

Project A.P.E.S

Active Platform Electromagnetic Stabilization



Critical Design Review

Table of Contents

List of Figures	6
List of Tables	8
1. Team Summary.....	10
2. Project A.P.E.S. Overview	11
2.1. Mission Statement	11
2.2. Mission Success Criteria	11
2.3. Launch Vehicle Summary	11
2.4. Payload Summary	13
3. Changes since PDR	14
3.1. Changes to the Launch Vehicle System.....	14
3.2. Changes to the Payload and Flight Systems Design	14
3.3. Changes to the Activity Plan.....	14
4. Launch Vehicle.....	15
4.1. Overview	15
4.2. System Design Overview	15
4.3. Recovery System.....	18
4.3.1. Overview.....	18
4.3.2. Parachute Dimensions.....	19
4.3.3. Ejection Charges	21
4.3.4. Altimeters.....	22
4.3.5. Assembly.....	23
4.3.6. Testing.....	24
4.4. Booster Section	25
4.4.1. Material Requirements.....	27
4.4.2. Manufacturing and Quality Assurance	27
4.4.3. Finite Element Analysis	28
4.4.4. Fin Overview	29
4.4.5. Testing Facility	31
4.4.6. Static Loading Testing	31
4.5. iMPS – Integrated Modular Payload System	31
4.5.1. Design and Analysis	31
4.5.2. Structure Fabrication and Manufacturing	35
4.5.3. Structure Testing & Results	35
4.6. Vesputa Mass Breakdown.....	38

4.7.	Vespula Overall Dimension	39
5.	Launch Vehicle Performance Predictions	40
5.1.	Flight Simulation.....	41
5.2.	AeroTech L1390G-P Simulated Thrust Curve.....	42
5.3.	Stability Margin.....	42
5.4.	Drift Profile Simulation.....	43
5.5.	Kinetic Energy Upon Landing	44
6.	Launch Vehicle Testing.....	45
6.1.	Subscale Testing.....	45
7.	Launch System and Platform.....	50
8.	Payload	51
8.1.	Introduction to the Experiment and Payload Concept Features & Definition	51
8.1.1.	Motivations	51
8.1.2.	Scientific Merit	51
8.2.	Success Criteria	52
8.3.	Experimental Requirements and Objectives	53
8.4.	Experiment Overview	54
8.4.1.	Hypothesis and Premise	54
8.4.1.	Experimental Method and Relevance of Data	55
8.4.2.	Ground Test Plan	56
8.5.	Ground Testing.....	57
9.	Flight Systems	60
9.1.	Flight Avionics.....	60
9.1.1.	Overview and Requirements.....	60
9.1.2.	Requirements and Products.....	60
9.1.3.	Flight Computer	62
9.2.	A.P.E.S. System Computer	65
9.2.1.	Control Theory	66
9.3.	Power Systems	68
9.3.1.	Power Budget.....	68
9.3.2.	Power Supply	70
9.4.	Telemetry and Recovery	71

9.4.1.	Ground station.....	71
9.4.2.	Transmitter Design.....	71
9.5.	Integration	72
9.5.1.	Modularity and Motivation	72
9.5.2.	Universal Mounting Bracket.....	73
9.6.	Sensing Capabilities	75
9.6.1.	Flight Avionics Sensors	75
9.6.2.	A.P.E.S. System Sensing	77
9.7.	“De-Scope” Options.....	80
9.7.1.	Payload “De-Scope”	80
9.7.2.	Flight Computer “De-Scope”.....	80
9.8.	General Safety	80
9.9.	Payload Hazards.....	81
9.10.	Vehicle Safety.....	83
10.	Project Budget.....	86
10.1.	Funding Overview	86
10.2.	Projected Budget Update	86
10.3.	Actual Project Costs	87
10.3.1.	CDR Budget Summary	87
10.3.2.	Flight Hardware Expenditures.....	89
10.3.3.	Actual Costs vs. Projected Costs	90
11.	Project Schedule.....	92
11.1.	Schedule Overview.....	92
11.2.	Critical Path Chart: CDR to PLAR.....	92
11.3.	Schedule Risk	94
11.3.1.	High Risk Tasks.....	94
11.3.1.	Low-to-Moderate Risk Tasks	95
12.	Educational Outreach.....	96
12.1.	Overview	96
12.2.	FIRST LEGO League.....	96
12.3.	Civil Air Patrol Model Rocketry Program	97
12.4.	National Air and Space Museum Discovery Station	98
12.5.	Young Astronauts Program	98

Reference	99
Appendix I: Project A.P.E.S. Gantt Chart	100
Appendix II: Launch Checklist.....	104
Appendix III: Ground Test Plan	107
Appendix IV: Mathematical and Physical Modeling of Magnetic Fields	109
Appendix V: Recovery MATLAB code.....	115
Appendix VI: FIRST LEGO League Lesson Plan.....	119
Appendix VII: Civil Air Patrol (CAP) Model Rocketry Program	Lesson Plan

121

List of Figures

Figure 1: Main Chute Deployment altitude as a function of Descent Rate and Chute Size	19
Figure 2: Section View of Launch vehicle	19
Figure 3: Detail of Drogue chute section	20
Figure 4: Detail of Main Chute section.....	20
Figure 5: Location of Recovery system within the Launch Vehicle	22
Figure 6: Electrical Schematic of Stratologger	23
Figure 7: Stratologger Configuration.....	23
Figure 8: AeroTech 75/3840 Motor Casing.....	25
Figure 9: Thrust Retention System	25
Figure 10: Thrust Plate Assembly.....	26
Figure 11: U-bolt Attachment.....	26
Figure 12: Assembled retention plate	27
Figure 13: Fin Placement	27
Figure 14: Motor retention and Fin Assembly.....	27
Figure 15: Booster Section with Recovery	27
Figure 16: Thrust Plate Stresses (top-view).....	29
Figure 17: Thrust Plate Stress (bottom-view).....	29
Figure 18: Booster section stresses	29
Figure 19: Booster section displacement	29
Figure 20: Fin Dimensions.....	30
Figure 21: CAD model of the iMPS	32
Figure 22: Dimensions for the stringer	33
Figure 23: Cross-sectional view of the rod with the fastener hole	33
Figure 24: FEA of rib with lightening holes (note that units are in base SI).....	34
Figure 25: Impact testing rig.....	36
Figure 26: iMPS structure test article	37
Figure 27: Evidence of minor compression damage occurring at F.S = 2.5.....	38
Figure 28: Mass Fraction for Vespula	39
Figure 29: Dimensions for Vespula	40
Figure 30: Flight profile with AeroTech L1390 motor for a total takeoff weight of 41.5 pounds	42
Figure 31: Thrust curve for Aerotech L1390 motor	42
Figure 32: Stability margin calibers vs. Time.....	43
Figure 33: Drift from launch pad at various wind speeds.....	44
Figure 34: Korsakov (a) layout and (b) flight vehicle	45
Figure 35: Stability profile for Korsakov vehicle.	46
Figure 36: Korsakov Flight Profile as predicted by OpenRocket.....	48
Figure 37: Korsakov Predicted Drift Profile.....	49

Figure 38: Korsakov Drift Distance.....	49
Figure 39: Vespula on Launch Pad.....	50
Figure 40: Section view of the proposed flight model of the A.P.E.S. system.....	56
Figure 41: The A.P.E.S. system ground test platform	57
Figure 42. Field Strength in the X-Direction of the solenoid vs. radial distance at various current settings.	58
Figure 43. Response Surface of the field strength in the X-Direction.....	59
Figure 44: General products of Flight Avionics	60
Figure 45: Generalization of flight computer software.....	63
Figure 46: Proposed layout of flight computer. Larger copy included in Appendix 4.....	63
Figure 47: Generalization of A.P.E.S. system software	66
Figure 48: Layout of A.P.E.S. computer system hardware	66
Figure 49. PID Controller Block Diagram.....	67
Figure 50. (a) Power budget for the A.P.E.S. computer and the Flight Computer; (b) subtotals of the A.P.E.S. computer and the Flight Computer.....	69
Figure 51: Discharge characteristics of the A123 battery.....	70
Figure 52: A single A123 LiFePO battery	71
Figure 53: Antenna performance as a function of range.....	72
Figure 54: Universal mounting bracket bolted to rib.....	73
Figure 55: Basic finite-element-analysis of the universal mounting bracket	74
Figure 56: ADXL345 accelerometer	76
Figure 57: HMC1043 Magnetometer.....	77
Figure 58: OVM7690 Camera Cube.....	79
Figure 59. Projected total project cost.	87
Figure 60. Project expenditures as of the CDR milestone.	88
Figure 61. Actual total project costs and project reserves at each milestone.	88
Figure 62. Summary of Flight Hardware expenditures up to the CDR milestone.....	89
Figure 63. Total and Projected Flight Vehicle expenditures	90
Figure 64. Actual vs. Projected Costs for the 2011-2012 competition year.....	91
Figure 65. Critical Path Chart from CDR to PLAR.....	93
Figure 66. Online Outreach Contact Form through which educators may contact the Mile High Yellow Jackets.	96
Figure 67. Example of a First LEGO League autonomous robot.	96
Figure 68. A Civil Air Patrol Model rocket constructed by a cadet during the TITAN phase of the Model Rocketry Program.....	97
Figure 69: field generated by a single dipole.....	111
Figure 70: field generated by multiple dipoles	111

List of Tables

Table 1: Mission Success Criteria.....	11
Table 2: System design requirement overview.....	16
Table 3: System design requirement overview.....	17
Table 4: System design requirement overview.....	18
Table 5: Parachute parameters.....	21
Table 6: Ejection charge equation variables.....	21
Table 7: Ejection pressurization and black powder charge.....	22
Table 8: Summary of the electrical schematics for recovery system.....	23
Table 9: Success Criteria.....	24
Table 10: Failure Modes.....	25
Table 11: FEA results for the thrust plate and the assembly.....	29
Table 12: Drag calculation values.....	31
Table 13: Values for factor of safety calculation.....	34
Table 14: Impact test runs.....	36
Table 15: Testing results matrix, where X signifies damage, P signifies pass.....	37
Table 16: iMPS component weight.....	38
Table 17: Booster Section Weight Budget.....	39
Table 18: Subsection Mass Break.....	39
Table 19: Best motor per launch vehicle weight and altitude reached.....	41
Table 20: Flight Simulation Conditions.....	41
Table 21: Kinetic energy upon landing for each section of Vespula.....	44
Table 22: Characteristics of Korsakov vehicle.....	46
Table 23: Material and cost for Korsakov.....	47
Table 24: Success Criteria.....	52
Table 25: A.P.E.S. system requirements.....	53
Table 26: A.P.E.S. ground testing objectives.....	54
Table 27. RSE coefficients and terms.....	59
Table 28: Flight Avionics Requirements.....	61
Table 29: Major Flight Computer Components.....	65
Table 30: Universal Mounting Bracket Specifications.....	75
Table 31: Possible A.P.E.S. distance sensors.....	78
Table 32: Hazards, Risks, and Mitigation.....	81
Table 33: A.P.E.S. payload failure modes.....	82
Table 34: Risk Identification and Mitigation Steps.....	84
Table 35: Launch vehicle failure modes and mitigation.....	85
Table 36. Summary of sponsors for the Mile High Yellow Jackets.....	86
Table 37. Design milestones set by the USLI Program Office.....	92

Table 38. Identification and Mitigations for High-Risk Tasks	94
Table 39. Low to Moderate Risk items and mitigations.....	95
Table 40: Ground Test goals.....	107
Table 41. Range of test values used during Test Sequence 1	107

1. Team Summary

<i>Team Summary</i>	
School Name	Georgia Institute of Technology
Team Name	Mile High Yellow Jackets
Project Title	Active Platform Electromagnetic Stabilization (A.P.E.S.)
Launch vehicle Name	Vespula
Project Lead	Richard
Safety Officer	Matt
Team Advisors	Dr. Eric Feron, Dr. Marilyn Wolf
NAR Section	Primary: Southern Area Launch vehiclery (SoAR) #571 Secondary: GA Tech Ramblin' Launch vehicle Club #701
NAR Contact	Primary: Matthew Vildzius Secondary: Jorge Blanco

2. Project A.P.E.S. Overview

2.1. Mission Statement

To maintain a sustainable team dedicated to the gaining of knowledge through the designing, building, and launching of reusable launch vehicles with innovative payloads in accordance with the NASA University Student Launch Initiative Guidelines.

2.2. Mission Success Criteria

The criteria for mission success are shown in Table 1.

Table 1: Mission Success Criteria

<i>Requirement</i>	<i>Design feature to satisfy that requirement</i>	<i>Requirement Verification</i>	<i>Success Criteria</i>
Provide a suitable environment for the payload	The payload requires a steady, but randomly vibrating platform to test the APES system. Unsteadiness in the motor's thrust and launch vehicle aerodynamics cause vibrations.	By measuring the acceleration with the payload's accelerometers	The APES system dampens out a recordable amount of vibration.
To fly as close to a mile in altitude as possible without exceeding 5,600 ft.	A motor will be chosen to propel the vehicle to a mile in altitude	Through the use of barometric altimeters	The altimeters record an altitude less than 5,600 ft
The vehicle must be reusable	The structure will be robust enough to handle any loading encountered during the flight	Through finite element analyses and structural ground testing of components	The vehicle survives the flight with no damage

2.3. Mission Timeline

Figure 1 graphically illustrates the Mission Profile of Project A.P.E.S.

Mission Profile

ONE MILE

PHASE II

PHASE I

PHASE III

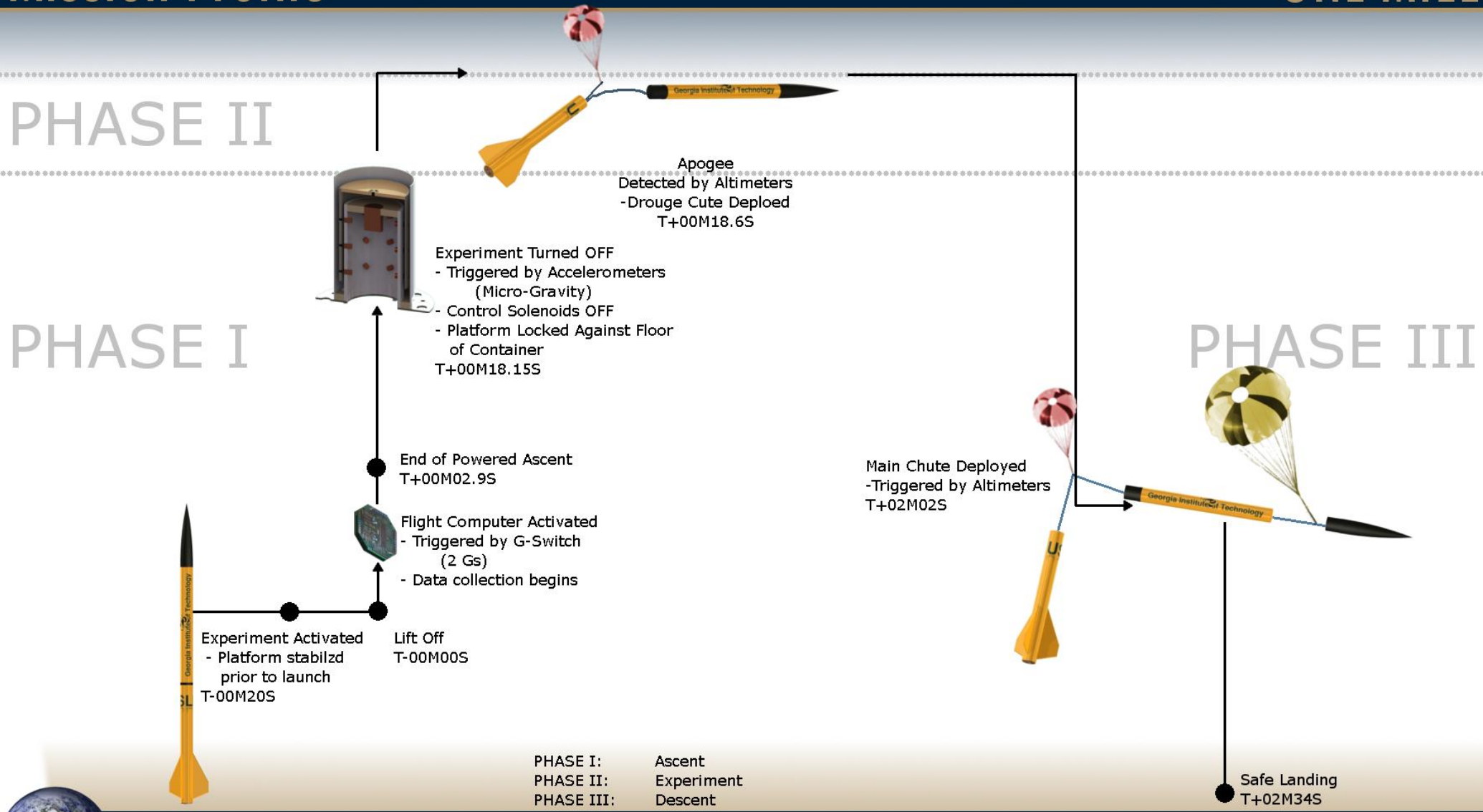


Figure 1. Project A.P.E.S. Mission Timeline

2.4. Launch Vehicle Summary

The *Vespula* launch vehicle features a modular design that allows for simplified integration of various payloads up to 10 lbs, and has a maximum launch weight of approximately 40 pounds using the preferred AeroTech L1390G-P motor. The structure of the launch vehicle features a rib-and-stringer design covered by a thin skin to minimize weight. The recovery system utilizes a 48” drogue parachute slowing the launch vehicle down to 50 feet per second (ft/s) and a 144” main parachute to slow the launch vehicle down to 15 ft/s from an apogee of approximately one mile above ground level.

2.5. Payload Summary

The Mile High Yellow Jackets will design, build, test, and fly an electromagnetically levitated plate within their launch vehicle. This plate will be stabilized against the motion of the launch vehicle providing a vibration-free environment for a theoretical payload in an experiment known as A.P.E.S., or Active Platform Electromagnetic Stabilization. Flight Systems will utilize an ATmega 2560 for all data collection activities and the ARM Cortex M3 for the A.P.E.S. control law implementation.

3. Changes since PDR

3.1. Changes to the Team

The following individuals have either graduated or are studying abroad:

- Kevin (Project Systems Engineer, Flight Systems Lead)
- Xiao (Rocket Lead)
- Alex B. (Mechanical Lead)

The following individuals have joined the Mile High Yellow Jackets this semester:

- Alex T
- Alzar T
- Franz B
- Katie S
- Hunter S

Lastly, the following individuals have been reassigned to a new leadership role within the Team:

- Matt S. (Flight Systems Lead)
- Robert R. (Flight Avionics Lead)
- Jason T. (Rocket Lead)

3.2. Changes to the Launch Vehicle System

- The main parachute and drogue were changed to 12 ft and 4 ft in diameter respectively.
- The larger drogue slows down the vehicle to 50 ft/s. The larger main slows the vehicle down to a landing speed of 15 ft/s.
- Ejection charge masses have been updated to account for parachute packing.
- A cardboard motor tube has been added to the booster section to allow for increased fin epoxy surface area
- The thrust plate has been redesigned to be cut from a wood block using a waterjet instead of being machined from an aluminum billet
- The thrust retention ring has been updated to be cut from an aluminum plate on a waterjet instead of machined from an aluminum billet
- L-brackets have been added to the fins and recovery system bulkheads at epoxy joints for added strength

3.3. Changes to the Payload and Flight Systems Design

- The Universal Mounting System has been redesigned to have greater annularity and strength allowing for a decrease in mass with-out compromising safety.

3.4. Changes to the Activity Plan

- A Discovery Station has been submitted to the National Air and Space Museum in DC
- The Mile High Yellow Jackets will be working with a local Civil Air Patrol squadron in teaching a Model Rocketry Program.

4. Launch Vehicle

4.1. Overview

The purpose of the launch vehicle is to carry a payload up one mile in altitude and safely return it to the surface of the Earth. Additionally, the launch vehicle will also be designed to carry a wide range of possible experiments so that the launch vehicle can be reused in the future. The overall design is to be as flexible as possible, encouraging reuse for future research and multiple launches.

The chosen launch vehicle design provides an adequate amount of space for a variety of payload designs. Prior to test flights, extensive ground testing will be performed to verify successful integration of the payload into the fully assembled launch vehicle. A subscale test flight occurred in December 2011 to test the launch vehicle's skin design and a full scale test will be performed in the spring. The objective of the full scale test launch, from a vehicle perspective, is to verify the recovery system with delayed apogee ejection and the integrity of the overall structure during flight. These tests will ensure a successful launch and recovery of the vehicle to meet all requirements for the final launch

Though a kit launch vehicle would be easier to construct, a custom internal structure was designed to have lower mass and lower cost. The launch vehicle will have a 5 inch outer diameter to fit the chosen nose cone. The vehicle's diameter of 5 inches supports a wide range of payloads on a level two motor, while providing support for up to a 40-inch-long payload bay. Strength, durability, and safety are ensured as the structure is solely composed of fiberglass components.

4.2. System Design Overview

Table 2, Table 3, and Table 4 list the derived system-level requirements in order to meet the success criteria.

Table 2: System design requirement overview

<i>Requirement</i>	<i>Design feature that will satisfy that requirement</i>	<i>Requirement Verification</i>	<i>Verification Status</i>	<i>Verification Reference</i>
The launch vehicle shall carry a science or engineering payload	The launch vehicle will carry the A.P.E.S. experiment in the integrated modular payload section (iMPS)	The A.P.E.S. experiment will undergo extensive ground testing prior to flight testing	Completed	Section 4.5.1
The launch vehicle shall deliver the payload to an altitude of 1 mile above ground level	The motor will be chosen per the final launch vehicle mass	Verification via OpenRocket vehicle simulations of the design	Completed	Figure 31, Table 19
The launch vehicle shall carry one approved altimeter for recording purposes	An approved altimeter will be included in the recovery design	Engineering inspection from manufacturer	Completed	Figure 8
The recovery system shall meet all requirements listed in requirement 4 in the handbook	The recovery system will feature a drogue and main parachute	Ground testing of the independent recovery systems and flight testing of the integrated system	In Progress	Section 4.3
The recovery system electronics shall be shielded from all interference	Faraday shielding will be incorporated into design to protect electronics from payload interference	Ground testing of the independent recovery systems and flight testing of the integrated system	In Progress	
The launch vehicle shall have a pad stay time of one (1) hour	The hardware and battery will be able to function after remaining on the pad for a hour	Ground testing of the integrated system	Completed	Figure 51, Section 9.3.2
The launch vehicle shall have aerodynamic stability before leaving the launch rail	The launch vehicle will have launch buttons mounted to the booster section and will launch from a rail of adequate length	OpenRocket vehicle Simulations	Completed	Figure 33

Table 3: System design requirement overview

<i>Requirement</i>	<i>Design feature that will satisfy that requirement</i>	<i>Requirement Verification</i>	<i>Verification Status</i>	<i>Verification Reference</i>
The launch vehicle shall remain subsonic throughout flight	The motor will be chosen per the final launch vehicle mass	Through OpenRocket vehicle simulations of the design	Completed	Figure 31
The launch vehicle shall be reusable	The structure will be robust enough to handle any loading encountered during the flight	Ground testing of the independent recovery systems and flight testing of the integrated system	Completed	Figure 17, Figure 18, Figure 25, Table 11, Table 15
The launch vehicle shall stage the deployment of its recovery devices	The recovery system will feature a drogue and main parachute	Ground testing of the independent recovery systems and flight testing of the integrated system	Completed	Section 4.3
Removable shear pins shall be used for both the main and drogue chute compartments	Plastic shear pins are designed to be installed in the recovery compartments	Ground testing of the independent recovery systems and flight testing of the integrated system	In progress	Section 4.3.6
The launch vehicle shall have a maximum of four (4) independent or tethered sections	There are three (3) sections: nosecone, payload, and booster	Engineering inspection	Completed	Figure 6
Each section shall have a maximum kinetic energy of 75 ft-lb _f	The recovery system will feature a drogue and main parachute	Analysis and simulation	Completed	Table 21
All sections shall be designed to recover within 2,500 feet of the launch pad assuming 15 mph wind	The recovery system will feature a drogue and main parachute	OpenRocket vehicle simulations	Completed	Figure 34

Table 4: System design requirement overview

<i>Requirement</i>	<i>Design feature that will satisfy that requirement</i>	<i>Requirement Verification</i>	<i>Verification Status</i>	<i>Verification Reference</i>
The launch vehicle shall be capable of being prepared for flight at the launch site within 2 hours from the time the waiver opens	Assembly Checklist	Construction testing and instructions will be made before launch day	In Progress	
The launch vehicle shall be launched from a standard firing system using a 10 second countdown	NAR launch regulations will be followed	Inspection	Completed	Section 5.1
The launch vehicle shall require no external circuitry or special ground support equipment to initiate the launch other than what is provided by the range	The vehicle will implement standard ground support equipment	Inspection	Completed	Section 5.1
The launch vehicle shall use a commercially available solid motor	An L-class NAR approved motor will be incorporated into the design	Engineering inspection from manufacturer	Completed	Section 5.1
The total impulse provided by the launch vehicle shall not exceed 5,120 N-s	An L-class NAR approved motor will be incorporated into the design	Engineering inspection from manufacturer	Completed	Section 5.1

4.3. Recovery System

4.3.1. Overview

The recovery system is intended to mitigate difficulties encountered due to variable wind speeds and to prevent destruction from impact. These objectives will be accomplished with a dual-deployment system. OpenRocket vehicle analysis of the drogue chute indicates that the maximum descent rate will be 50 ft/s with deployment at apogee. Using the MATLAB code included in Appendix V, Figure 2 was produced to determine that main chute deployment will

slow the launch vehicle to a maximum descent rate of 15 ft/s and will be deployed at 450 ft AGL altitude.

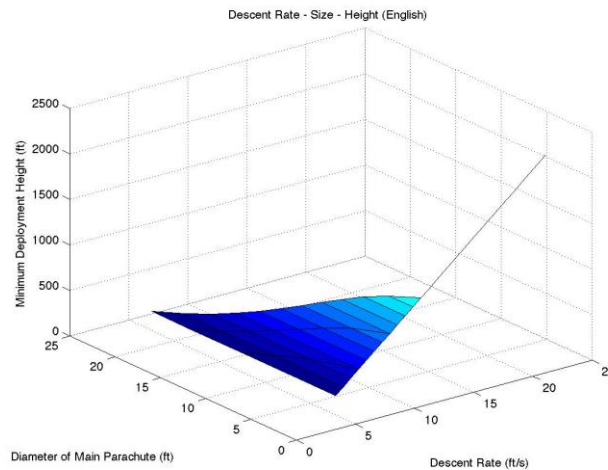


Figure 2: Main Chute Deployment altitude as a function of Descent Rate and Chute Size

The drogue chute is assumed to have a C_D of 1.2, and the main chute is assumed to have a C_D of 1.4. Figure 3 shows a section drawing of the launch vehicle and where the parachutes are contained.

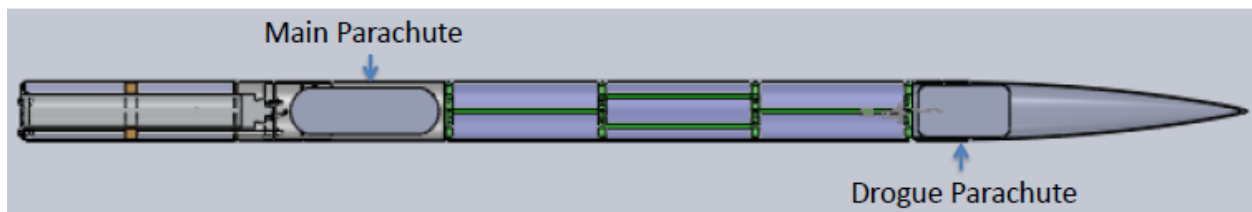


Figure 3: Section View of Launch vehicle

4.3.2. Parachute Dimensions

The drogue chute will be placed inside the nose cone – which has an outer diameter of 5 inches, an inner diameter of 4.7 inches, and a length of 25.5 inches. A bulkhead connected to a 1-inch wide nylon webbing on one end will serve to take the impulse of the ejection charge blast and prevent the drogue chute from being stuck inside of the nose cone (see Figure 4).

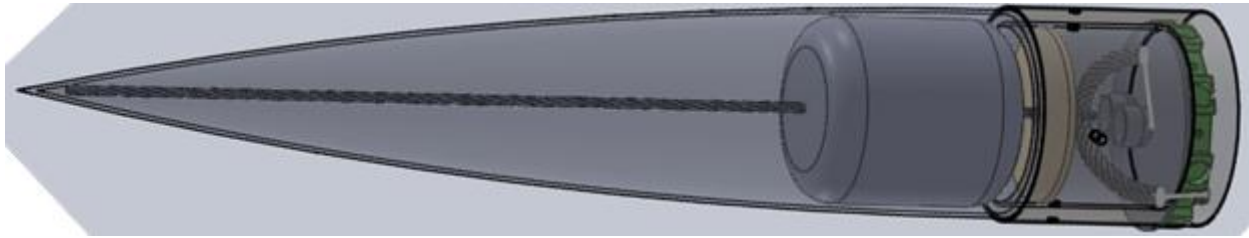


Figure 4: Detail of Drogue chute section

Nomex cloth will be used to prevent the shock cord from burning. Once ejected, the inertia of the nose cone will allow the drogue chute to be pulled freely from storage. The main chute will be housed in a cylindrical compartment attached to the thrust plate within the launch vehicle. The main chute compartment has a 5 inch outer diameter and a height of 12 inches. Shock cords, made of 1-inch wide nylon webbing, will connect the parachutes to all sections of the launch vehicle such that in the recovery phase the entire system remains a single unit. For the main chute, the shock cord is attached to a U-Bolt that is on the reverse side of the thrust plate, and will be connected through a steel wire drilled into a fiberglass bulkhead (see Figure 5).

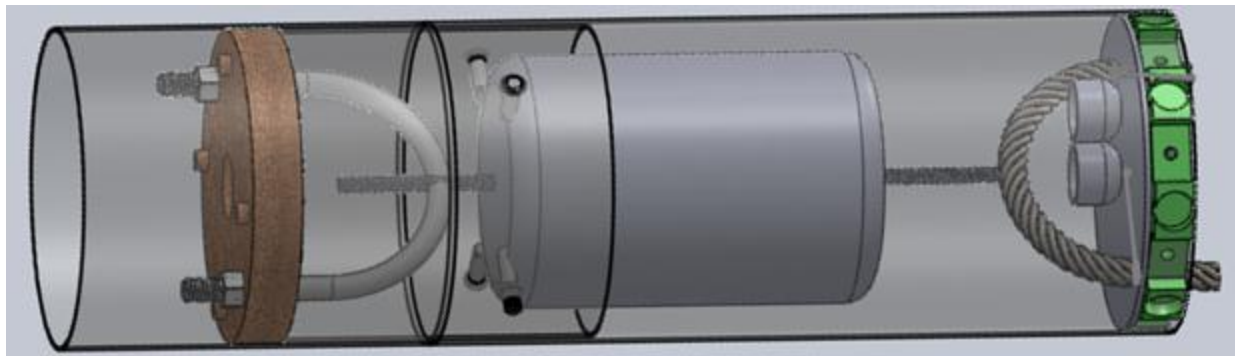


Figure 5: Detail of Main Chute section

Similarly, the shock cord of the drogue parachute is connected to the nose cone and to the steel wire on the upper end of the payload section bulkhead.

Table 5 outlines the dimensions and the weights of the parachutes.

Table 5: Parachute parameters

	<i>Main Parachute</i>	<i>Drogue Parachute</i>
Dimensions	12 ft diameter	4 ft diameter
Surface Area	113.10 ft ²	12.56 ft ²
Estimated C _D	1.4	1.2
Weight	2.5 lb	1.5 lb
Target Descent Rate	15 ft/s	50 ft/s

4.3.3. Ejection Charges

Black powder masses were calculated using Equation 1 with variables defined in Table 6.

$$W = \frac{VDP}{RT} \quad 1.$$

Table 6: Ejection charge equation variables

<i>Variable</i>	<i>Description</i>	<i>Units</i>
W	Weight of the black powder in pound mass	454 · W _{gram}
V	Volume of the container to be pressurized	in ³
DP	Pressure Differential	psia
R	Gas Combustion Constant for black powder	$\frac{22.16 \text{ ft} \cdot \text{lb}_f}{\text{lb}_m \cdot \text{R}}$
T	Gas Combustion Temperature	3307 °R

Volume, V, is set by the design, while the black powder determines the gas constant and temperature. In order to find the pressurization, the strength and number of shear pins that will hold the parachute compartments together is needed. A quarter-inch shear pin can take up to 35 pounds of shear force before it fails. The two compartments will be held together with four (4)

1/16” diameter Nylon shear pins, thus implying only a force of 150 pounds per compartment is needed to achieve separation from Equation 2 using a tensile yield strength of 12 ksi.

$$F_{pin} = \frac{\sigma \pi d^2}{4} \tag{2}$$

However, accounting for frictional resistance from the tubes, 10 pounds of force per compartment will be added. The corresponding amounts of black powder are summarized in Table 7. Figure 6 shows how the two (2) chutes will be attached throughout the launch vehicle.

Table 7: Ejection pressurization and black powder charge

	<i>Main Parachute</i>	<i>Drogue Parachute</i>
Total Pressurization	24.7 psia	23.7 psia
Pressure at Deployment Altitude	14.4 psia	12.1 psia
Differential Pressurization	10.3 psia	11.6 psia
Ejection Force	202.2 lbf	227.8 lbf
Amount of Black Powder	4.5 grams	3.6 grams
Factor of Safety	1.26	1.42

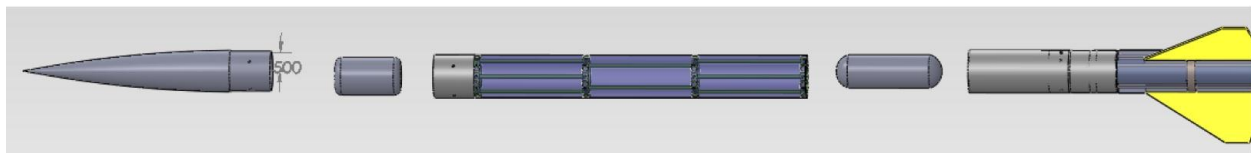


Figure 6: Location of Recovery system within the Launch Vehicle

4.3.4. Altimeters

The StratoLogger collects flight data at a rate of twenty samples per second throughout the flight and stores the data for later download to a computer. The altimeter is capable of recording flights of up to 100,000 ft in altitude. Two (2) altimeters will be used, each with an independent power supply. The system for each altimeter will be set up as shown in Figure 8, while the pin connections to be used are shown in Stratologger Configuration

Table 8. A picture of the StratoLogger is shown in Figure 7.

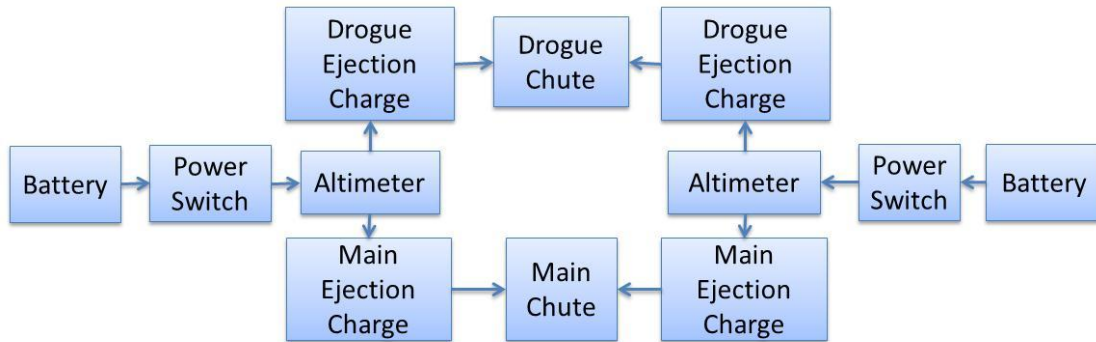


Figure 7: Electrical Schematic of Stratologger

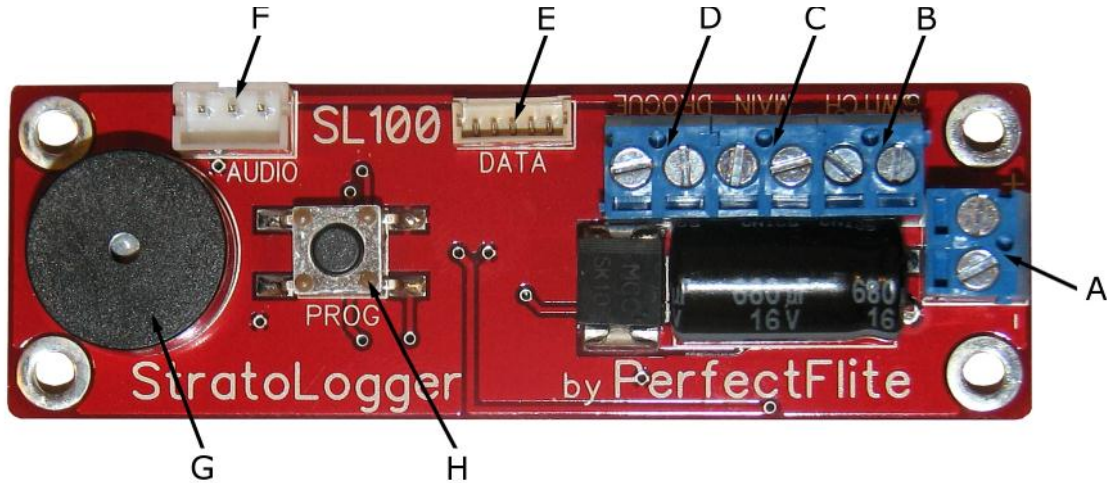


Figure 8: Stratologger Configuration

Table 8: Summary of the electrical schematics for recovery system

Port	Name	Description
A	Battery Port	Connect to a 9 V power source
B	Power Switch Port	Connect to a power switch
C	Main Chute Port	Connect to Main Chute E-matches
D	Drogue Chute Port	Connect to Drogue Chute E-matches
G	Beeper	Audibly reports settings, status, etc. via a sequence of beeps

4.3.5. Assembly

4.3.5.1. Launch Vehicle Recovery

Both the main and drogue parachutes are legacy hardware and the casings are made of G10 fiberglass. The bulkhead that goes underneath the main parachute will be made out of wood, since it will serve a dual function as the thrust plate. Four shear pins will hold the assembly in launch configuration. The ejection charge will be directed with the use of PVC end-caps to protect the casings from thermal shock and a NOMEX shield will be used to protect the chutes from thermal shock. The charges will be ignited by an e-match. Each casing will undergo two tests: a distance test and a feasibility test. These tests will enable the estimation of the mass of black powder to be placed both forward and aft of each compartment. In addition, the tests will confirm whether the black powder charges are enough to achieve separation. Supporting equipment will be provided to prevent launch vehicle parts or debris from hitting bystanders during testing.

4.3.5.2. Recovery Setup

Assembly will be straightforward. The main coupler will be fixed to the compartment using epoxy. The top half of the compartment will then slide onto the coupler up to the inner wall of the compartment and will be held in place by shear pins. The ejection charges will be placed on the outer side of the payload bulkheads and will be detonated by an e-match, which will be manually controlled by a switch box at a safe distance from the test structure. The actual chutes will be inside the compartments; a NOMEX shield will protect them.

4.3.6. Testing

For testing to be considered a success, it must meet all of the success criteria (shown in Table 9). Only if none of the criteria are met, or if one of the failure modes occurs, would the test be considered a failure. The failure modes are also shown in Table 10.

Table 9: Success Criteria

<i>Success Criteria</i>	<i>Risk Level</i>	<i>Mitigation</i>
Ejection charge ignites	Low	Keep Personnel a safe distance away
Shear pins break	Low	Keep Personnel a safe distance away
Launch vehicle moves half the distance of shock cord	Medium	Keep Personnel a safe distance away

Table 10: Failure Modes

<i>Failure Criteria</i>	<i>Risk Level</i>	<i>Mitigation</i>
The fiberglass or the tube coupler shatters due to the charge	Medium	Keep Personnel a safe distance away
The shear pins don't shear, and the launch vehicle stays intact	Low	Keep Personnel a safe distance away
The NOMEX shield fails and the parachute is burned	Medium	Properly folding the parachute and shield
Ematches fail to ignite black powder	Low	Redundant ignition system

4.4. Booster Section

The booster system of the Mile High Yellow Jackets launch vehicle uses traditional motors combined with a unique structure. The main focus is to have a highly integrated design and to lighten the total weight of the launch vehicle. The primary components of the launch vehicle booster section are the launch vehicle motor and the thrust retention system. Both of these primary components are shown in Figure 9 and Figure 10 below.

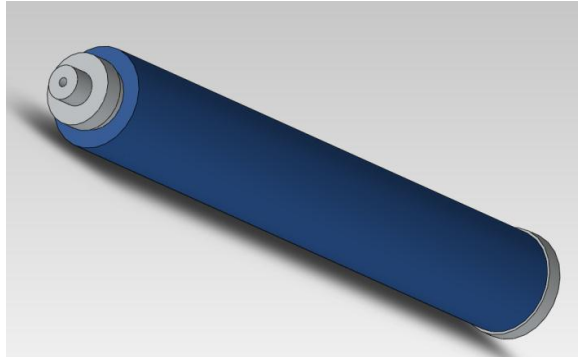


Figure 9: AeroTech 75/3840 Motor Casing

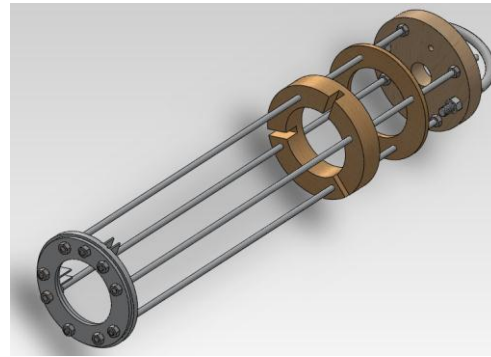


Figure 10: Thrust Retention System

The Motor Retention System (MRS) can be broken down into several modular parts. The first part is the thrust plate located at the top of the MRS. The thrust plate will provide contact area necessary for the ignited launch vehicle motor to provide thrust to the rest of the structure. The thrust plate will also be part of the recovery system for chute deployment as it will serve as a bulkhead with a U-bolt for attachment of the main chute. Finally, the thrust plate will prevent the motor from penetrating through the booster section and it will provide torsional rigidity to the mounting rods running along the MRS. The current thrust plate is manufactured using marine

grade plywood and the assembly of the thrust plate with the motor casing, mounting rods, and the U-Bolt attachment in Figure 11 and Figure 12, respectively.

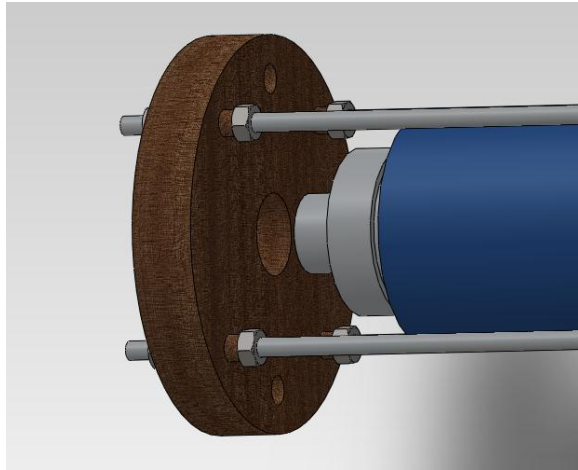


Figure 11: Thrust Plate Assembly



Figure 12: U-bolt Attachment

The major components of the MRS are the two support plates at the rear of the booster section, the centering rings, and the cardboard motor tube. The main purpose of the support plates is to prevent the motor from falling out of the launch vehicle. Additionally, the rear retention plate will provide a base for L-brackets that will be bolted on. The L-brackets are designed to seat each fin and provide torsional support for the mounting rods. The assembled retention plate with L-brackets and fin placement are shown in Figure 13 and Figure 14, respectively.

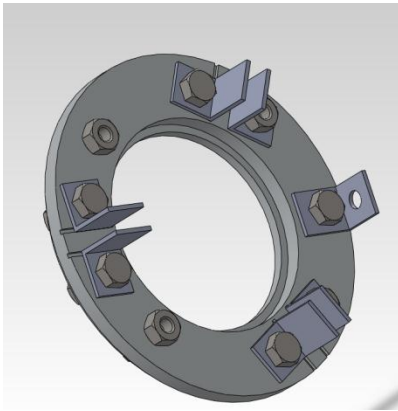


Figure 13: Assembled retention plate

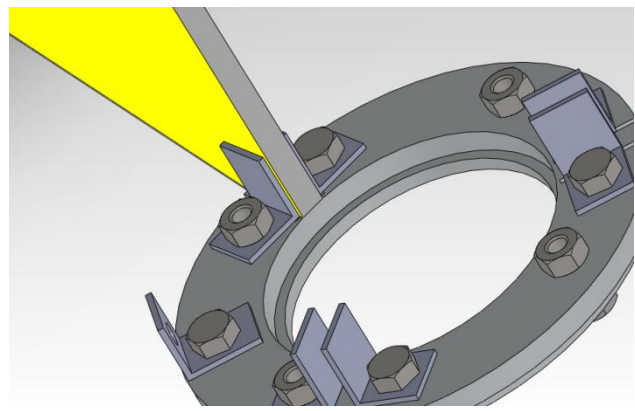


Figure 14: Fin Placement

The centering rings and the cardboard motor tube provide additional support to the fins and recovery section tubes. The motor retention and fin assembly are shown in Figure 15 and the total assembly including the recovery system is shown in Figure 16.

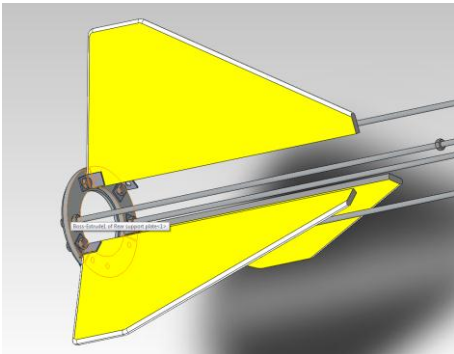


Figure 15: Motor retention and Fin Assembly

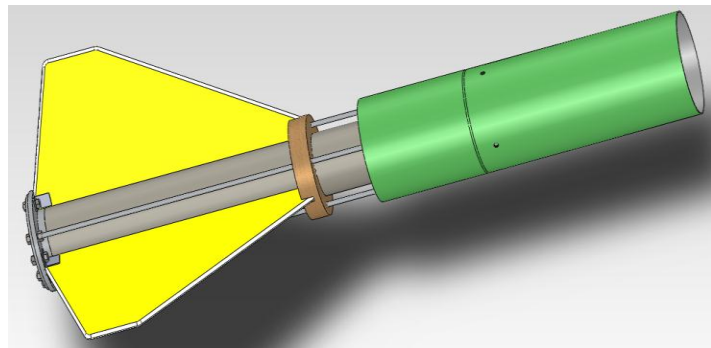


Figure 16: Booster Section with Recovery

4.4.1. Material Requirements

The majority of the booster section will be constructed from 1/2" BS1088 marine grade plywood and thin sheets of 6061 aluminum. These materials will reduce the weight of the system while maintaining structural integrity. Epoxy will serve as an adhesive for attaching the fins to the L-brackets, centering ring, and motor tube.

4.4.2. Manufacturing and Quality Assurance

Quality will be assured by utilizing proper manufacturing techniques that are appropriate for the materials and part designs. First, the thrust plate and rear support plates will be cut using a water jet, which will be used for cutting out the plywood for the centering rings. Next, the booster section will be assembled using epoxy and hex nuts on a threaded rod. For motor preparation, the rear retention plates will be removed by unscrewing the hex nuts. Afterwards, the motor propellant will be placed inside the motor casing and the rear retention plates will be reattached. The booster section will then undergo several test firings to ensure reliability and quality for the official launch date. Four motors will be used for testing and the final launch. Furthermore, the MRS will undergo torsional buckling tests to ensure structural integrity.

4.4.3. Finite Element Analysis (FEA)

Finite Element Analysis (or FEA) is a method of finding approximate solutions to partial differential equations. This method is helpful in analyzing complex structures for design and development analysis. Solidworks contains a design validation tool that carries out a basic FEA, which was used to structurally analyze the thrust plate and the overall booster section. The force applied during the analysis is 408 lb_f , which is the maximum thrust expected for an Aerotech L1390G-P. The first simulation contained only the thrust plate (Figure 17 and Figure 18), which resulted in a maximum displacement of 0.00838 inches and an induced maximum stress of 404.6 psi. The next simulation was for the entire booster section (Figure 19 and Figure 20). It is important to note both figures have deformation scaled to a high level so that it appears as if the rods are buckling when they are not. To reduce complexity, the shape was generalized as a single part similar to the actual booster section which included the thrust plate, mounting rods, fin centering ring, and the two support plates. The material used for the simulation was Aluminum 6061-T6. This simulation resulted in a maximum displacement of 0.00526 inches and an induced maximum stress of 483.3 psi. The results of the two simulations are summarized in Table 11 below.

Table 11: FEA results for the thrust plate and the assembly

Part	Material	Force Applied (lb _f)	Max. Displacement (inches)	Max. Stress (psi)	Factor of Safety
Thrust Plate	BS 1088	408	0.00838	404.6	3.3
Stringers	6061	408	0.00526	483.3	2.9

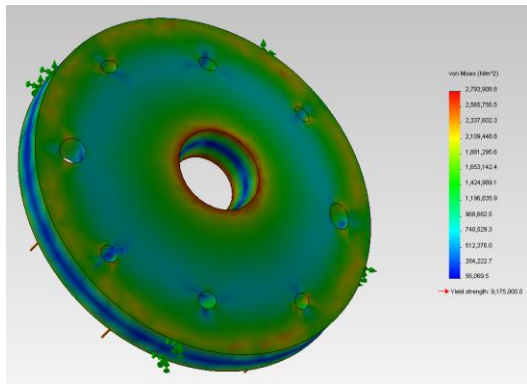


Figure 17: Thrust Plate Stresses (top-view)

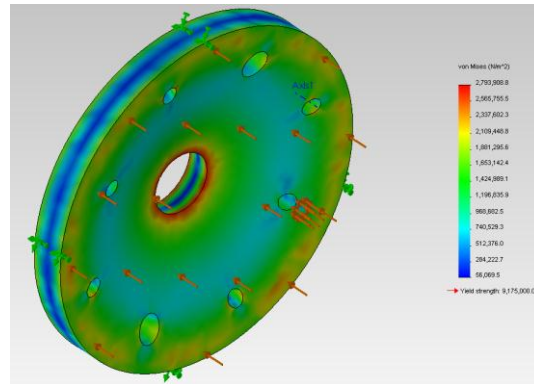


Figure 18: Thrust Plate Stress (bottom-view)

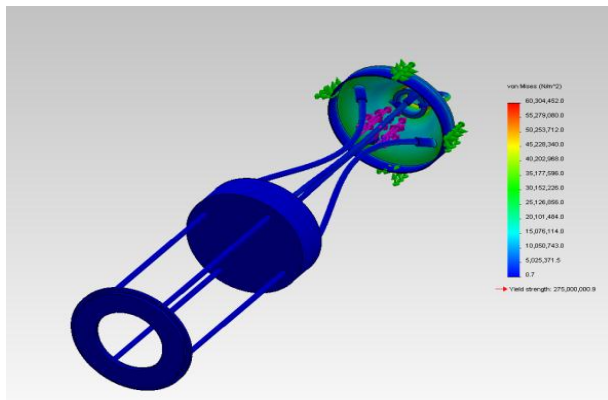


Figure 19: Booster section stresses

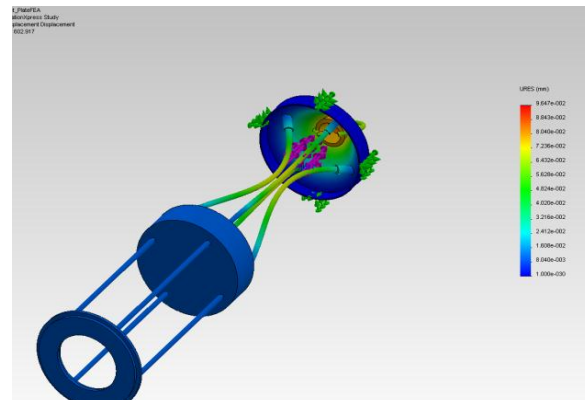


Figure 20: Booster section displacement

4.4.4. Fin Overview

Fins are used to keep the launch vehicle stable and the flight path straight. In addition, the shape and location of the fins places the center of gravity in front of the center of pressure. The trailing edge of the fins is located forward of the end of the rocket body the fins are more protected from impact damage during landing (Figure 21).

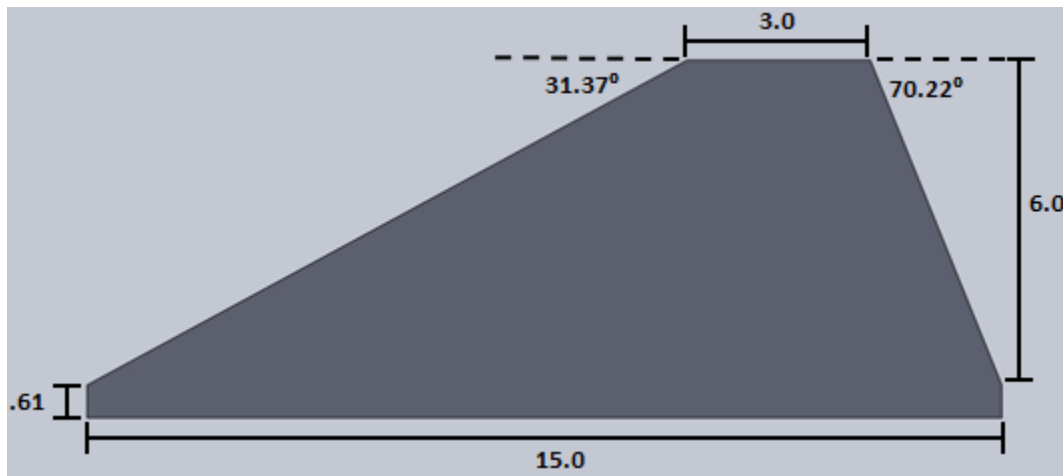


Figure 21: Fin Dimensions

The fins are made out of a composite honeycomb core with carbon fiber skins on both sides. This sandwich design provides strength to the fin structure while reducing weight. The leading edge will be constructed of foam crafted in a triangular shape and attached to the fin through epoxy. The fins will connect to the launch vehicle structure through two L brackets on each side of the fin attaching it to the thrust plate and epoxy fillets down the length of the fin to a cardboard motor tube. During flight, if the drag becomes too great the fins can detach from the launch vehicle structure due to the high moment acting at the interface between the fins and the structure of the launch vehicle. Another mode of failure is drag causing the leading edge to detach from the fin resulting in the carbon fiber honeycomb panel disintegrating. Calculations of the max drag force per fin were performed utilizing Equation 3 and the moment was calculated as the product of force and the distance from the tip of the fin.

$$D = \frac{1}{2} \rho v^2 C_D A \tag{3}$$

Further, the maximum velocity occurs at an altitude of 1,015 feet, which corresponds to a density of $0.07423 \text{ lb}_m/\text{ft}^3$. The results are summarized in Table 12.

Table 12: Drag calculation values

<i>Variable</i>	<i>Value</i>
Density	$0.07423 \text{ lb}_m/\text{ft}^3$
Velocity	613.88 ft/sec
Cross section area	0.0695 ft^2
C_D	0.295
Max drag force per fin	8.9 lb_f
Moment	6.78 $\text{lb}_f \cdot \text{ft}$

4.4.5. Testing Facility

The test rig that will be used for testing the fin structures is designed to test the worst case scenario by applying the force at the maximum moment. The fin test rig will be portable and consists of an L-structure that can be attached to any flat surface with a clamp. The fin structure connects directly to the test rig with a qualification motor tube and fin unit.

4.4.6. Static Loading Testing

Various tests will be used to determine the capabilities of the test article while undergoing static loading. This is representative of the thrust during the boost phase of flight. The weight will be applied until part failure. The weight will be added in 2 lb_m increments starting at 2 lb_m and ending at 22 lb_m . The fin must withstand the force of the weight for one minute for the run to be considered a success. Additionally, a 2.5 factor of safety shall be achieved for the testing to be considered a success.

4.5. *iMPS – Integrated Modular Payload System*

4.5.1. Design and Analysis

A lightweight structure is essential to maximizing payload mass fraction. Most launch vehicles use a thick walled body tube as structural member of the launch vehicle. Though simple, this design is inefficient in its use of material. The Mile High Yellow Jackets' launch vehicle will be unique amongst high power launch vehicles as it utilizes an internal structure consisting of ribs and stringers as illustrated by Figure 22. The ribs and stringers are fashioned out of G-10 fiberglass. The skin of the launch vehicle consists of a thin, flexible, heavy-weight paper.

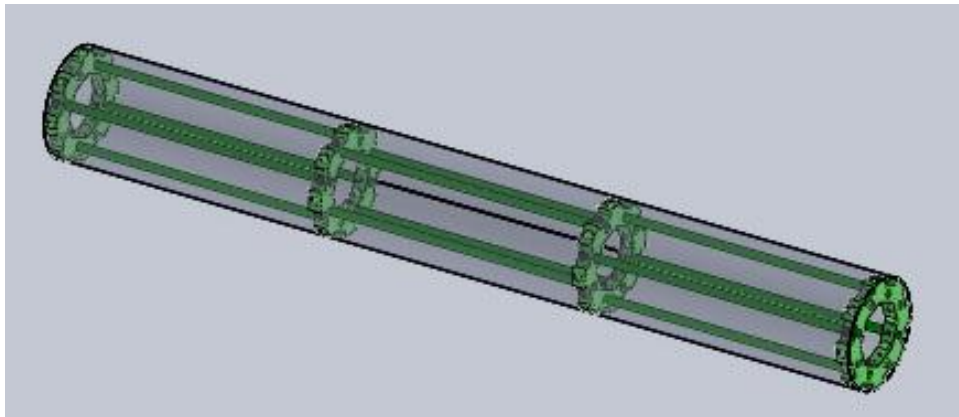


Figure 22: CAD model of the iMPS

To ensure the validity of the design, structural calculations were performed in order to ensure a factor of safety (F.S.) of at least 2.5 on the static loading for the structure. Consider a two dimensional view of the stringer in Figure 23. As a result of the hole, the loading path of the rod has changed significantly. That is, instead of the load being transferred through the entire cross-section of the rod, only a smaller cross-sectional area is carrying the load. The smallest cross-sectional area occurs along the diameter of the fastener hole. Thus, the point of failure will be about this hole due to increased stresses.

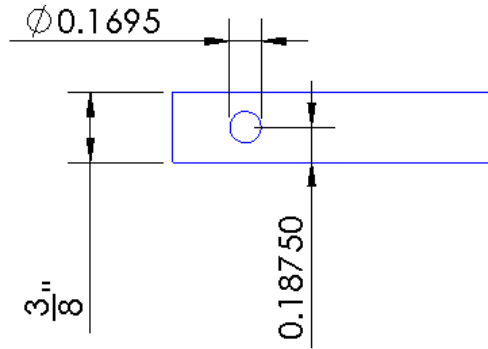


Figure 23: Dimensions for the stringer

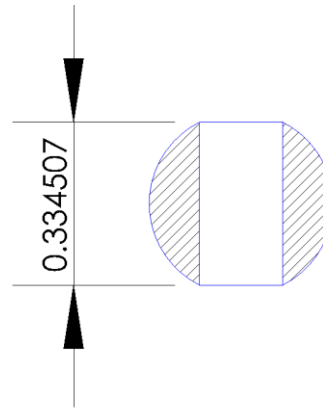


Figure 24: Cross-sectional view of the rod with the fastener hole

The smallest cross-sectional area that will carry the load is 0.0537 in^2 (see Figure 24). The stress concentration factor (SCF) for this particular geometry is 2.0, and was calculated utilizing Equation 4.

$$SCF = \frac{A_{rod}}{A_{min}} \quad 4.$$

Essentially, this indicates that for a given load, the area around the hole will experience at least twice the amount of stress than compared to any other part. Therefore, for a maximum stress of 38 ksi, the maximum force that one rod can handle before breaking is 995.4 lb_f as calculated utilizing Equation 5.

$$F_{max} = \frac{S_{max}}{SCF} \quad 5.$$

Since four stringers will be used, and the max thrust from the motor is known, the factor of safety was calculated to be 9.75, and the results are summarized in Table 13. The size of the

stringers and ribs were determined by creating adequate fastener edge clearance. This is the cause of the high factor of safety.

Table 13: Values for factor of safety calculation

Condition	Values
Max thrust from motor	408 lb _f
A _{rod}	0.1104 in ²
A _{min}	0.0537 in ²
SCF	2.05
F.S.	9.75

In order to reduce structure mass, lightening holes have been added to the design of the ribs. These holes run radially about the structure and are the same diameter as the stringer holes. To ensure that these holes would not compromise the integrity of the structure, a FEA was run using ANSYS (see Figure 25). The maximum and min stresses were found to be 9,220 psi and 82 psi, respectively.

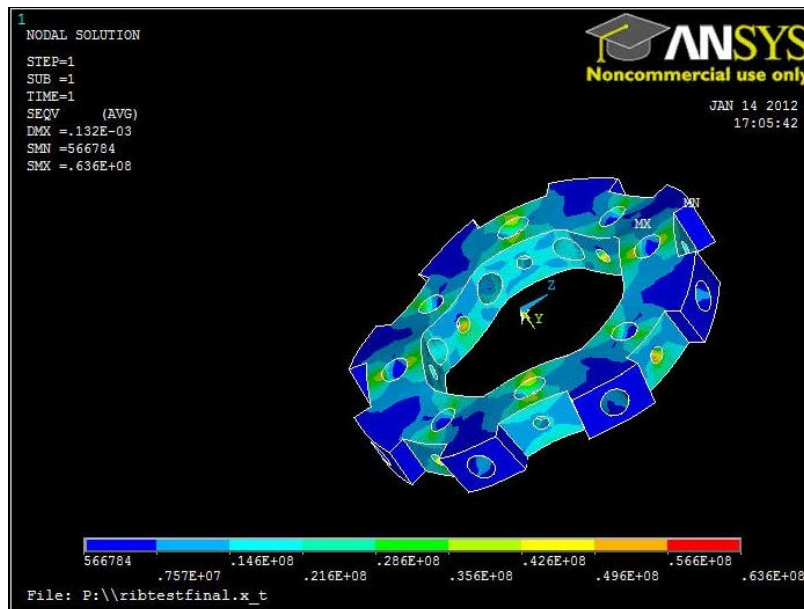


Figure 25: FEA of rib with lightening holes (note that units are in base SI)



The analysis utilized a loading of 684 lbf, which occurs during parachute deployment and is the maximum loading that will act upon the ribs. The factor of safety on the ribs is 4.7 using the maximum loading and a yield stress of 43.5 ksi.

4.5.2. Structure Fabrication and Manufacturing

Because fiberglass is a laminate composite, machining it can be difficult. To simplify manufacturing, the ribs were limited to being 2-D designs. This allows the ribs to be cut from a sheet using a water-jet. Starter holes are drilled in the plate in order to prevent delamination of the G-10 fiberglass when the water-jet pierces the material. The cutting jet can then be traversed from these starter holes to the part. The stringers are cut from lengths of 3/8 inch diameter G-10 rods. They are match drilled to the ribs to create a good fit with the fasteners. To attach the skin, hook and loop fasteners are secured using epoxy to the outer surfaces of the ribs and to the inner surface of the skin. This method was tested on the subscale rocket, Korsakov, to be discussed in Section 6.1

4.5.3. Structure Testing & Results

Testing was performed to ensure a F.S. of 3.0 on the impact energy during launch. The test rig that was used for these tests was designed to complete multiple types of test, such as static and dynamic structural loading – This was done to decrease test costs through the use of a multipurpose test device as shown in Figure 26. The testing device features a rail-mounted impact machine that can hold various amounts of mass and can be lifted to various heights up to five feet for various sized test articles and/or impact energies.



Figure 26: Impact testing rig

Each test consisted of a known mass (3.98 kilograms) being dropped from a known distance, whose energy correlated to a design impulse (I) of 9.35 N*s. This value was determined from the calculated acceleration of the launch vehicle from the OpenRocket vehicle simulation. The height for the mass was derived using conservation of energy in Equation 6, where m_t is the drop mass. Table 14 features the details of the test runs.

$$height = \frac{1}{2} \frac{1}{g} \left(\frac{I}{m_t} \right)^2 \tag{6}$$

Table 14: Impact test runs

<i>Test Number</i>	<i>Impactor mass (kg)</i>	<i>Factor of Safety</i>	<i>Impact Energy (J)</i>	<i>Impactor Height (m)</i>	<i>Impactor Height (in)</i>
1	3.98	1.0	5.23	0.064	11.08
2	3.98	1.5	7.85	0.096	16.62
3	3.98	2.0	10.47	0.128	22.16
4	3.98	2.5	13.08	0.160	27.70
5	3.98	3.0	15.70	0.192	33.24

The test article, which consisted of half of the iMPS structure illustrated in Figure 27, was inspected at various locations after each run, and passed the performance criteria, with only minor damage. The results are listed in Table 15.

Table 15: Testing results matrix, where X signifies damage, P signifies pass.

Fastener location	F.S. = 1.0	F.S. = 1.5	F.S. = 2.0	F.S. = 2.5	F.S. = 3.0
1	p	P	p	p	P
2	P	P	P	P	P
3	P	P	P	P	P
4	P	P	P	P	P
1A	P	P	P	P	X
2A	P	P	P	X	X
3A	P	P	P	X	X
4A	P	P	P	P	P
5	P	P	P	P	P
6	P	P	P	P	P
7	P	P	P	P	P
8	P	p	P	P	P



Figure 27: iMPS structure test article

The damage was very minor and featured discoloration from compression of the fiberglass at the faster locations in the stringers, but no fracturing occurred as seen in Figure 28.

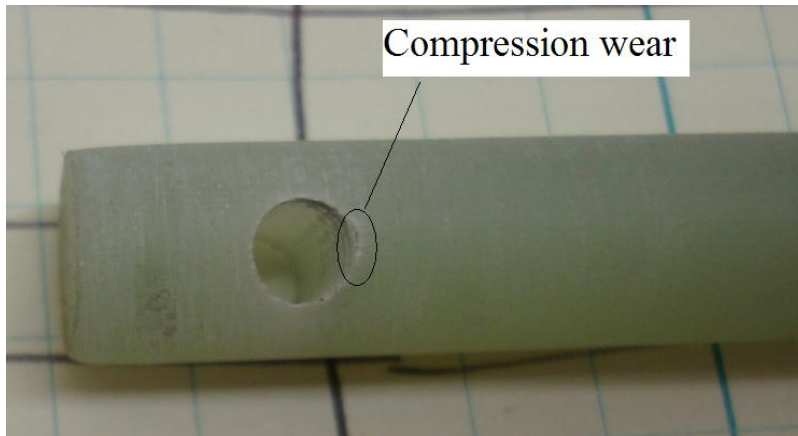


Figure 28: Evidence of minor compression damage occurring at F.S = 2.5

An internal review for this novel structural design was held to decide to continue with this option. Future testing will include full scale impact testing using a payload mass simulator.

4.6. Vespula Mass Breakdown

Mass breakdown for each subsystems are summarized in Table 16 and

Table 17 with the systems level summary shown in Table 18. The values obtained for the booster section were estimated utilizing Solidworks. However, since material properties were entered manually, the estimated weight is fairly accurate. The values for the nose cone, drogue chute, main chute, shock cords, iMPS structures, and motor case are weights obtained from a scale. Additionally, the mass breakdown is also presented in terms of mass fractions, as illustrated in Figure 29.

Finally, a complete CAD model of Vespula with dimensions is shown in Figure 30.

Table 16: iMPS component weight

<i>Payload Section</i>	<i>Weight (lbs)</i>	<i>Quantity</i>	<i>Total Weight (lbs)</i>
G10 Fiberglass Ribs	0.42	4	1.69
Fiberglass Stringers	0.11	12	1.32
1" bolts	0.004	24	0.105
Hook and loop fasteners	0.004	32	0.141
Skin	0.1	1	0.1
Total			3.27

Table 17: Booster Section Weight Budget

<i>Booster Section</i>	<i>Weight (lbs)</i>	<i>Quantity</i>	<i>Total Weight (lbs)</i>
Mounting Rod	0.10	4	0.40
Cardboard Tube	0.06	1	0.06
Fin Centering Ring	0.07	1	0.07
Empty Motor Casing	2.60	1	2.60
Skin	0.1	1	0.1
Fin	0.20	3	0.6
Rear Plate	0.28	1	0.28
Rear Cap	0.16	1	0.16
Thrust Plate	0.21	1	0.21
Booster fiberglass tube (6")	0.42	1	0.42
TC Centering Ring	0.01	1	0.01
L-Brackets	0.01	7	.07
Bolts	0.002	4	0.009
Nuts	0.011	26	0.286
Total			5.276

Table 18: Subsection Mass Break

<i>Component</i>	<i>Weight (lbs)</i>
Nose Cone	1.61
Drogue Chute + Shock Cords	1.50
Main Chute + Shock Cords	2.30
Avionics System	5.00
Allotted Payload	10.0
Payload & Recovery Structure	5.42
Booster Structure	6.18
AeroTech L1390 at launch	8.55
Contingency Mass	1.0
Total	40.7

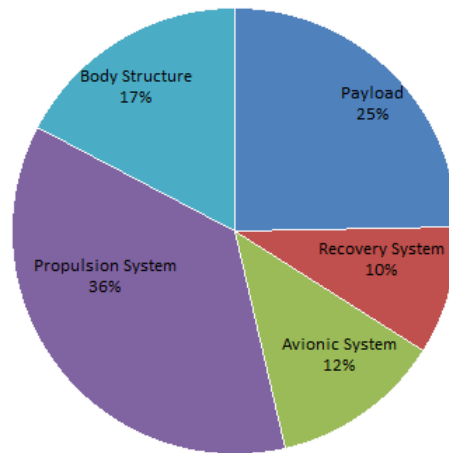


Figure 29: Mass Fraction for Vespula

4.7. Vespula Overall Dimension

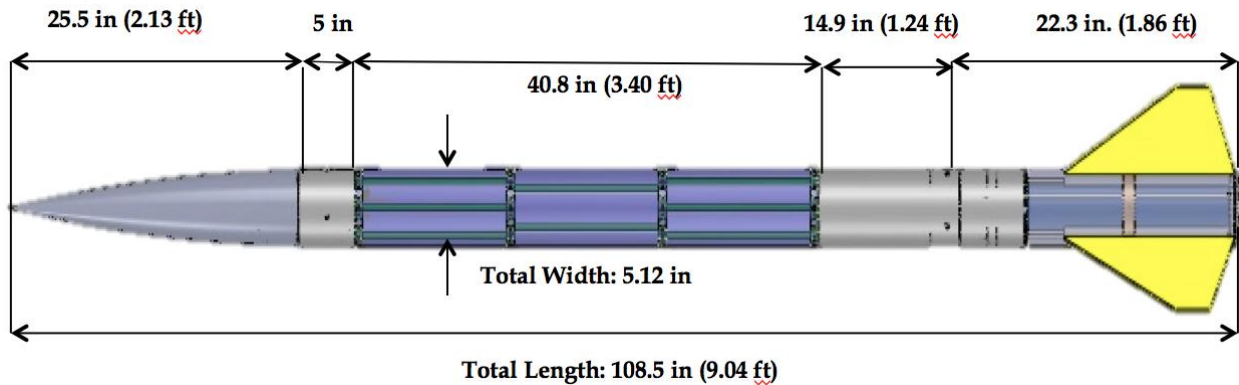


Figure 30: Dimensions for Vespula

5. Launch Vehicle Performance Predictions

Current mission performance predictions are based on a worst case scenario assuming a launch vehicle mass of approximately 41 pounds and an AeroTech L1390G launch vehicle motor. As the payload is finalized, mission performance predictions will be updated to reflect a more accurate mass and appropriate motor selection.

For the launch vehicle to fly along the predicted trajectory, the launch vehicle must leave the launch rail at a certain velocity. For the preliminary launch vehicle design, the launch vehicle becomes stable, with a stability margin caliber of 1, at 47 ft/s, which occurs at 60 inches up the launch rail. Thus so long as our launch rail is at least 97 inches, the launch vehicle will be stable when the rail buttons leave the guide rail. 97 inches leaves 60 inches to reach stability plus the necessary distance between rail buttons, which is 37 inches. The current launch pad is the Apogee “Gun Turret” Pad. The system consists of a rail and a base. Altogether the system costs roughly \$500.00. The rail is a T-slot aluminum extrusion of approximately eight ft in length and satisfies the distance required for the launch vehicle to reach an acceptable static stability margin. Depending on budgetary constraints, we may build our own launch pad to reduce cost. Table 19 takes a range of possible launch weights, without motor, for the launch vehicle and an optimal motor selection for each weight.

Table 19: Best motor per launch vehicle weight and altitude reached.
The highlighted row represents the design point.

<i>Total Weight without Motor (lbs)</i>	<i>Total Weight with Motor (lbs)</i>	<i>Motor Required</i>	<i>Apogee (ft)</i>
28.0	36.0	AeroTech L1150R-P	5242
30.0	38.0	AeroTech L850W-P	5253
32.0	40.0	AeroTech L1520T-PS	5170
32.0	40.5	AeroTech L1390G-P	5315
33.0	41.5	AeroTech L1390G-P	5259

All simulations utilized the highest gross launch weight on the chart and the corresponding motor selection. The assumptions for all simulations are listed in Table 20,

Table 20: Flight Simulation Conditions

<i>Condition</i>	<i>Value</i>
Windspeed	5 mph
Temperature	60.8 ⁰ F
Latitude	34 ⁰ N
Pressure	14.7 psi
Gross launch weight	41.5 lb
Motor	Aerotech 1390G-P

5.1. Flight Simulation

Figure 31 shows the flight profile of the launch vehicle utilizing flight simulation conditions from Table 20. Velocity, altitude, and acceleration were plotted as a function of time. Apogee occurs at approximately 19 seconds at an altitude of 5315 ft. At apogee, the ejection charge for the drogue chute will fire; slowing the decent rate to 80 ft/s. Deployment of the main chute will occur at 450 feet above ground level to further decelerate the launch vehicle to 14 ft/s. The entire flight duration is approximately 110 seconds.

Simulated flight
Vertical motion vs. time

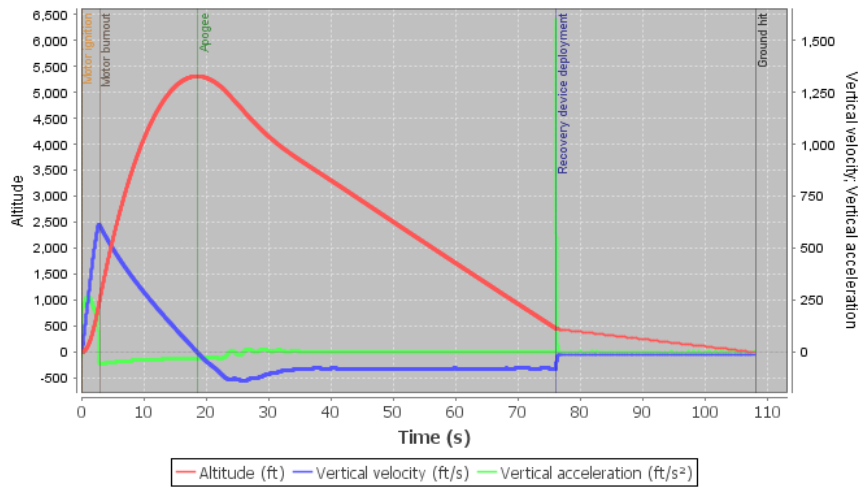


Figure 31: Flight profile with AeroTech L1390 motor for a total takeoff weight of 41.5 pounds

5.2. AeroTech L1390G-P Simulated Thrust Curve

The simulated thrust curve for Aerotech L1390G-P is shown in Figure 32. It is the optimum projected motor for the preliminary launch vehicle to reach an altitude of 5,280 feet. The motor will follow this thrust curve closely, however it is important to keep in mind that the performance of the motor may vary slightly in actual flight.

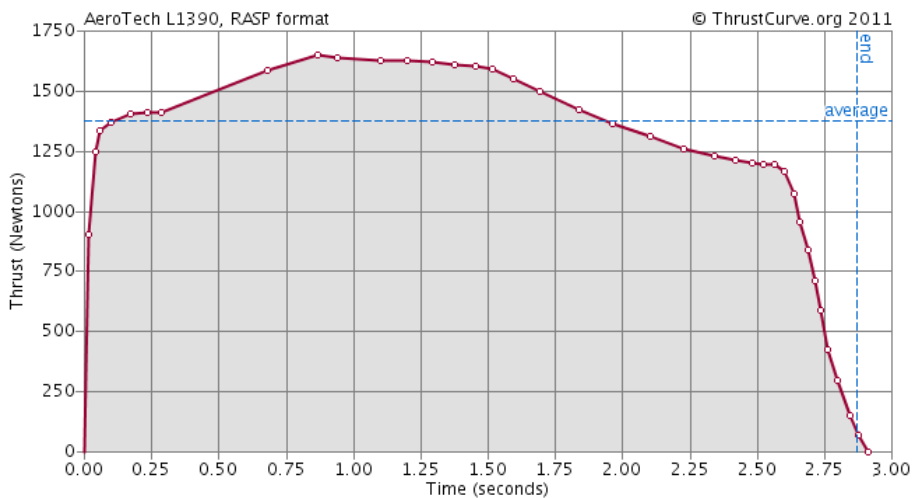


Figure 32: Thrust curve for Aerotech L1390 motor

5.3. Stability Margin

In addition, a stability analysis was performed to ensure a safe flight profile as shown in Figure 33. The stability margin of our launch vehicle during most of the flight is four calibers, where one caliber is the maximum body diameter of the launch vehicle. This is higher than the general rule of thumb among model rocketeers that the C_P should be one to two calibers aft of the C_G . However, being over-stable is not bad; it simply means that the launch vehicle will have a greater tendency to weathercock if there is any wind at launch. To counter this, our launch rod will be at least 97 inches long to ensure stability when the rail buttons leave the guide rail as mentioned previously; additional length will be added to prevent weathercock.

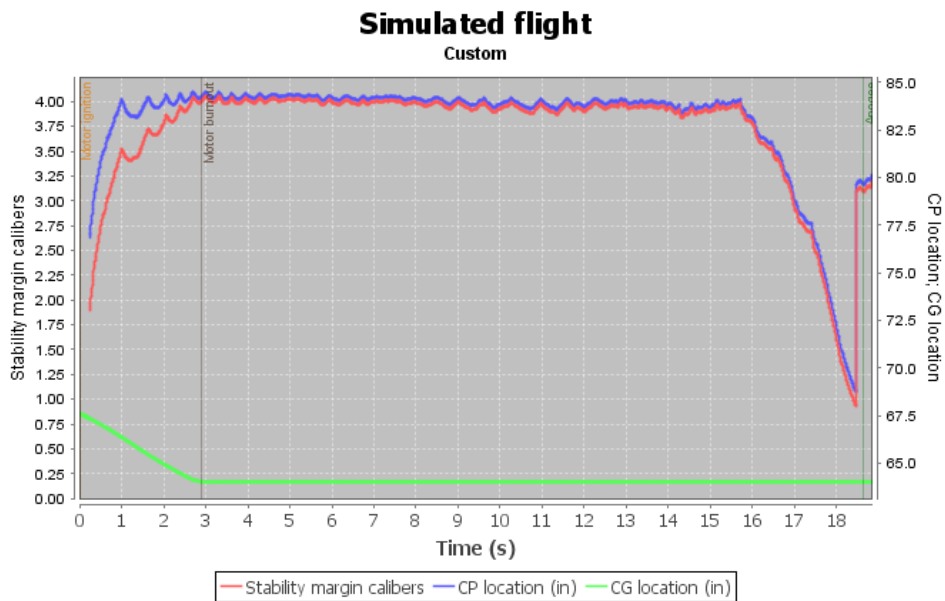


Figure 33: Stability margin calibers vs. Time

5.4. Drift Profile Simulation

The effect of wind speeds on launch vehicle apogee is clearly demonstrated in Figure 34. The green curve illustrates our simulation data, the red triangles are to better assist the reader to visualize apogees reached at wind speeds of 0, 5, 10, 15 and 20 MPH. As illustrated, there is a monotonic relationship between wind speed and apogee; the higher the wind speed, the lower the apogee. This is fundamentally due to a horizontal force created by the wind, which ultimately alters the angle of attack of the launch vehicle, and thus a lower apogee.

In addition, the rocket must be recoverable within 2,500 ft of the launch pad in a 15 mph head wind. The plot of lateral distance during the flight into a 15 mph headwind is shown in Figure 34. Here it is seen that the vehicle will land approximately 1,300 ft from the launch pad.

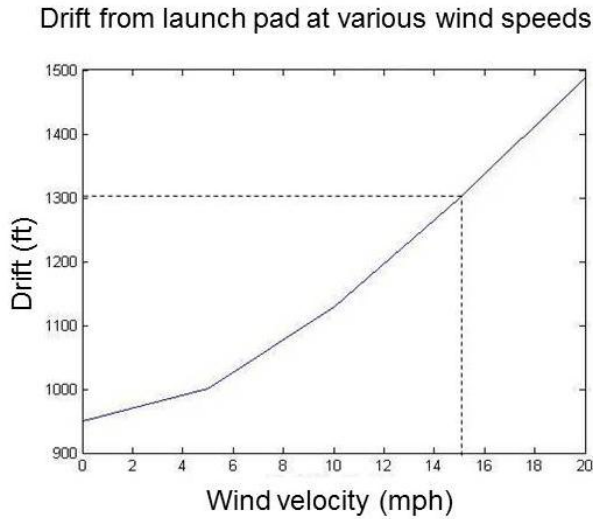


Figure 34: Drift from launch pad at various wind speeds

5.5. Kinetic Energy Upon Landing

The kinetic energy at landing for each independent and tethered section of Vespula was calculated utilizing Equation 7 where m is the mass of each section and v is the velocity. The results are summarized in Table 21.

$$KE = \frac{1}{2}mv^2 \tag{7}$$

Table 21: Kinetic energy upon landing for each section of Vespula

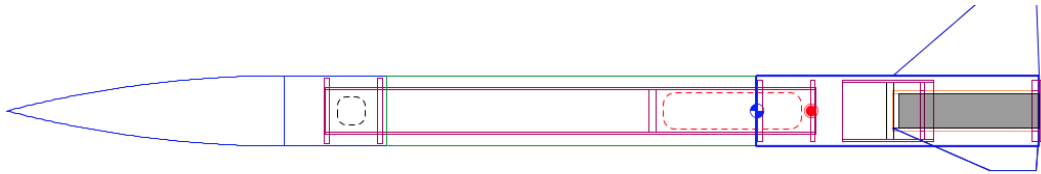
	Mass (lbs)	Velocity (ft/sec)	KE (ft-lb)	KE Margin (ft-lb)
Nose Cone	1.610	15	8.12	89.2 %
Booster Section	10.62	15	37.13	50.5 %
Payload Section	20.42	15	71.4	4.8 %

6. Launch Vehicle Testing

6.1. Subscale Testing

A subscale flight test will be performed prior to CDR to determine the feasibility of specific aspects of our design. This testing primarily focuses on the performance of our exterior skin covering the booster and payload section during flight. The basic design of our subscale launch vehicle, to be called “Korsakov” features a smaller diameter body tube, which is covered by a non-load bearing, thin-walled skin (Figure 35). Korsakov will utilize two 0.5 inch diameter launch lugs, with one placed on the top section and one on the bottom. The launch lugs will be two inches long and epoxied onto the sides. The thrust will transfer through the internal cardboard tube from the booster section to the nose cone. Due to the configuration of the launch vehicle, a dummy mass of 0.3 pounds was added beneath the nose cone to provide a stability margin of around 3.25 calibers for most of the flight (see Figure 36). The characteristics of Korsakov are summarized in

Table 22.



(a)



(b)

Figure 35: Korsakov (a) layout and (b) flight vehicle

Table 22: Characteristics of Korsakov vehicle

Condition	Value
Length	55.5 inches
Outer Diameter	3 inches
Motor	Aerotech H128
Max Mach Number	0.44

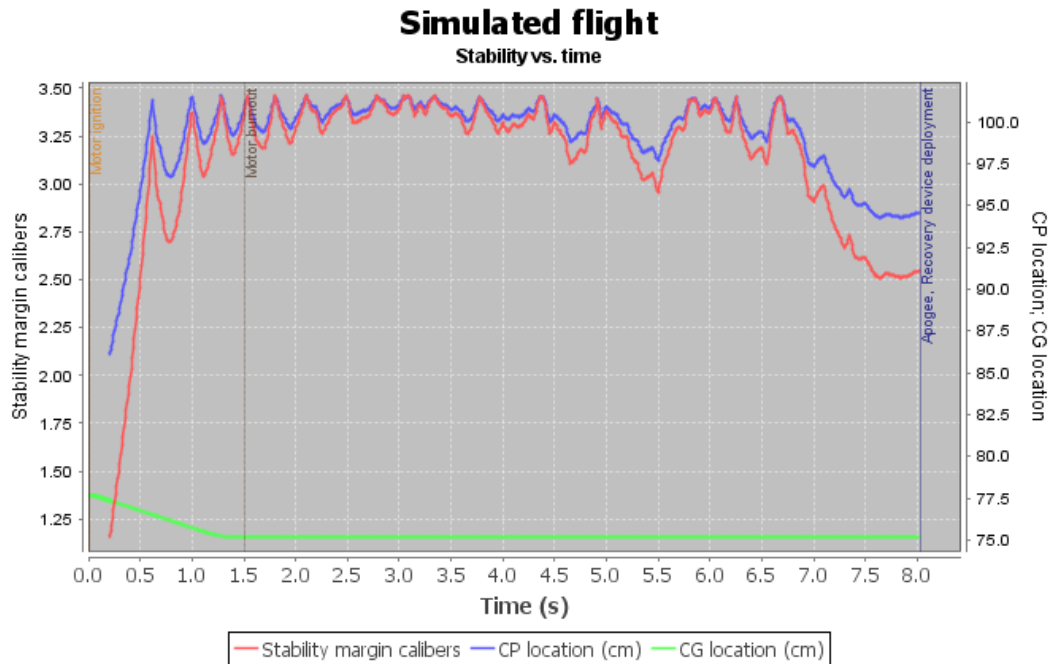


Figure 36: Stability profile for Korsakov vehicle.

Table 23 shows all the materials required for building Korsakov with a total cost of \$165.28 and the total weight was found to be 3.4 lb_f.

Table 23: Material and cost for Korsakov

<i>Item</i>	<i>Use</i>	<i>Cost (\$)</i>
Motor reload kit	Launch vehicle motor	31.99
Airframe Tube 74/18 (Thin Wall 3" tube)	Main body	20.57
Airframe Tube 29/13	Inner body	8.790
Airframe Tube 56/18 (Estes BT-70 size)	Motor tube	11.52
Baltic Birch Plywood 6mm-1/4" x 24" x 30"	Fins	8.99
1/4" plywood	Centering rings	10.00
U-bolts	Recovery	2.000
Poster board	Skin	4.990
Hook and Loop fasteners	Skin fasteners	14.58
Parachute	Recovery	33.00
Nose cone	Aerodynamics	18.85
Total		165.28

Unfortunately, Korsakov landed in a tree and was unrecoverable. Therefore, the actual loading on the skin from the onboard accelerometers could not be retrieved. However, upon visual inspection of the rocket, the skin remained intact throughout the flight and landing. In conclusion, the test was considered a success and the skin and hook and loop fasteners are rated for the flight characteristics predicted by the OpenRocket simulation as seen in Figure 37.

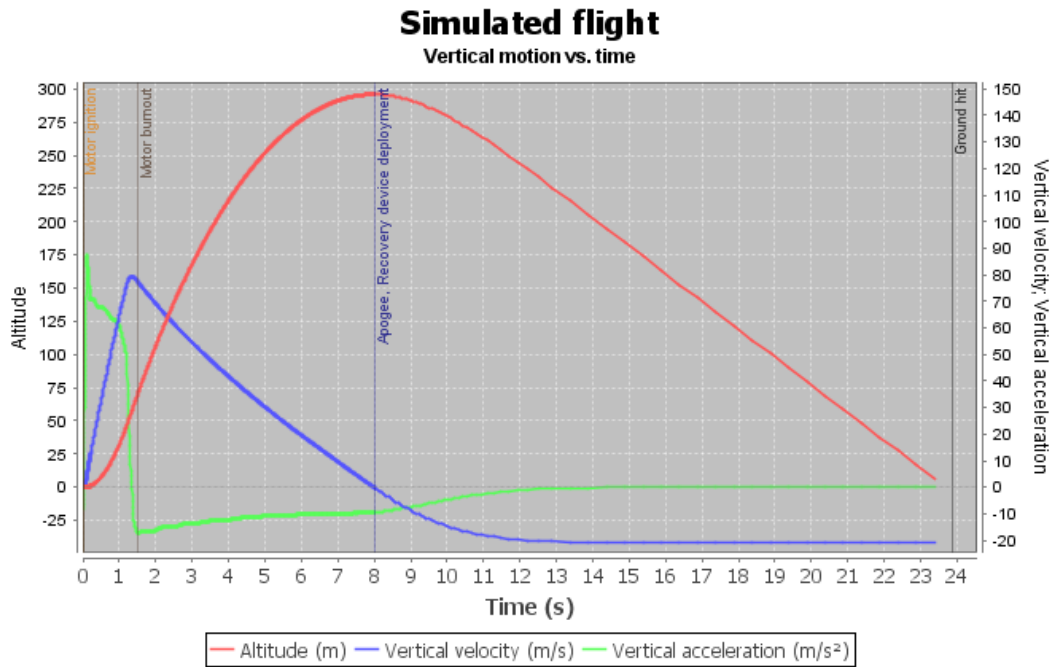


Figure 37: Korskakov Flight Profile as predicted by OpenRocket

In the 25 mph gusting winds of North Georgia, OpenRocket predicted a drift of 1,800 ft (Figure 38), when in reality, Korskakov landed in the trees approximately 1,970 ft from the launch pad (Figure 39). This supports that OpenRocket’s drift calculations are within approximately 10% of test data.

Simulated flight
Custom

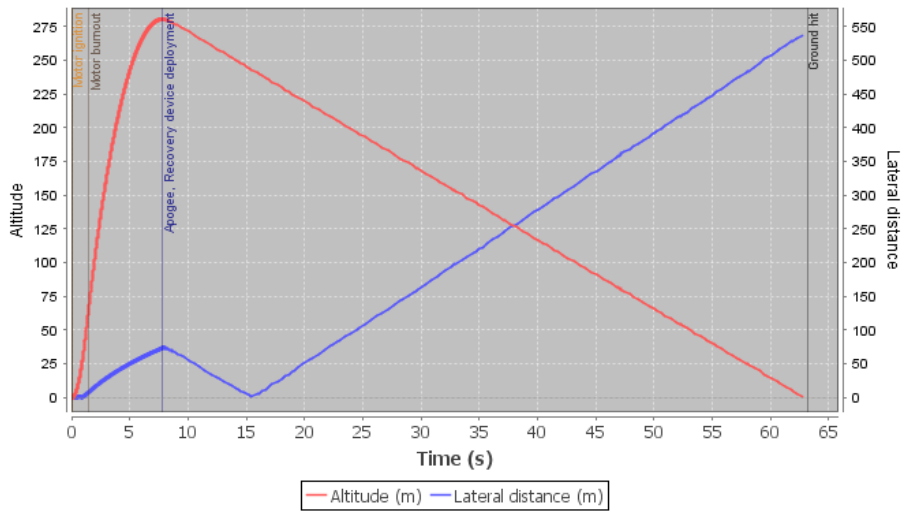


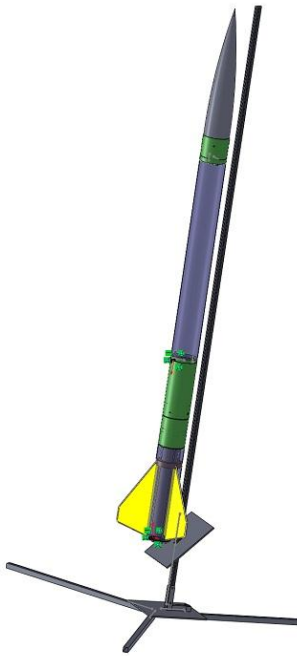
Figure 38: Korsakov Predicted Drift Profile



Figure 39: Korsakov Drift Distance

7. Launch System and Platform

As mentioned previously, the launch system that is showing the most promise is the Apogee “Gun Turret” Pad (Figure 40). The system consists of the “rail” and the base. Altogether the system costs \$500.00. The rail is a T-Slot aluminum extrusion of approximately 8 feet in length and satisfies the requirements of the distance required for our launch vehicle to reach an acceptable static stability margin. The blast deflection pad is angled with the dimensions 9 x 9 x 0.25 inches, and is made of heavy-gauge steel. The rail and the deflection pad are attached to the head of the base, which can pivot horizontally for easy loading of launch vehicles. Three legs with leveling screws are attached to the base so that the launch angle can be adjusted to desired conditions, with all parts also being constructed from heavy-gauge steel. The entire system weighs roughly 30 approximately pounds; and is collapsible for transportation.



Our launch vehicle will have two rail buttons attached in such a way that they do not interfere structurally with any other components. The rail buttons slide into T-shaped aluminum extrusion and limit the launch vehicle’s motion except in the desired launch direction. The first button will be attached to the thrust plate in the booster section, where there is a pre-existing attachment interface with minimal structural interference. The second button will be attached to the rear thrust retention plate. This will ensure that both buttons will be on the rail for enough time to reach an acceptable static stability margin upon launch.

The launch procedure checklist is presented in Appendix II.

Figure 40: Vespula on Launch Pad

8. Payload

8.1. Introduction to the Experiment and Payload Concept Features & Definition

8.1.1. Motivations

Today, many entrepreneurs are beginning to build newer and more cost-effective launch vehicles. Every one of these launch vehicles must address a specific challenge in their design process: integration with the spacecraft payload. This integration presents difficulties in launch vehicle design because harmonic oscillations of the spacecraft mass could cause structural damage to either the launch vehicle or the spacecraft itself. To solve this dilemma, industry typically utilizes large mechanical springs – in addition to the placement of certain structural constraints on the payload spacecraft for use of a particular launch vehicle. Repeated deformation on vibration dampers and springs used in launch vehicles presents a further issue in providing reusability, as these parts must be intermittently replaced. Furthermore, modifications must be made to both payload and launch vehicle to tune the natural frequencies of both and prevent harmful oscillation. The net result of the present situation is an increase in overall structural mass, which combined with the necessary increase in fuel required and maintenance, dramatically increases the launch cost to the detriment of mission capability. The Mile High Yellow Jackets intend to provide a possible alternative solution in a demonstration of the ability of electromagnetic levitation to lower the necessary structural masses currently required to prevent harmonic oscillation, decreasing launch cost.

8.1.2. Scientific Merit

The problem of magnetic force interactions from n-solenoids on a single sample is a non-trivial problem in electromagnetics. The difficulty in describing complex field relationships is similar to the difficulty in aerodynamics for describing complex fluid flows, and many of the computational techniques are similar. However, due to the nature of the complexity, the study of complex magnetic interactions must be a data-driven process, as in aerodynamics. The A.P.E.S. system will depend upon a theory-informed, data-driven model for control. This data will be generated through a series of ground test experiments that gradual increase the complexity of the

problem. Final model testing on the ground will involve only permanent magnets and solenoids, simplifying the force interactions to compensate for complex geometry.

The A.P.E.S. project may be considered as a dual scientific-engineering payload. A period of scientific analysis is necessary, as stated above. However, the actual product flown in the launch vehicle will be flown for verification and validation purposes after the conclusion of ground testing; the flight will test the performance of the derived model, and engineering design, during the dynamics of the ascent phase. This process of scientific investigation followed by engineering development is not entirely unlike the development of experimental aircraft and spacecraft, where some scientific investigation may be needed before the engineering can proceed.

8.2. Success Criteria

A fully successful launch of the A.P.E.S. system will demonstrate a capability to respond and dampen impulses delivered to the levitated platform from the launch vehicle during ascent. Namely, the platform shall, ideally, not touch any other A.P.E.S. components during ascent. However, failure to achieve total isolation of the platform is only a partial failure, as conditions during launch could lead to unforeseen perturbations of the launch vehicle. Any failure to levitate the platform, dampen motion, shutdown, or start up, would be a critical failure. Specified preliminary success criteria are given in Table 24: Success Criteria. An attempt has been made to provide a reasonable goal for system performance before any physical testing has begun. It is not certain whether it will be possible to provide the same level of control for many disturbances.

Table 24: Success Criteria

<i>Success Criteria</i>	
The A.P.E.S. system shall be successful if	
1	For an impulse response the system shall have a 2% settling time of less than 0.5 seconds
2	And for the flight of the launch vehicle that the platform should not touch other components of the A.P.E.S. system.

8.3. Experimental Requirements and Objectives

Included within the Mile High Yellow Jackets terminology of “Flight Systems” is included all avionics and experimental material necessary for a successful mission. Therefore, the Flight Systems group must deliver based on two sets of functional requirements. Requirements for A.P.E.S. are detailed in Table 25. These four basic requirements have been updated for functionality from those originally listed in the proposal and all elements necessary to the smooth operation of the experiment are tied to these requirements.

Table 25: A.P.E.S. system requirements

<i>Requirement Number</i>	<i>Requirement Definition</i>	<i>Verification Method</i>	<i>Status</i>	<i>Verification Reference</i>
1	A platform shall be levitating without rotation during the ascent of the launch vehicle and coordinate data provided through optical and infrared sensing.	Ground Testing	In progress	
2	All elements of the A.P.E.S. system shall weigh no more than 10 pounds total, including all hardware and electronics in direct support of the A.P.E.S. system.	Analysis	In progress	
3	The A.P.E.S. system must actively correct for accelerations of the launch vehicle.	Ground Testing	Not started	
4	The A.P.E.S. system must shut down at apogee.	Ground Testing	Not started	

There are several options available to Flight Systems to satisfy the functional requirements. The use of the word “platform” is necessarily open-ended as the team investigates several types of platforms. Ground testing requirements necessitate that several platform configurations be used

to formulate the final system model. Table 26 outlines some of the ground testing objectives for A.P.E.S.

Table 26: A.P.E.S. ground testing objectives

<i>Goal Number</i>	<i>Goal Definition</i>
1	Ground testing should develop a data-driven model for the interaction of ferromagnetic materials and permanent magnets in one-, two-, and three-dimensional dynamical systems of magnetic fields.
2	Ground testing should test the feasibility of de-scope and full flight designs.
3	Ground testing should provide the computational basis for control of the A.P.E.S. system during ascent of the launch vehicle.

If ground testing results are successful and combined with a thorough theoretical understanding of the phenomena involved in dynamic magnetic fields, ground testing will enhance the ability of Flight Systems to successfully accomplish the most important objective of the A.P.E.S. system –

– that the A.P.E.S. platform shall not touch any part of the container during the ascent phase.

Optical sensing of the visible spectrum will serve to inform the control system of the location of the platform. A full flight model – illustrated in a section view in Figure 41 – would include a series of concentric cylinders, wherein the center cylinder would contain permanent neodymium magnets and a platform, while the inner cylinder would store solenoids and a CMOS camera for optical detection of fiducial markers.

8.4. Experiment Overview

8.4.1. Hypothesis and Premise

The premise of the experiment is that –

If a platform can be levitated and stabilized in a dynamic magnetic field during the flight of a launch vehicle, then greater stability and lower structural mass may be achieved.

The payload will utilize dynamic three-dimensional magnetic fields to create an Active Platform Electromagnetic Stabilization, or A.P.E.S., system for use during the ascent phase of the launch vehicle's trajectory. The launch vehicle ascent will provide a high vibrational intensity environment in which to test the stabilization system. Two further premises are necessary for this A.P.E.S. system, namely:

- 1. Under appropriate conditions, it is possible to control complex oscillating magnetic fields such that a system of ferromagnetic materials or permanent magnets may be levitated in non-rotational stability.*
- 2. A design exists such that a platform of some size and low mass may be levitated using ferromagnetic materials or permanent magnets.*

Therefore, after completing a thorough analysis of the dynamics of materials being levitated and stabilized in magnetic fields, the Mile High Yellow Jackets will implement a design to apply this science to a platform within the Vespula launch vehicle.

8.4.1. Experimental Method and Relevance of Data

The parameters to be measured in the experiment are the coordinates of the position of a test sample – in the case of ground testing – and the coordinates of the platform for the ascent of the launch vehicle. To ensure full implementation of the scientific method, the experiments will be carried out such that the results are controlled by comparison – i.e. a series of tests of increasing complexity will be conducted such that the control theory of the A.P.E.S. system is constructed methodically. Analysis of optical and infrared data will provide Cartesian coordinates, which, in a known design, can be used to specify the position and displacements of the platform, defining all kinematics to a level of accuracy proportional to the sample and computational rates of the data acquisition system. This data provides an empirical basis for confirmation or rejection of an experimental hypothesis – a newly written control program can be considered as a hypothesis – and for the improvement of the system as a whole.

8.4.2. Ground Test Plan

Ground testing will serve two general purposes: (1) the development of data algorithms and control laws, and (2) the verification and validation of theory and control systems. By understanding and modeling the kinematics of a sample plate driven by dynamic magnetic fields, steady-state models can be formed allowing for stable non-rotating levitation with oscillation dampening. The testing process will ramp the complexity of the model, beginning with simple 1-dimensional tests, and increasing the number of solenoids and dimensions until a 3-dimensional multi-solenoid model has been created. Data collected from ground testing will directly inform the control of the flight A.P.E.S. system design. The flight design is depicted in Figure 41, and the ground test platform design is illustrated in Figure 42. See Appendix III for specific details on the Ground Testing Plan.



Figure 41: Section view of the proposed flight model of the A.P.E.S. system



Figure 42: The A.P.E.S. system ground test platform

8.5. Ground Testing

Using the equations developed in the Modeling General Magnetic Fields, section XXX, the solenoid parameters NI were back solved for to 260 Ampere-Turns. The current was restricted to 80% of maximum allowable for the wire 0.86 Amperes and the solenoid was then constructed using a jig to wind 300 turns. Maximum field strength when run the solenoid was run at full current achieved over 1100 μ T. Using the 3-axis AKM 8975 magnetic field sensor, the field strength in the X-direction was tested at several currents and distances as per the Ground Test Plan. The results are illustrated in Figure 43.

Furthermore, in order to determine the field strength in the X-direction for any given position and current setting within the range tested, a Response Surface Equation (RSE) was created. The Response Surface is illustrated in Figure 44. The resulting RSE has the form of

$$\ln(B_x) = b_0 + \sum_{i=1}^n b_i X_i A_i + H.O.T. \quad 8.$$

where b_0 is the intercept, b_i is the coefficient of the i^{th} term, X is the position within the range tested and A_i is the current within the range specified. The resulting RSE is listed in Table 27.

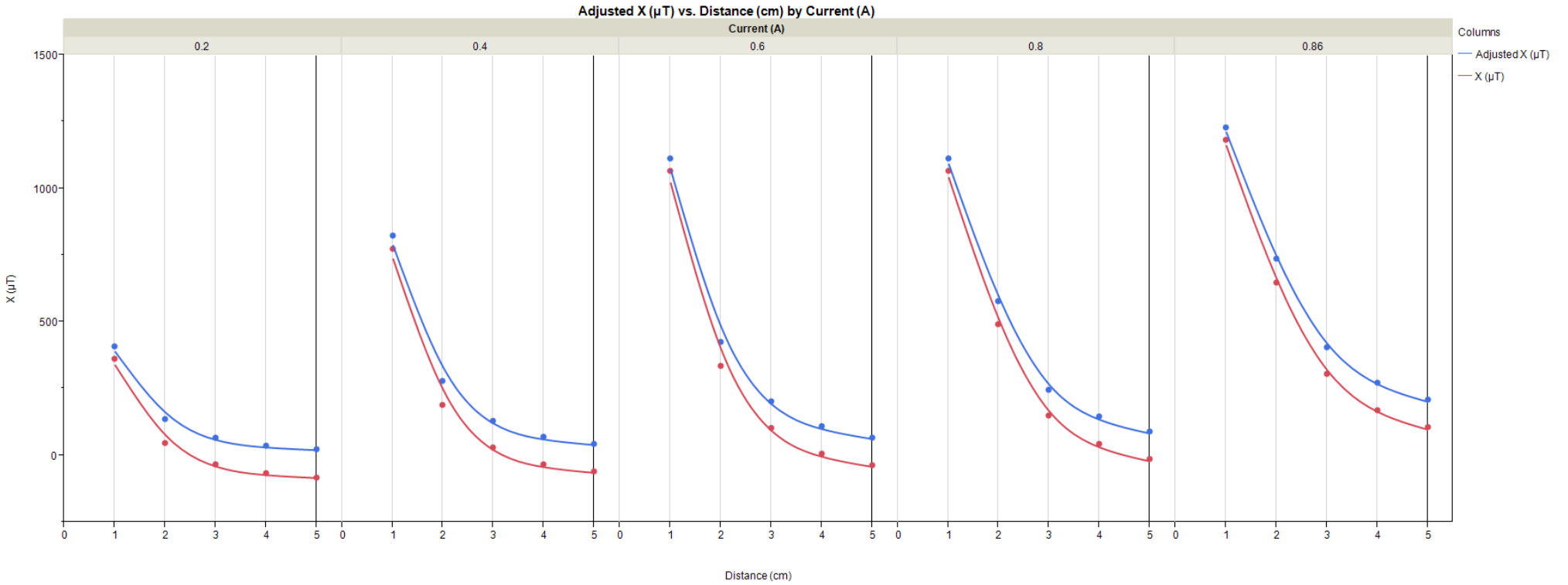


Figure 43. Field Strength in the X-Direction of the solenoid vs. radial distance at various current settings.

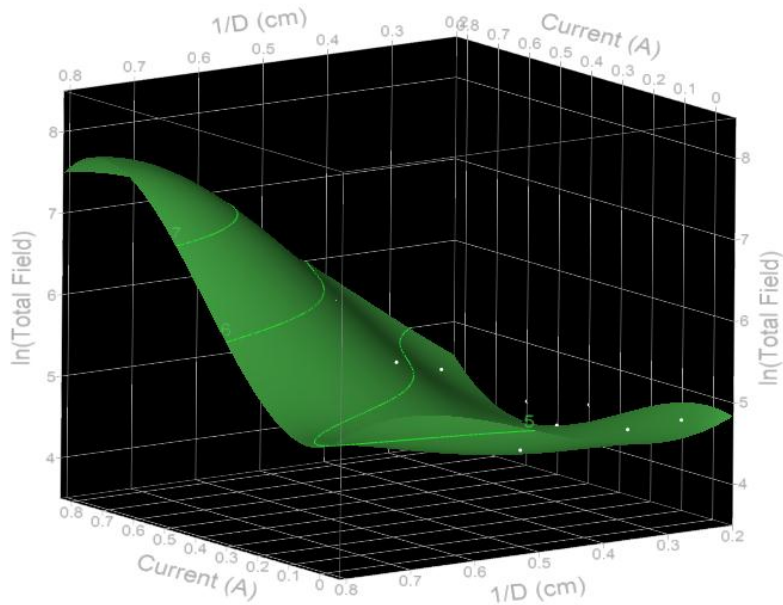


Figure 44. Response Surface of the field strength in the X-Direction.

Table 27. RSE coefficients and terms

Term	Estimate	Std Error	t Ratio	Prob> t
b_0	2.81755501	0.59373639	4.74546459	0.00021945
A	-1.4251419	1.04427097	1.36472423	0.19122614
X	-5.37987105	4.39097585	-1.2252108	0.23822696
X*X	10.8426075	9.35256543	1.15931908	0.26333572
X*X*X	-6.36499083	5.58455774	1.13974841	0.27116687
A*X	17.1758472	11.1812302	1.53613215	0.14404375
A*X*X	-57.4138468	33.6670109	1.70534435	0.10746498
A*X*X*X	46.1097665	23.8093525	1.93662413	0.07065691
A*A*X*X*X	-170.759236	65.1181151	2.62230004	0.0184835
A*A*X*X	218.596471	88.1941886	2.47858135	0.02471551
A*A*X	-53.8621328	24.275883	2.21875072	0.04131437
A*A*A*X*X*X	142.367636	50.1506082	2.83880178	0.01185239
A*A*A*X*X	-190.6841	67.9226079	2.80737307	0.01264749
A*A*A*X	51.1175767	18.696031	2.73414056	0.01470551

9. Flight Systems

9.1. Flight Avionics

9.1.1. Overview and Requirements

To successfully complete the USLI mission, flight systems is further responsible for providing a fully functional flight computer system. Avionics is the second subsystem of Flight Systems, responsible for data acquisition, experimental control, recovery electronics, and features necessary as per the USLI Handbook. Avionics requirements are listed in Table 28.

9.1.2. Requirements and Products

Two major products of the Avionics subsystem are the flight computer and the experiment computer for A.P.E.S as detailed in Figure 45. The flight computer interfaces with all sensors not directly involved with A.P.E.S. and controls most sensing, logging, and telemetry for the launch vehicle. The A.P.E.S. computer focuses entirely on the control of the A.P.E.S. system.

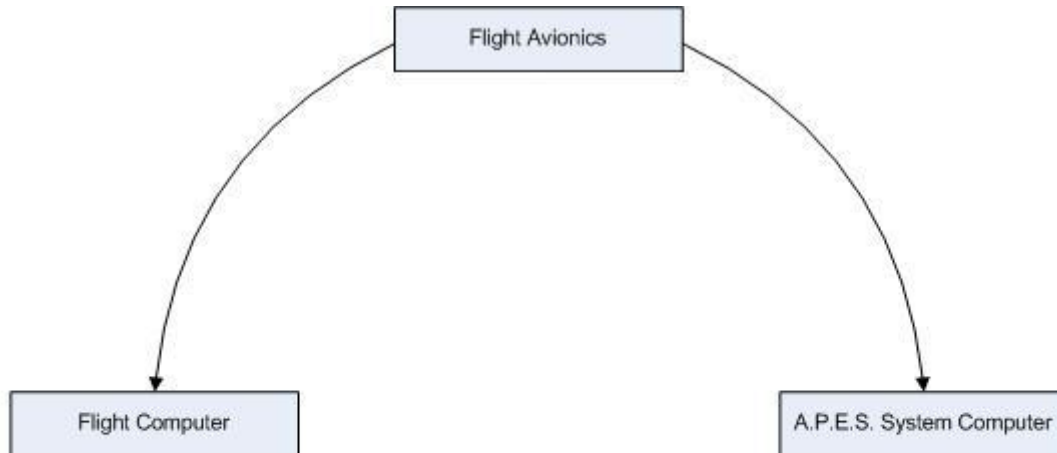


Figure 45: General products of Flight Avionics

The A.P.E.S. computer will calculate the position of the platform and control the solenoids in order to change the magnetic field and stabilize the platform. Independent computing systems

provides modularity for ease of implementation and debugging. The methodology for component selection shall include consideration of clock speed, I/O, and voltage requirements. Electromagnetic interference will be shielded by a Faraday cage. The system will incorporate redundancy to tolerate the loss of one or more sensors and/or communication lines.

Table 28: Flight Avionics Requirements

<i>Requirement Number</i>	<i>Requirement Definition</i>	<i>Verification Method</i>	<i>Status</i>	<i>Verification Reference</i>
1	The avionics shall be a thoroughly tested custom design.	Based on fulfillment of other avionics requirements	In Progress	Fig. 37
2	The flight computer shall be based off of the ATMEGA 2560 chip.	Inspection	Completed	Fig. 37
3	The A.P.E.S. computer shall be able to perform real-time image processing	Ground Testing	In Progress	
4	The flight avionics shall collect data on acceleration, altitude, and data necessary to the A.P.E.S. payload and execute the A.P.E.S. control laws.	Ground testing and drop testing of all sensors, logging of data and transmission to A.P.E.S. computer	In progress	
5	Key elements of the flight systems shall operate on independent power supplies.	Ground testing will utilize independent power supplies	In progress	
6	Power supplies should allow for successful payload operation during launch vehicle flight with up to 1 hour of wait on the launch pad and 2 hours of wait during launch vehicle preparation.	Two methods: calculate max current draw of all devices over the given time and ensure below maximum. Also have a dry run with sensors and A.P.E.S. running for given time on charged batteries.	In progress	
7	The flight avionics, with the exception of the recovery avionics, shall begin at launch and these systems should be capable of being armed externally to the launch vehicle structure.	Arming screws shall be a component of ground testing.	Not started	

<i>Requirement Number</i>	<i>Requirement Definition</i>	<i>Verification Method</i>	<i>Status</i>	<i>Verification Reference</i>
8	The avionics should provide for the communication of ground location to base station for recovery.	Communication with XBees will be tested at a maximum predicted distance and verified to work.	In progress	
10	GPS coordinates of all independent launch vehicle sections shall be transmitted to a base station.	Communications Ground Testing	In progress	
11	The recovery avionics and system shall be separate from the main flight avionics.	Design verification and ground testing.	In progress	
12	The base stations shall be capable of receiving and displaying data transmitted from on board the launch vehicle.	To be verified during ground communications test.	In progress	

9.1.3. Flight Computer

The flight computer will run the ATMEGA 2560AU processor with the Arduino bootloader and other necessary components for ease of programming. The chip has sufficient I2C, serial, and analog inputs to read data from all sensors and log to an SD card based on Sparkfun's OpenLog break-out board. Additionally, the chip will run the Fastrax UP501 GPS module and send the data to an Xbee PRO for transmission to the ground station. An OpenLog board will provide logging capabilities. The chip will be programmed in the Arduino language, a subset of C++ with some additional libraries. Figure 46 provides a generalization of proposed flight computer software.

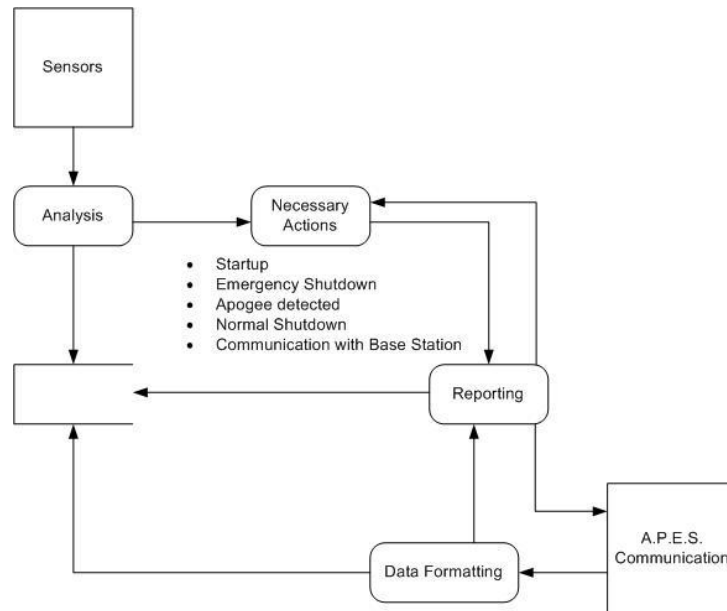


Figure 46: Generalization of flight computer software

The flight computer must accomplish several tasks and handle multiple responsibilities. The main goal of this system is to collect and monitor all the relevant data from the environment around it such as the strain on the launch vehicle, environmental factors such as temperature, stray magnetic flux from the A.P.E.S system, launch vehicle acceleration, and GPS position. During flight, the flight computer must also monitor the payload's control system and data through a serial bus and provide an emergency secondary disengage for the A.P.E.S. system in the case of a necessary emergency shutdown. During flight the avionics will log all data to a SD card. Solid state memory should allow recovery of flight data if a recoverable failure occurs. Post-recovery, the flight computer must switch to location and communication systems to transmit a GPS signal through the telemetry system to the ground station. and Table 29 provide the current proposed flight computer schematic and major components, respectively.

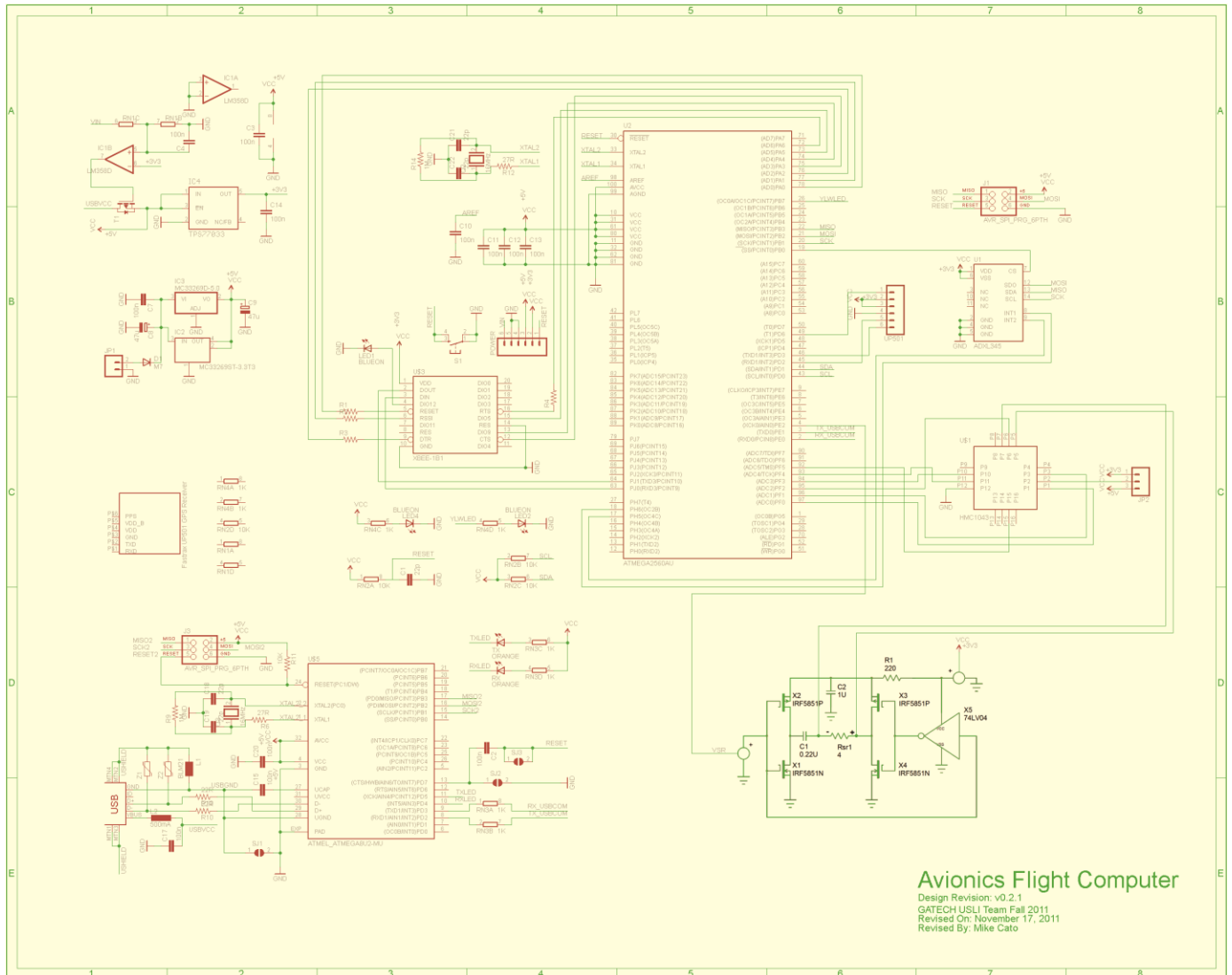






Figure 47: Proposed layout of flight computer

Table 29: Major Flight Computer Components

<i>Part Number</i>	<i>Component Picture</i>	<i>Description</i>
1		The flight computer microprocessor, the ATmega 2560
2		The GPS receiver, the Fastrax UP501 GPS module
3		The Xbee PRO 900-XSC module for communication between launch vehicle and ground station
4		The OpenLog board will provide logging capability

9.2. A.P.E.S. System Computer

The A.P.E.S. system and its computer will focus on the stabilization of the isolated platform. The computer system will be a commercially purchased ARM Cortex M3 breakout board named a “Blueboard”. The Cortex M3 will provide up to 100 MHz of clock speed for the rapid computation necessary in analyzing optical data. The Blueboard will also allow the Cortex M3 to handle all control of the magnetic fields through pulse-width modulation (PWM), and delivery of data to the flight computer. A.P.E.S. system software will also include steps to shut down the experiment at or around apogee, and physical constraints will be built into the A.P.E.S. system

structure to improve shutdown and recovery safety. An outline of the A.P.E.S. system software is given in Figure 48 and a high-level schematic layout of the A.P.E.S. computer hardware is given in Figure 49.

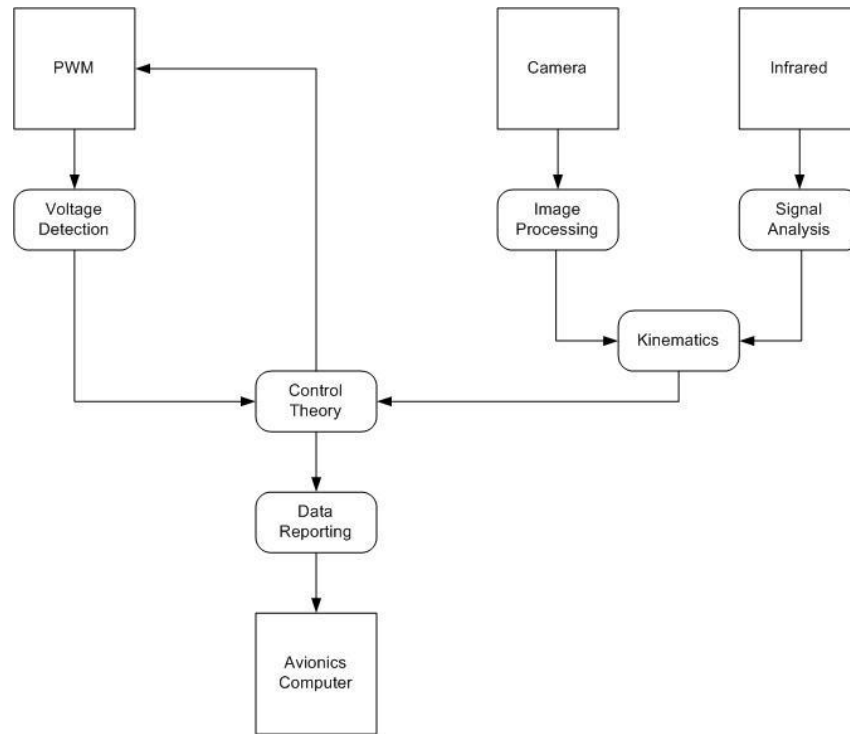


Figure 48: Generalization of A.P.E.S. system software

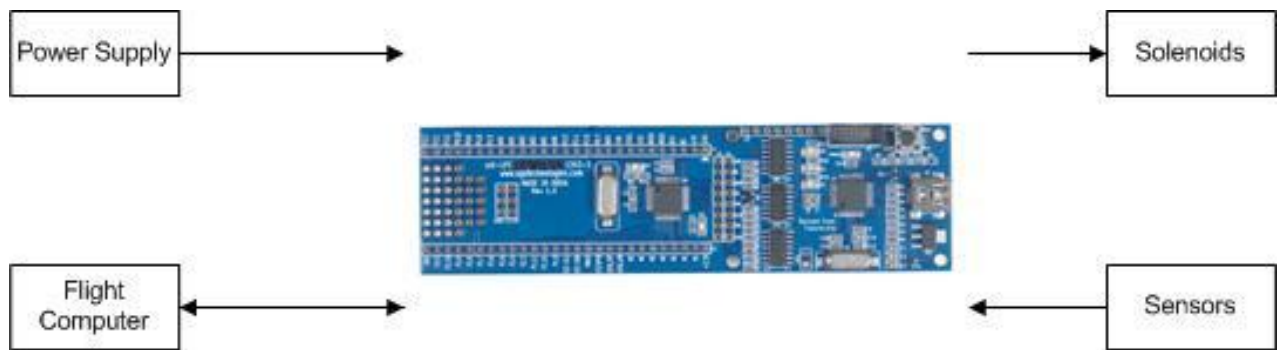


Figure 49: Layout of A.P.E.S. computer system hardware

9.2.1. Control Theory

9.2.1.1. Introduction to PID control

A proportional-integral-derivative (PID) controller is a common control loop feedback mechanism, as illustrated in Figure 50. The basis of the method is the measurement and minimization of an ‘error’ term, defined as the difference between a measured process variable and a setpoint, the desired state of the process. The PID controller attempts to minimize that error by appropriately adjusting the process control inputs. The “P” term corresponds to the present error, the “I” term the accumulation of past errors, and the “D” term is a prediction of future errors based on the current rate of change, or derivative, of the process. The weighted sum of these three actions is used to adjust the process.

Various sensors are used to measure the state of the process and the information is fed back into

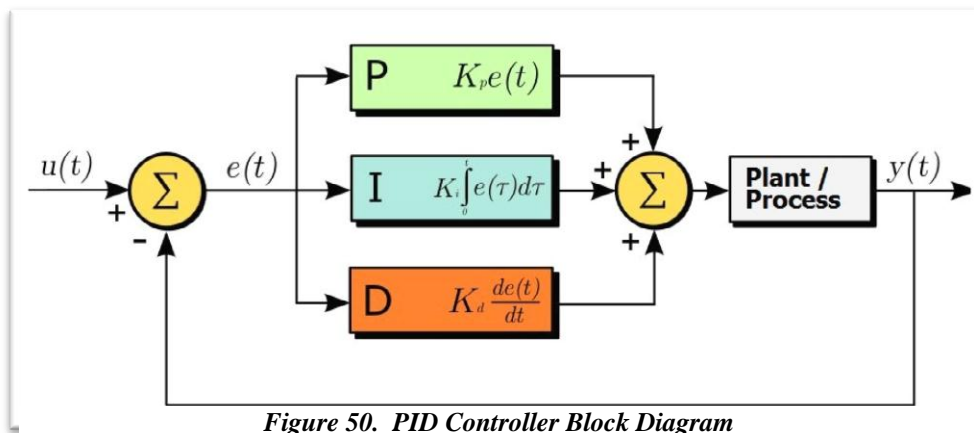


Figure 50. PID Controller Block Diagram

the control loop. The rate at which the system shall adjust to changes is given by the “P” term. The degree to which the adjustment itself should be increased or decreased in order to converge with the desired state is given by the “I” term. Finally, the “D” term slows down the adjustment of the present state to the desired state to prevent the overcompensation that could be caused by the “I” term.

9.2.1.2. A.P.E.S. PID Control Design

In this application, a series of camera modules will be used to measure the output state of the controller, corresponding to the 3 dimensional Cartesian position of the A.P.E.S. platform. This position data will then be fed back into the PID controller. The error term in this implementation corresponds to the distance the platform is from the desired setpoint: in the absolute center of the

payload module. After calculating the necessary adjustments, the strength of the magnetic field required of each solenoid will be computed and the power to each adjusted accordingly via digital control.

9.2.1.3. Design Considerations

The speed of this loop is critical in ensuring the system achieves a marginally stable output. If the time between reading the output state and adjusting the solenoids is too long, the system state will have already changed between the periods of measurement and adjustment and the system will become unstable. The implementation will be verified to run in an acceptable timeframe to ensure stable control of the platform.

9.2.1.4. Tuning

The PID controller depends on appropriate coefficient values being chosen for each term. This process is called ‘tuning’. The Zeiger-Nichols technique is a method that tunes the control loop while it is online by automating the trial and error systematically according to a given heuristic, and adjusting each term until a stable output is reached. In order to tune the control loop efficiently the Zeiger-Nichols technique will be utilized with the platform’s average distance from the module center as the heuristic.

9.3. Power Systems

9.3.1. Power Budget

The power budget for both the A.P.E.S. computer and the Flight Computer are illustrated in Figure 51. The duty cycle is representative of one (1) flight, or 140 seconds. For the A.P.E.S. computer and components, it is assumed that the hardware is active for only 40 seconds of the entire flight – from T-20s to T+20s.

Power Consumption			Modes								
			Standby			Typical			Max		
Subsystem	Component	Voltage	Amps	Watts	Duty Cycle	Amps	Watts	Duty Cycle	Amps	Watts	Duty Cycle
Avionics	adx1345	3.3	0.000	0.000	1.000	0.000	0.000	1.000	0.000	0.001	1.000
	hmc1043	3.3	0.012	0.040	0.000	0.012	0.040	1.000	0.012	0.040	1.000
	atmega8u2	5	0.000	0.002	1.000	0.014	0.070	1.000	0.021	0.105	1.000
	atmega2560	5	0.000	0.002	1.000	0.020	0.100	1.000	0.029	0.145	1.000
	UP501	3.3	0.005	0.017	1.000	0.023	0.077	1.000	0.035	0.117	1.000
	Xbee-XCS	3.3	0.000	0.000	1.000	0.330	1.089	1.000	0.330	1.089	1.000
	OpenLog	5	0.002	0.010	1.000	0.005	0.025	1.000	0.006	0.030	1.000
A.P.E.S.	OVM7690	2.8	0.000	0.000	0.000	0.100	0.280	0.182	0.100	0.280	0.182
	Sharp GP2Y0D805Z0F	5	0.000	0.000	0.000	0.009	0.045	0.182	0.011	0.053	0.182
	MLX90363	5	0.005	0.023	0.000	0.013	0.063	0.182	0.016	0.078	0.182
	mbed	3.3	0.002	0.007	0.000	0.067	0.221	0.182	0.067	0.221	0.182
Other	Solenoids	2.4	0.000	0.000	0.000	0.688	1.651	0.182	0.860	2.064	0.182
Max Power Draw (W)			0.099			3.661			4.221		
Duty Cycled Power Consumption (W)			0.031			1.812			2.016		
10% Contingency (W)			0.003			0.181			0.202		
Power Consumption with Contingency (W)			0.034			1.993			2.218		

(a)

SubTotals						
Standby		Typical		Maximum		
Amps	Watts	Amps	Watts	Amps	Watts	
0.020	0.070	0.404	1.401	0.434	1.526	Avionics
0.007	0.029	0.189	0.609	0.193	0.631	A.P.E.S.
0.000	0.000	0.688	1.651	0.860	2.064	Other

(b)

Figure 51. (a) Power budget for the A.P.E.S. computer and the Flight Computer; (b) subtotals of the A.P.E.S. computer and the Flight Computer.

9.3.2. Power Supply

The avionics system, including computers and sensors, will be powered by a 9V battery. The supply will be attached to the Avionics Computer Board which is designed to have a voltage regulator circuit providing 3.3V and 5V rails. The supply will provide 1200mAh of power.

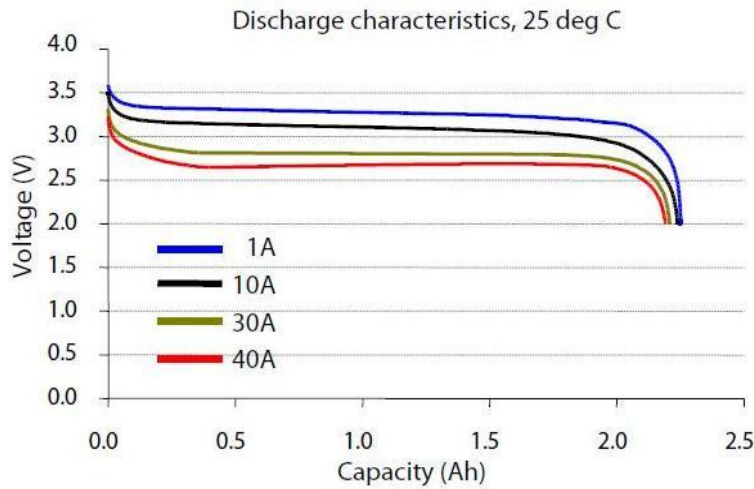


Figure 52: Discharge characteristics of the A123 battery

The avionics use a negligible amount of power in sleep mode providing a minimum of 5 hours of wait capability for the launch pad. Upon launch the system is activated and will have greater than needed power capacity to perform its duties until the launch vehicle is retrieved. Separately, the A.P.E.S. system will utilize a four-pack of A123 lithium iron phosphate (LiFePO) rechargeable batteries, one of which is shown in Figure 53. These batteries have a per-unit nominal capacity and voltage of 2.3 ampere-hours and 3.3V, respectively. Furthermore, the A123 batteries provide a maximum discharge rate of 70 amperes. Figure 52 illustrates the discharge characteristics of the A123 at four discharge rates. The ability of the A123 to provide a large current is critical to the A.P.E.S. system, which will rely on pulse-width modulation to change magnetic field intensity via manipulation of a root-mean-square current.



Figure 53: A single A123 LiFePO battery

9.4. Telemetry and Recovery

9.4.1. Ground station

The ground station for receipt of data shall consist of a laptop connected via USB to an Xbee Pro and Xbee Explorer with a rubber duck antenna. This will ensure simplicity, portability, and operability of the ground station.

9.4.2. Transmitter Design

In order to satisfy recovery requirements that the launch vehicle be found, a GPS module is included with the avionics in addition to radio communication equipment. The Fastrax UP501 provides a 10Hz update rate, rapid satellite acquisition, and low current draw. Position data is logged on-board and transmitted over the 900MHz radio band to our ground station. The telemetry system is designed to utilize two Xbee PRO 900-XSC modules for one-way communication from the launch vehicle to the ground station. Using a simple, loss-tolerant protocol with reliable delivery ensures the data is received if at all possible and that the information is correct. To extend the range beyond 1 mile, each module has a 900MHz monopole-monopole vertically polarized rubber duck antenna with 2 dBi gain and 10W of power. This antenna's performance is depicted graphically in ory.

. Receipt of GPS data via radio to the ground station will satisfy the recovery requirement and bolster kinematics data of the launch vehicle trajectory.

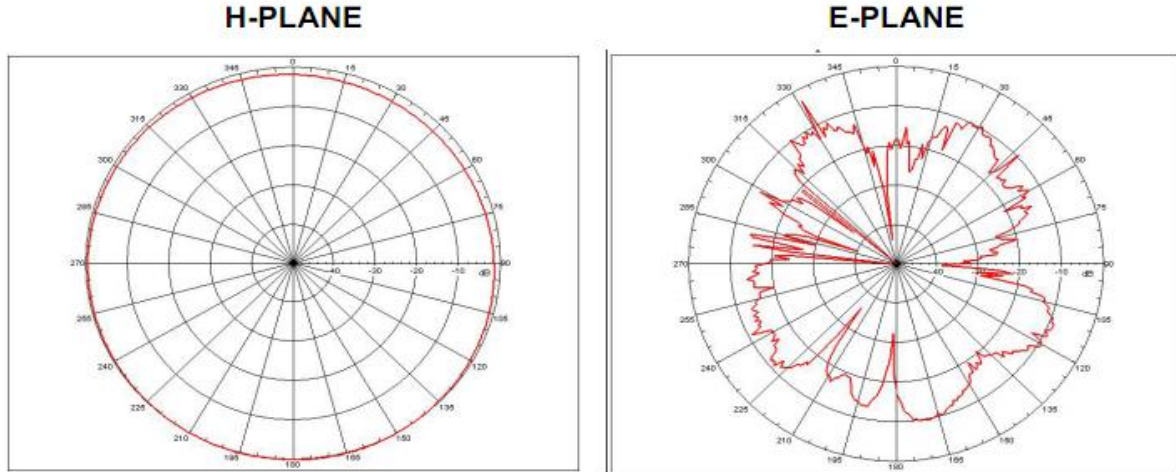


Figure 54: Antenna performance as a function of range

9.5. Integration

9.5.1. Modularity and Motivation

The modular internal launch vehicle structure permits integrating the payload with minimal effort. A section of the internal launch vehicle structure is reserved for the altimeters, payload experiment, and flight computer. The ends of the modular section are fitted structurally with solid fiberglass to sustain the bursts of the recovery system. These solid fiberglass sections are fitted with shear pins to maintain stability during flight. The entire system stacks together for dual deployment. The volume designed for the payload is an area between the struts 8 inches long with an average diameter of 3.2 inches within the hexagonal inner side of the ribs. The A.P.E.S. device will be anchored to the top of this section via a "universal bracket" to one of the ribs, shown in

. Below A.P.E.S. will be the flight system computer will in a shielded compartment. The computer will also be mounted to a rib using a universal bracket.

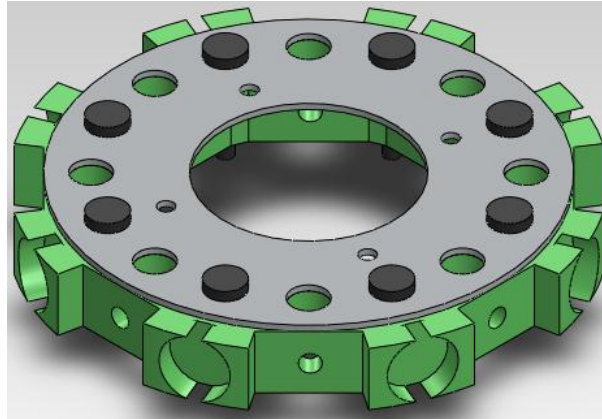


Figure 55: Universal mounting bracket bolted to rib

9.5.2. Universal Mounting Bracket

The unique and robust structure of the Vespula launch vehicle will allow greater reusability and modularity for integration of the flight and payload subsystems. In order to speed up integration time a generalized universal mounting system will be employed so that current and future subsystems can be quickly and effectively mounted to the major rib sections of the launch vehicle structure. When these and future internal components are designed and produced, minimal design consideration will be needed to account for attachment to the universal mounting bracket. This continues on the Georgia Tech Mile High Yellow Jackets tradition of simplifying and unifying the structural elements of the launch vehicle, simplifying design and improving construction time and structural robustness. The universal mounting bracket shall be built to accommodate structures such as the A.P.E.S. device with minimal fabrication and design requirements, and to fit within rib structures with few necessary design parameters on the ribs themselves, increasing the potential reusability of the universal mounting bracket should future teams alter the modular structure further. As shown in **Figure 41**, the A.P.E.S. structure mounts easily with the universal bracket. The use of the bracket also allows for the whole A.P.E.S. system to be removed more easily in case there any modifications are required. Furthermore this frees up the designs for the payload structure as it is fundamentally non-load bearing as the internal launch vehicle structure is taking care of that already.

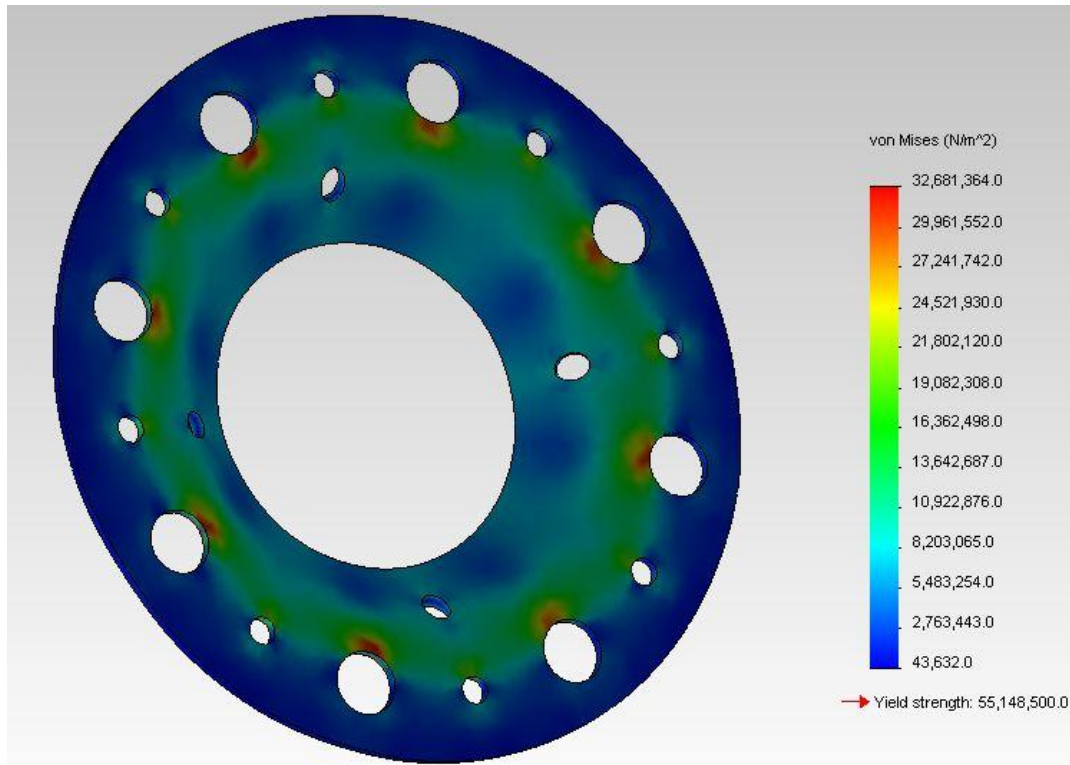


Figure 56: Basic finite-element-analysis of the universal mounting bracket

Finite-element-analysis carried out in the Solidworks Office environment details an axial load of 150 lb_f placed in the center of the mounting bracket. High stress regions appear due to the fallibilities of the Solidworks finite-element-analysis software and the difficulty of specifying distributed reaction loads. The results of the finite-element-analysis appear in Figure 56. While quarter inch (0.0625”) aluminum was necessary to provide a factor of safety of 1.6 in the case of point application of resistive loads, it is more likely that the actual safety factor is closer to 1.8 or 2 meaning that 1/16” is more than sufficient for the loads experienced. Further study will be done to specific an exact safety factor and the design may be modified to ensure a minimum safety factor of 2.

The universal mounting bracket will mount into the launch vehicle structural ribs at approved attachment points using number 8 bolts. Initial designs allow for the A.P.E.S. structure to then bolt directly to the bracket also using number 8 bolts. Table 30 provides further characteristics of the universal mounting bracket.

Performance evaluation metrics will be developed further as elements of Flight Systems begin to be produced. However, several basic metrics exist already, namely, the reduction of all motion of the A.P.E.S. plate in a timely manner, i.e. a well-damped impulse response. The flight computer must survive for several hours on the launch pad. All data must be handled and recorded accurately by both the flight and experimental computers.

Table 30: Universal Mounting Bracket Specifications

<i>Universal Mounting Bracket Parameter</i>	<i>Design Value</i>
Thickness	0.0625 in.
Diameter	4.409 in.
Bolt Hole Diameter	0.164 in.
Rib Mount Bolt Radius from Center	1.809 in.
Number of Bolts to Rib	8 bolts maximum
A.P.E.S. System Mount Bolt Radius from Center	1.282 in.
Avionics System Mount Bolt Radius from Center	1.282 in.
Stringer through Holes Diameter	0.376 in.
Stringer Hole Radius from Center	1.809 in.
Mounting Bracket Material	6061-Aluminum

9.6. Sensing Capabilities

9.6.1. Flight Avionics Sensors

9.6.1.1. General Sensing

Sensing data will be provided to the flight computer through ten (10) different sensors chosen to give the most relevant data regarding experimental and launch vehicle performance. The sensing system must account for difficulties arising in communication interfaces, voltage requirements, and material sourcing. Components must survive periods of potentially strong magnetic flux density and sensors placed in launch vehicle modules which undergo separation must resist explosive impulses which may interfere or damage sensing components.

9.6.1.2. Kinematics and Location

The accelerometer ADXL345 (shown in Figure 57) will provide acceleration data and, combined with the GPS module, provide rotation and position data for the launch vehicle trajectory. Three axis capabilities will implicitly define velocity, position, and rotational motion. The ADXL345 accelerometer can record up to $\pm 16G$. The ADXL345 is capable of entering a “standby” mode

for periods of inactivity, an advantage for periods of inactivity during setup and preparation to launch.



Figure 57: ADXL345 accelerometer

9.6.1.3. Magnetic Fields

The chosen magnetometer for detection of potentially harmful fields in the vicinity of the avionics is the HMC1043, and will determine the effectiveness of our shielding to contain the magnetic fields from the APES system. The sensor detects the magnetic field in three dimensions and “static” testing will allow for compensation for the contributions of the Earth’s magnetic field. The sensor will be used to determine the flux within the avionics bay of the launch vehicle to help monitor the influence of the magnetic field to our other equipment. The HMC1043, in **Error! Reference source not found.**, can sense up to ± 6 gauss. A combination of distance and mu-metal shielding should diminish the A.P.E.S. fields significantly that such a small range should be appropriate.

Figure 58: HMC1043 Magnetometer

9.6.2. A.P.E.S. System Sensing

The A.P.E.S. computing system will require two types of sensors for feedback and control. Position of the levitating test platform inside of A.P.E.S. will be tracked and displacement data used for derivation of platform kinematics. The magnetic fields generated by the solenoids will

also be monitored and compared to models and thresholds developed during ground testing. There are several serious issues to sensing in the A.P.E.S. experiment. First is the possibility of large magnetic flux – potentially as large as several hundred gauss. Strong magnetic flux will induce current in wiring often destroying sensitive digital electronics. High current such as the solenoids power cables may also risk induced current in electronics. To counteract these issues, mu-metal Faraday shielding and distancing from the computational elements will be utilized. However, sensors and detection equipment will be chosen to satisfy the expected parameters of the environment around the A.P.E.S. system.

Table 31: Possible A.P.E.S. distance sensors

<i>Sensor</i>	<i>Cartesian Coordinate Axes</i>	<i>Viewing Angle >45 Degrees</i>	<i>Range <5cm</i>	<i>Resolution <1mm</i>	<i>Delay <20ms</i>	<i>Interference</i>	<i>Flux Sensitive</i>	<i>Reliable under Shock and Vibrations</i>	<i>Small Form Factor <15mm</i>
Ultrasonic Distance	1	No	No	No	No	No	No	No	No
IR Distance	1	No	Yes	Yes	Yes	No	Yes, w/Shielding	Yes	Yes
Laser Distance	2	Yes	Yes	Yes	No	No	Yes, w/Shielding	Yes	No
CMOS Camera	2	Yes	Yes	Yes	Yes	Yes	Yes, w/Shielding	Yes	Yes

9.6.2.1. A.P.E.S. Distance Sensing

The full three-dimensional design would utilize two to three CMOS cameras. The OVM7690 Camera Cube CMOS camera meets all current design requirements and expected environmental conditions, as outlined in Table 31. The camera sensor is a small form factor (2x2x1mm) color image camera module, as illustrated in Figure 59, with integrated optical glass lens and on-chip image processing. A test pattern is used for initial software pixel-to-distance mapping and calibration for the camera output data and is mounted on the opposite side of the test structure as the camera. The test pattern must be an easily identifiable pattern – this will be made of fiber optic cables mounted on a panel attached to a specific color light emitting diode (LED). A second camera and test pattern are mounted perpendicular to the first, using a second specific color.



Figure 59: OVM7690 Camera Cube

Once the calibration is complete, the cameras output is read at 30-60 frames per second (FPS). The levitating platform is painted another specific color which is not the same as the colors already used for calibration patterns of the two cameras. Several white LEDs are used for flooding light to make the painted platform visible. A simple edge detection algorithm is used to find the displacement of the platform in each sample frame. Using the pixel to distance mapping from the initial calibration, the displacement between samples is calculated which in turn is used to update the Cartesian coordinate for the platform in three dimensions. The use of one camera for sensing on three axes was rejected because the small movements along the forward line of sight (depth perception) would not be interpreted with high enough resolution. Movement along the horizontal and vertical plane will be sufficient, so two axes can be used.

9.6.2.2. A.P.E.S. Magnetic Field Sensing

While not critical to the flight mission of the A.P.E.S. system, sensing of magnetic fields during ground testing of the A.P.E.S. system will allow for better model generation as well as full confirmation of the theoretical basis of the project. Therefore, the MLX90363 magnetometer has been proposed for use in ground testing applications. The sensor is sensitive up to 0.7-1.0 Tesla, has a sample rate of 1 millisecond, and outputs magnetic field direction as a three coordinate vector. This sensor was chosen for its high magnetic flux sensitivity, decent resolution

increments, and three axis direction vector output. The magnetometer controls on-chip digital signal processing.

9.7. “De-Scope” Options

9.7.1. Payload “De-Scope”

The de-scope option for the payload will utilize a single infrared distance detection along a single axis of linear motion, where a sample plate is levitated vertically at constant distance between the sensor and a solenoid during the ascent of the launch vehicle. The objective of the flight experiment would be to then maintain a constant position with a 2% settling time of less than 0.5 seconds for a unit impulse. This option provides an opportunity to develop many of the same control theories without the necessity to grapple complex 3-dimensional magnetic fields.

9.7.2. Flight Computer “De-Scope”

The de-scope option for the flight computer is to use a commercially available Arduino Mega board, rather than fabricate a custom board. This option provides full capability should timelines not permit the completion of design and construction of the custom board. Safety

9.8. General Safety

Ensuring the safety of our members during building, testing and implementation of the payload experiment is an ideal condition. Procedures have been created and implemented in all of our build environments to ensure safety requirements are met and exceeded. A key way the Yellow Jackets ensure team safety is to always work in teams of at least two when using equipment or during construction. This guarantees that should an incident occur with a device the other member could provide immediate assistance or quickly get addition help if required. The Invention Studio where the team does a majority of its work is equipped with safety glasses, fire extinguishers, first aid kits, and expert personnel in the use of each of the machines in the area. All the members of the payload and flight systems teams have been briefed on the proper procedures and proper handling of machines in the labs.

9.9. Payload Hazards

As already mentioned in General Safety, the same methodology to identify and assess risks for vehicle safety will be used to identify hazards for the payload. The entire payload and flight systems teams have been briefed on the possible hazards they may encounter while working with the payload and how to go about avoiding them. Hazards that relate specifically to the payload are listed in Table 32. Payload failure modes are outlined in Table 33.

Table 32: Hazards, Risks, and Mitigation

<i>Hazard</i>	<i>Risk Assessment</i>	<i>Control & Mitigation</i>
Electrocution	Serious Injury/death	Do not touch wires that are hot and not insulated. Wear rubber gloves when the device is in operation. Handle leads to the power supply with care. Use low voltage settings whenever possible.
Electromagnetic Fields	Interfere with electronic devices inside the body	Ground test equipment, keep people with electronic components in them away from the coil when the electromagnetic coil is in use.
Epoxy/glue	Toxic fumes, skin irritation, eye irritation	Work in well ventilated areas to prevent a buildup of fumes. Gloves face masks, and safety glasses will be worn at all times to prevent irritation.
Fire	Burns, serious injury and death	Keep a fire extinguisher in the lab. If an object becomes too hot or starts to burn, cut power and be prepared to use a fire extinguisher.
Soldering Iron	Burns, solder splashing into eyes	Wear safety glasses to prevent damage to eyes. Do not handle the soldering lead directly only touch handle. Do not directly hold an object being soldered.
Drills	Serious injury, cuts, punctures, and scrapes	Only operate tools under supervision of team mates. Only use tools in the appropriate manner. Wear safety glasses to prevent debris from entering the eyes

<i>Hazard</i>	<i>Risk Assessment</i>	<i>Control & Mitigation</i>
Dremel	Serious injury, cuts, and scrapes	Only operate tools under supervision of team mates. Only use tools in the appropriate manner. Wear safety glasses to prevent debris from entering the eyes
Hand Saws	Cuts, serious injury	Only use saws under supervision of team mates. Only use tools in the appropriate manner. Wear safety glasses to prevent debris from entering the eyes. Do not cut in the direction of yourself or others.
Exacto Knives	Cuts, serious injury, death	Only use knives under supervision of team mates. Only use tools in the appropriate manner. Do not cut in the direction of yourself or others.
Hammers	Bruises, broken bones, and serious injury	Be careful to avoid hitting your hand while using a hammer.
Power Supply	Electrocution, serious injury and death	Only operate power supply under supervision of team mates. Turn off power supply when interacting with circuitry.
Batteries Explode	Eye irritation, skin irritation, burns	Wear safety glasses and gloves. Make sure there are no shorts in the circuit. If a battery gets too hot stop using it and remove any connections to it.
Improper Dress during construction	Serious injury, broken bones	Wear closed toe shoes, clothing that is not baggy, and keep long hair tied back.
Exposed construction metal	Punctures, scrapes, cuts, or serious injury	Put all tools and materials away after use.
Neodymium Magnets	Pinching, bruising, and snapping through fingers.	Do not allow magnets to fly together from a distance, do not play with powerful magnets, keep free magnets away from powered solenoids.

Table 33:

A.P.E.S. payload failure modes

<i>Potential Failure</i>	<i>Effects of Failure</i>	<i>Failure Prevention</i>
No power	Experiment cannot be performed	Check batteries, connections, and switches
Data doesn't record	No experimental data	Ensure power is connected to the payload computer and that all connections are firmly secured
Magnetic field interferes with flight computer	No experimental data	Shield the flight computer from any EMF interference
Accelerometers	Record erroneous acceleration values	Calibrate and test accelerometers
Solenoids	Experiment cannot be performed, wires melt	Check connections, ensure over heating will not occur during testing
Too much current goes into the solenoids	The wires in the solenoids get very hot	Make sure current is only pulsed into the solenoids
Improper dress during construction	Maiming, cuts, scrapes, serious injury.	Do not wear open toed shoes in the build lab. Keep long hair tied back. Do not wear baggy clothing.
Avionics	Chips or boards are manufactured incorrectly causing equipment failures and misfires	Test avionics operations, and perform a flight test.

9.10. *Vehicle Safety*

To assist in the elimination of risks to all members and bystanders involved the launch vehicle risks must be identified to a reasonable degree. Relevant risks will be identified through the use of a four step method and tabulated afterwards. To mitigate potential failures of the launch

vehicle potential failure modes will be developed as well as ways to prevent them from taking place. The specific hazards will also be classified according to how likely it is to occur under normal operating procedures.

Risks continue to be identified for the launch vehicle and payload by exploiting a four-step risk management process. This process helps by pinpointing risks that could cause damage or harm to the environment or people. The steps are listed in Table 34.

Table 34: Risk Identification and Mitigation Steps

<i>Step Name</i>	<i>Step Definition</i>
1. Hazard Identification	The first step is to correctly identify potential hazards that could cause serious injury or death. Hazard identification will be achieved through team safety sessions and brainstorming.
2. Risk and Hazard Assessment	Every hazard will undergo extensive analysis to determine how serious the issue is and the best way to approach the issue.
3. Risk Control and Elimination	After the hazards are identified and assessed a method is produced to avoid the issue.
4. Reviewing Assessments	As new information becomes available the assessments will be reviewed and revised as necessary.

The steps outlined above are being used to develop a set of standard operating procedures for launch vehicle construction, payload construction, ground testing, and on all launch day safety checklists. Materials Safety Data Sheets of all materials used in construction are listed in Appendix 5.

Failure modes for the launch vehicle were developed to better ensure success of the entire project. Possible modes, resultant problem, and mitigation procedures are given for each failure mode. These modes will continue to evolve and expand in scope as the project progresses. The mitigation methods will be continuously incorporated into preflight checklists. The mitigation items detailed therein will be incorporated into the preflight checklist. Launch vehicle failure modes and mitigation are listed in Table 35.

Table 35: Launch vehicle failure modes and mitigation

<i>Potential Failure</i>	<i>Effects of Failure</i>	<i>Failure Prevention</i>
Fins	Launch vehicle flight path becomes unstable	Test fin failure modes at connection to launch vehicle to ensure sufficient strength
Structural ribs buckle on take off	Launch failure, launch vehicle destroyed, possible injury from shrapnel	Wear eye wear protection, test the internal structure to ensure a factor of safety against buckling
Thrust retention plate	Motor casing falls out	Test reliability of thrust retention plate
Skin zippering	Internal components are exposed to flowing air currents, launch vehicle becomes unstable	Test skin adhesion reliability
Launch buttons	Launch vehicle becomes fixed to launch rail, or buttons shear off	Ensure buttons slide easily in launch rail, ensure rail is of the proper size
Drogue separation	Main shoot takes full brunt of launch vehicle inertia, launch vehicle becomes ballistic	Do a ground test of drogue separation as well as a flight test
Main shoot	Launch vehicle becomes ballistic, severe injury, irrecoverable launch vehicle	Do a ground test of main shoot deployment, as well as a flight test.
Land directly on fins	Fins break, and launch vehicle cannot be flow twice without fixing	Test fin failure modes at connection to launch vehicle to ensure sufficient strength
Ignition failure	Launch vehicle does not launch	Follow proper procedure when setting up launch vehicle ignition system
Motor failure	Motor explodes	Install motors properly according to NAR standards

10. Project Budget

10.1. Funding Overview

In order to fund the 2011-2012 Competition year, the Mile High Yellow Jackets have sought sponsorships from academic and industry sources. The current sponsors of the Mile High Yellow Jackets and their contributions can be found in Table 36. As of CDR, the Mile High Yellow Jackets have received \$7,000 in funding. Furthermore, the Team has also received a dedicated room in which the Team can construct and store their rocket and non-explosive components. All explosive components (i.e. black power) are properly stored in Fire Lockers in either the Ben T. Zinn Combustion Laboratory or the Center for Space Systems Flight Hardware Laboratory.

Table 36. Summary of sponsors for the Mile High Yellow Jackets.

<i>Sponsor</i>	<i>Contribution</i>	<i>Date</i>
Georgia Space Grant Consortium	\$3,500	Sept. 2011
Georgia Tech School of Aerospace Engineering	\$1,000	Oct. 2011
Georgia Tech Student Government Association	\$1,000	Nov. 2011
SCITOR Corp.	\$500	Nov. 2011
SpaceX	\$1,000	Dec 2011
ATK Travel Stipend	\$400	Apr 2011
ATK Motor Stipend	\$200	Apr 2011
<i>Coca-Cola (est.)</i>	<i>(\$1,500)</i>	<i>Mar. 2011</i>
Total	\$7,600	

10.2. Projected Budget Update

During initial planning, it was estimated that the total project cost for Project A.P.E.S. would be approximately \$9,896.25 – or, including a 30% contingency, \$12,565.12. Figure 60 illustrates the updated projected project costs and project reserves levels at each milestone based on the funding schedule in Table 36. It is important to note that the projected budget includes the Coca-Cola sponsorship funding.

Projected Total Project Cost

	<i>Projected Cost</i>	<i>Project Reserves</i>
PDR	\$924.53	35.52%
CDR	\$3,636.80	62.43%
FRR	\$7,513.39	78.21%
Launch	\$9,854.58	42.14%

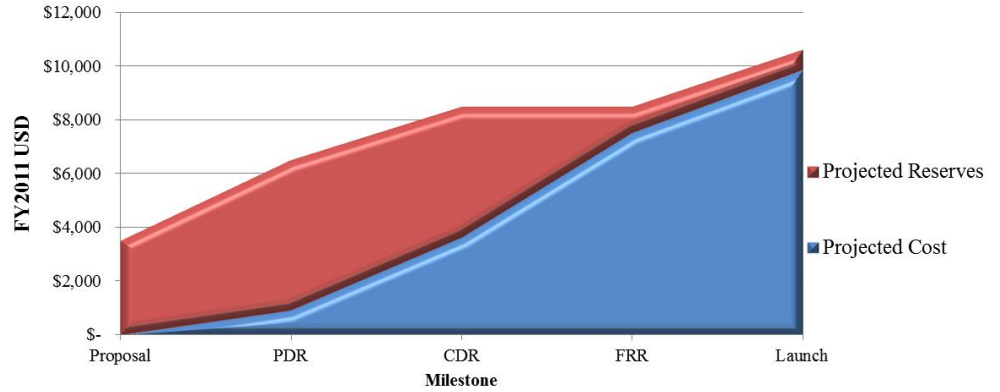


Figure 60. Projected total project cost.

10.3. Actual Project Costs

10.3.1. CDR Budget Summary

Figure 61 illustrates the budget breakdown as of the CDR Milestone. The summary is broken down into four (4) main categories: Launch Vehicle, Flight Systems, Operations, and Motors. The Launch Vehicle and Flight Systems categories are further broken down into two (2) sub-categories: Flight Hardware and Testing. Operational expenses include: non-system specific test equipment, Team supplies, non-system specific fabrication supplies, as well as any travel and outreach expenses. Any system-specific equipment bought for testing is charged against that specific system, whereas generic equipment. While motors are specific to the Launch Vehicle subsystem, they are critical component to the architecture and as such are tracked separately from the Launch Vehicle subsystem.

Figure 62 illustrates the actual total project costs - as of CDR - at each milestone. It is important to note that the total project cost estimates at FRR and the competition launch each include a 25% contingency. Due to the high project reserves, some risk associated with the novelty of the iMPS is mitigated should future unexpected testing is required.

2011-2012 Mile High Yellow Jackets Budget Summary

<i>2011-2012 Budget Breakdown</i>	
LV - Testing	\$ 530.17
FS - Testing	\$ 310.93
LV - Flight Hardware	\$ 458.90
FS- Flight Hardware	\$ 438.20
Operations - Spent	\$ 239.41
LV -Remaining	\$ 1,260.93
FS -Remaining	\$ 1,500.87
Motors	\$ 1,000.00
Operations - Remaining	\$ 1,260.59
<i>Total</i>	\$ 7,000.00

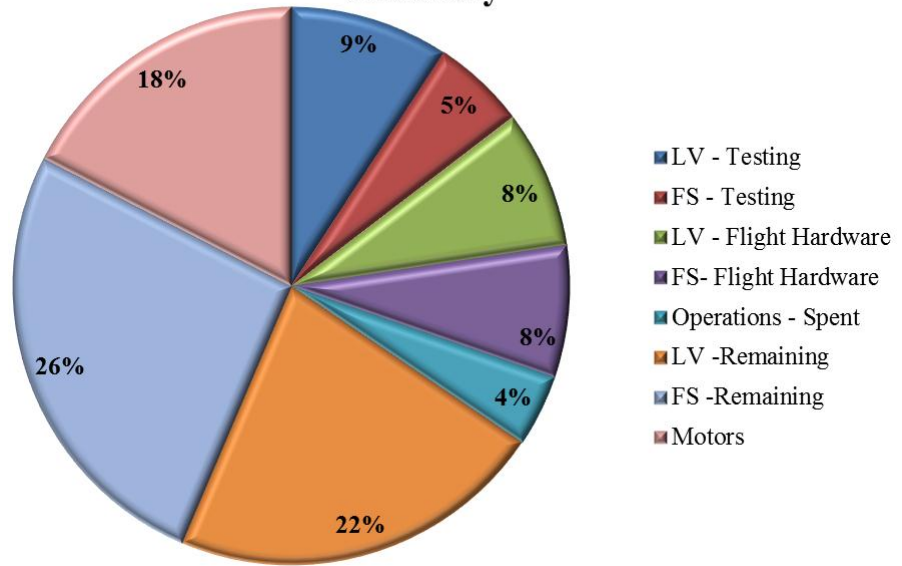


Figure 61. Project expenditures as of the CDR milestone.

	<i>Actual Cost</i>	<i>Project Reserves</i>
PDR	\$ 981.44	35.52%
CDR	\$2,032.62	62.43%
FRR	\$3,532.62	78.21%
Launch	\$5,657.62	42.14%

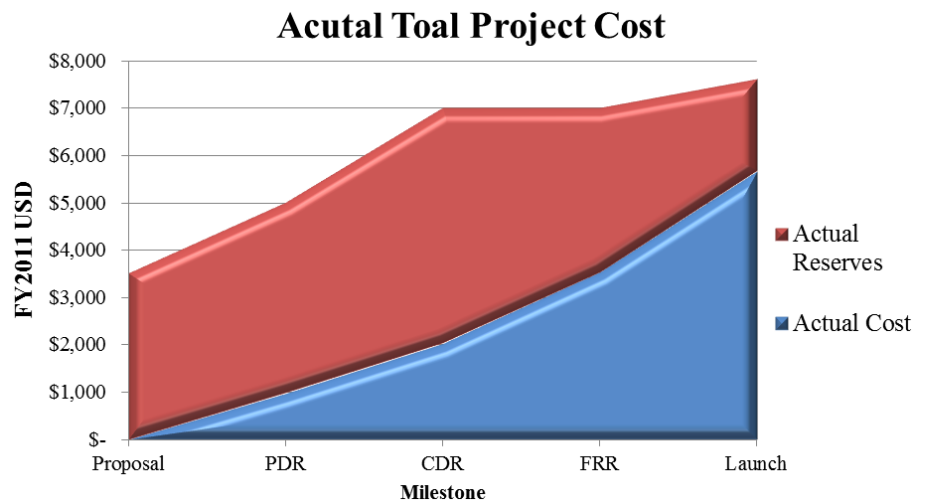


Figure 62. Actual total project costs and project reserves at each milestone.

10.3.2. Flight Hardware Expenditures

Figure 63 lists the overall expenditures for all Flight Hardware for the Launch Vehicle, Flight Avionics, and the Flight Experiment purchased up to the CDR milestone. Since motor costs are dependent upon lead time, up to \$300 has been allotted for the purchase of the Flight Motor. Figure 63 illustrates the total cost of the Flight Vehicle, Flight Avionics, and Flight Experiment at each milestone. It is estimated that the *Vespula* launch vehicle will cost just under \$2,800. It is important to note that the expenditure summary incorporates 15% contingency at both FRR and Competition Launch milestones.

Flight Vehicle & System Cost at CDR

<i>2011-2012 Overall Flight Vehicle Costs (\$5,000 Limit)</i>	
FS Flight Hardware	\$ 438.20
LV Flight Hardware	\$ 458.90
Motor	\$ 300.00
Remaining	\$ 3,802.90
<i>Total</i>	\$ 5,000.00

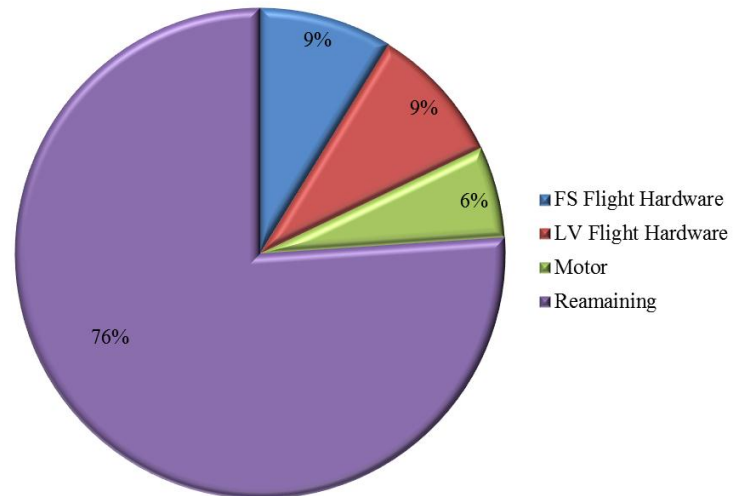


Figure 63. Summary of Flight Hardware expenditures up to the CDR milestone.

	<i>Remaining</i>	<i>Cumulative Costs</i>	<i>% Remaining</i>
PDR	\$ 4,713.10	\$ 286.90	94.26%
CDR	\$ 4,102.90	\$ 897.10	82.06%
FRR	\$ 3,067.90	\$ 1,932.10	61.36%
Launch	\$ 2,205.40	\$ 2,794.60	44.11%

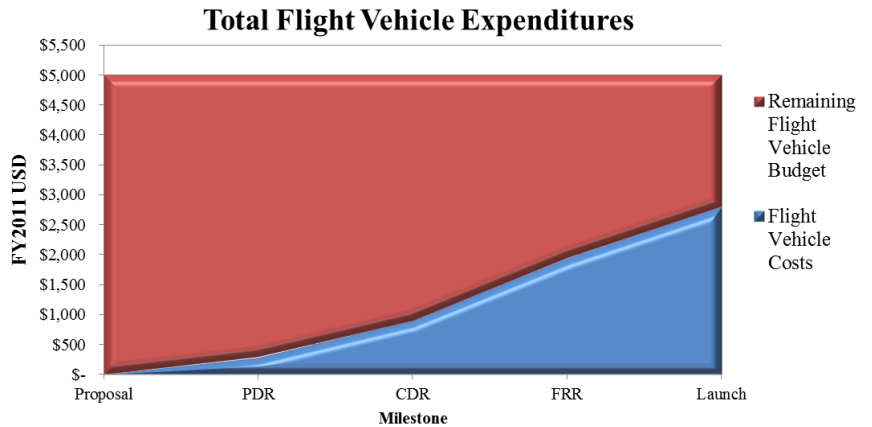


Figure 64. Total and Projected Flight Vehicle expenditures

10.3.3. Actual Costs vs. Projected Costs

Figure 65 compares the actual vs. projected total project costs. With the exception of the PDR milestone, all other milestones have achieved a lower total project cost or are expected to achieve a lower project cost. It is important to note that the total project cost at CDR is inflated due to (1) costs associated with furnishing a recently acquired workspace and (2) costs associated with starting-up an engineering team, such as generic test equipment, tools, and supplies.

The Mile High Yellow Jackets have been able to achieve these reduced project costs through:

- Internal design reviews at regular intervals
- Creation and review of Manufacturing and Fabrication Orders (MFO’s) prior to ordering materials
- Communication, proper analysis, and constructive criticism by peers all throughout the design, manufacturing, fabrication, and testing processes.

	<i>Predicted</i>	<i>Actual</i>	<i>% Difference</i>
PDR	\$ 924.53	\$ 981.44	5.80%
CDR	\$ 3,636.80	\$ 2,032.62	-44.11%
FRR	\$ 7,513.39	\$ 3,532.62	-52.98%
Launch	\$ 9,854.58	\$ 5,657.62	-42.59%

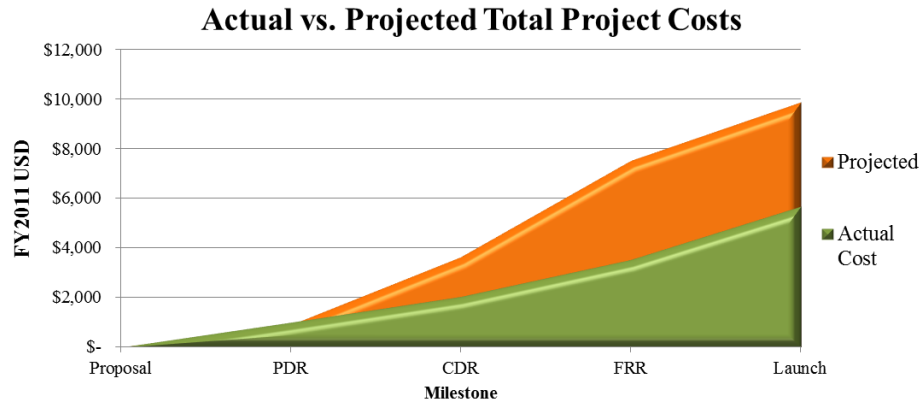


Figure 65. Actual vs. Projected Costs for the 2011-2012 competition year

11. Project Schedule

11.1. Scheudle Overview

The Mile High Yellow Jacket’s project is driven by the design milestone’s set forth by the USLI Program Office. The design milestones are listed in Table 37. The project Gantt Chart for Project A.P.E.S. – located in Appendix I – contains only high-level activities due to the unique launch vehicle and payload designs. A more detailed Critical Path chart is located in Section 11.2.

Table 37. Design milestones set by the USLI Program Office.

<i>Milestone</i>	<i>Date</i>
Proposal	26 SEP
Team Selection	17 OCT
Web Presence Established	4 NOV
PDR Documentation	28 NOV
PDR VTC	6 DEC
CDR Documentation	23 JAN
CDR VTC	2 FEB
FRR Documentation	26 MAR
FRR VTC	2-11 APR
Rocket Week	18-21 APR
PLAR Documentation	7 MAY

11.2. Critical Path Chart: CDR to PLAR

The critical path chart illustrated by Figure 66 demonstrates the highly integrated nature of Project A.P.E.S. The critical path chart identifies:

- High Risk Tasks
- Low-Moderate Risk Tasks
- Earned Value Management (EVM) Goal Tasks
- Looping Tasks
- Critical and Alternate Paths
- Major Inputs to Tasks

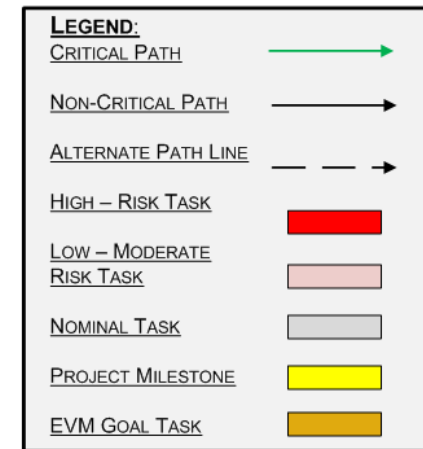
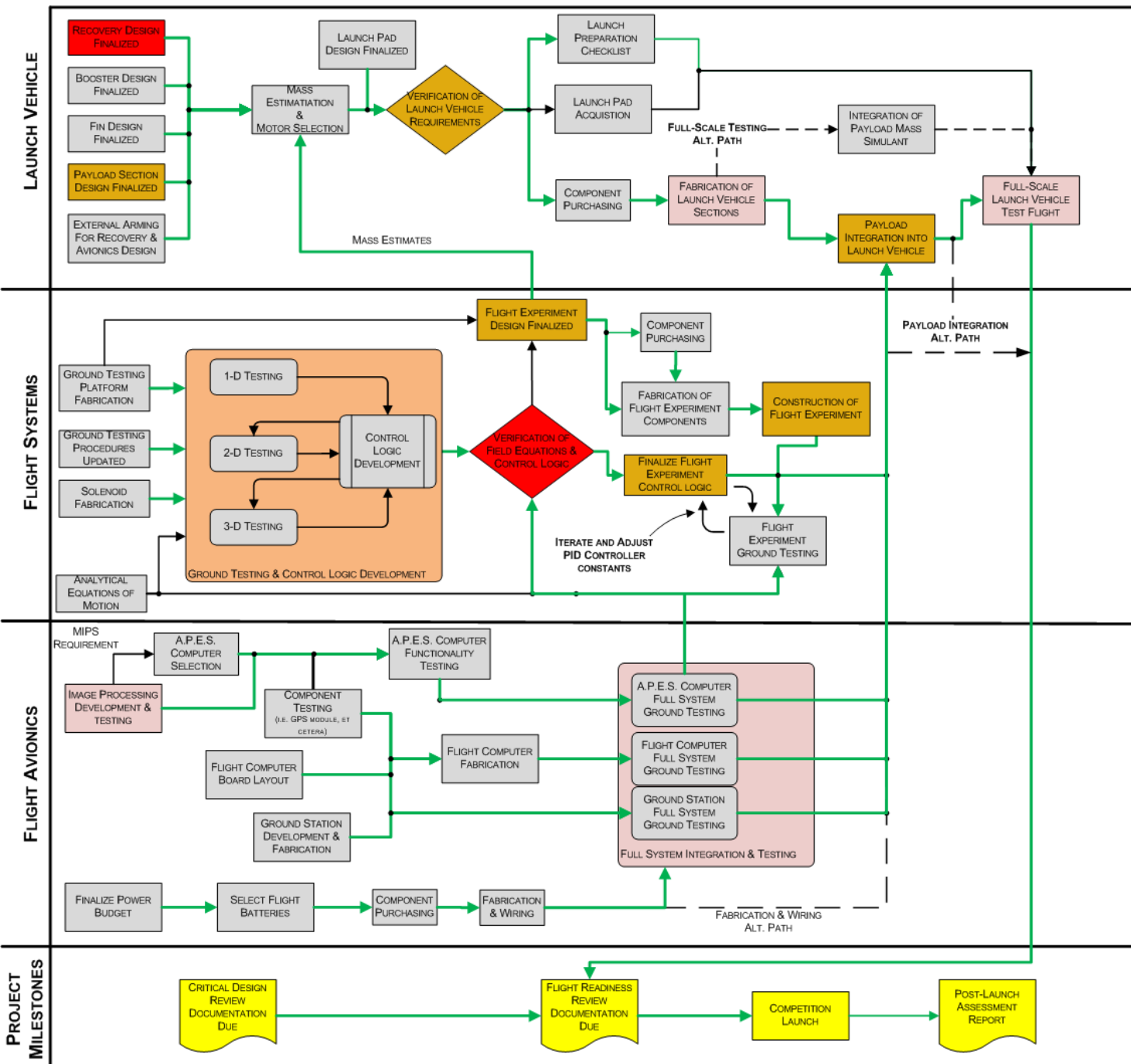


Figure 66. Critical Path Chart from CDR to PLAR

11.3. Schedule Risk

11.3.1. High Risk Tasks

From the Critical Path chart, two (2) items have been identified as “High Risk Items.” These are:

- Verification of Field Equations & Control Logic
- Recovery System Design

Table 38 lists the mitigations for these two (2) items.

Table 38. Identification and Mitigations for High-Risk Tasks.

<i>High-Risk Task</i>	<i>Potential Impact on Project A.P.E.S.</i>	<i>Mitigation</i>
Verification of Field Equations & Control Logic	<ol style="list-style-type: none"> 1) Unsuccessful flight demonstration 2) Flight Experiment does not function properly during flight 3) Flight Experiment encounters a flight anomaly that results in excessive draw and damage to the Flight Avionics, Power Supply, and/or Launch Vehicle 	<ol style="list-style-type: none"> 1) Develop multiple paths to achieve the end goal of developing thee robust control logic that is required for the successful demonstration of the Flight Experiment. 2) Ensure Flight Systems personnel have direct and free access to experienced personnel on and off of the team. 3) Ensure personnel have direct and free access to the simulation and analysis tools necessary for the development (and subsequent verification) of the control logic.
Recovery System Design & Fabrication	<ol style="list-style-type: none"> 1) Excessive kinetic energy at landing resulting in dis-qualification from the USLI competition at CDR 2) Excessive kinetic energy during landing resulting in damage to the rocket. 3) Failure to deploy the drogue and/or main parachute resulting in a high energy impact with the ground destroying the Launch Vehicle. 	<ol style="list-style-type: none"> 1) Ensure Recovery System Lead has direct and free access to experienced personnel on and off the team. 2) Provide real-time feedback of the design decisions to ensure all recovery-related requirements are meet with at least a 5% margin wherever possible. 3) Ensure proper manufacturing techniques are utilized during the fabrication of the recovery system.

11.3.1. Low-to-Moderate Risk Tasks

The “low-to-moderate risk tasks” are considered to be those risks that pose a risk to either the project schedule and/or project budget but little to no risk of not meeting the Mission Success Criteria in Table 1. The risks and mitigations are provided in Table 39.

Table 39. Low to Moderate Risk items and mitigations.

<i>Risk</i>	<i>Risk Level</i>	<i>Potential Impact on Project A.P.E.S.</i>	<i>Mitigation</i>
Fabrication of Launch Vehicle Sections	Moderate	<ol style="list-style-type: none"> 1) Schedule Impact 2) Budgetary Impact 3) Not qualifying for Competition Launch 	<ol style="list-style-type: none"> 1) Ensure Manufacturing and Fabrication Orders (MFO’s) are sufficiently detailed for the task prior to starting any fabrication. 2) Ensure proper manufacturing techniques are observed during fabrication.
Full-Scale Launch Vehicle Test Flight	Moderate	<ol style="list-style-type: none"> 1) Schedule Impact 2) Budgetary Impact 3) Not qualifying for Competition Launch 	<ol style="list-style-type: none"> 1) Ensure Launch Procedures are established practiced prior to any launch opportunity. 2) Have a sufficient number of launch opportunities that are in different geographical areas as to minimize the effects of weather on the number of launch opportunities.
Ground Testing & Control Logic Development	Moderate	<ol style="list-style-type: none"> 1) Schedule Impact 2) No Experimental Flight Data is recorded prior to the Competition Launch. 	<ol style="list-style-type: none"> 1) Ensure personnel have direct and free access to experienced personnel on and off of the team.
Image Processing: Development & Testing	Low	<ol style="list-style-type: none"> 1) Schedule Impact 2) Budgetary Impact 	<ol style="list-style-type: none"> 1) Ensure Flight Systems personnel have direct and free access to experienced personnel on and off of the team.
Flight Computer Fabrication	Low	<ol style="list-style-type: none"> 1) Budgetary Impact 2) Not able to collect in-flight data 	<ol style="list-style-type: none"> 1) Ensure proper manufacturing techniques are observed during fabrication. 2) Ensure Manufacturing and Fabrication Orders (MFO’s) are sufficiently detailed for the task.

12. Educational Outreach

12.1. Overview

The goal of Georgia Tech’s outreach program is to promote interest in the Science, Technology, Engineering, and Mathematics (STEM) fields. The Mile High Yellow Jackets’ intend to conduct various outreach programs targeting middle school students and educators. The Mile High Yellow Jackets have an outreach request form on their webpage – as shown in Figure 67 - for educators to request presentations or hands-on activities for their classroom.

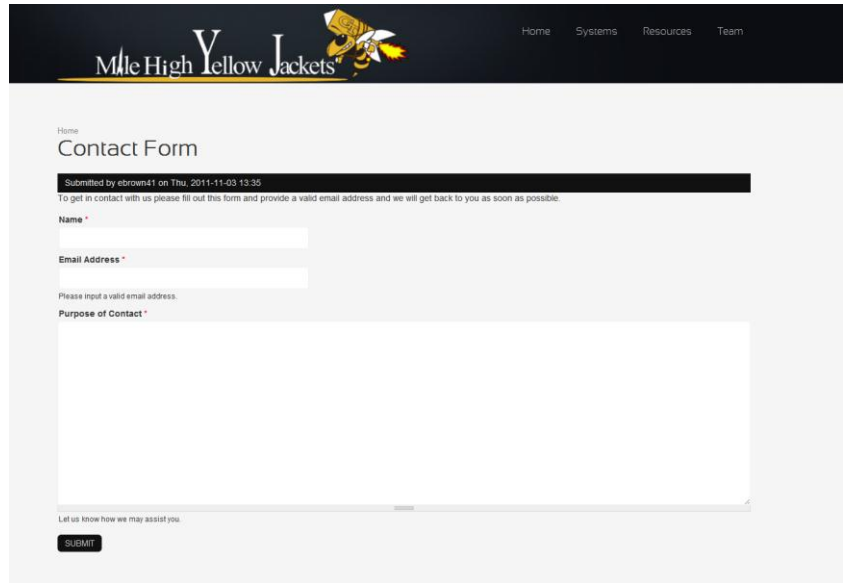


Figure 67. Online Outreach Contact Form through which educators may contact the Mile High Yellow Jackets.

12.2. FIRST LEGO League

FIRST LEGO League is an engineering competition designed for middle school children where they build an autonomous LEGO MINDSTORMS robot. An example robot is illustrated in Figure 68. Every year there is a new competition centered on a theme exploring a real-world problem. The Mile High Yellow Jackets will have a booth at the Georgia State FIRST Lego League Tournament where we will teach the fundamental concepts behind our payload and showcase our past rockets. In addition team members will aid in judging the tournament. This

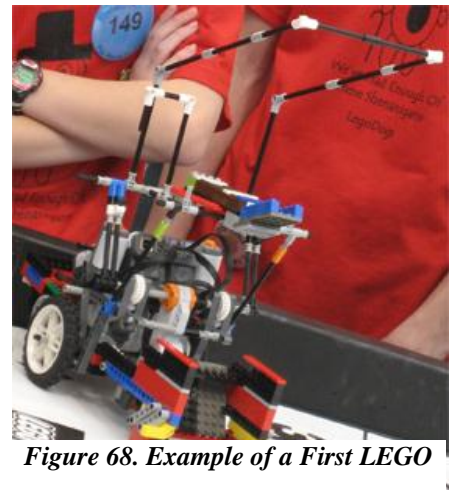


Figure 68. Example of a First LEGO League autonomous robot.

outreach event is anticipated to reach over 700 middle school students and educators. The lesson plan for First LEGO League can be found in Appendix .

12.3. *Civil Air Patrol Model Rocketry Program*

The Civil Air Patrol (CAP), the Official Auxiliary to the U.S. Air Force, is a volunteer organization whose primary missions are Emergency Services, Cadet Programs, and Aerospace Education. In the Aerospace Education program, Cadets have the opportunity to earn a Model Rocketry Badge by furthering their knowledge in the history and physics of rocketry as well as building five (5) separate rockets ranging from non-solid fuel rockets to scale models of historic rockets as well as rockets that must meet specific altitude and payload requirements. The Mile High Yellow Jackets will be working with a local Atlanta-based squadron, the DeKalb County Cadet Squadron (DCCS). This event is currently scheduled for March 2012 and is currently in the planning stage. The Mile High Yellow Jackets Educational Outreach Chair is working with the DCCS liaison in order to ensure that all program criteria are met. This outreach event is anticipated to reach approximately 20 to 30 Cadets in the 6th to 9th grade range. Specific details regarding the main concepts that are to be learned by the Cadets participating in the Model Rocketry Program can be found in the lesson plan in Appendix



Figure 69. A Civil Air Patrol Model rocket constructed by a cadet during the TITAN phase of the Model Rocketry Program.

12.4. National Air and Space Museum Discovery Station

We have designed a rocket themed Discovery Station to be used at the National Air and Space Museum in DC and the Udvar Hazy Center. The station focuses on the differences between rockets and airplanes and Newton's Third Law. Once approved, our Discovery Station will go into rotation. The average Discovery Station is seen by upwards of 10,000 visitors a year.

12.5. Young Astronauts Program

The Mile High Yellow Jackets are planning to work in conjunction with the Georgia Tech Space Systems Design Lab (SSDL) to put on the Young Astronauts program at Madras Middle School in Newnan, Ga. The intent of this program is to expose Middle School Students to various topics in the Aerospace and STEM fields. This will be accomplished by meeting twice a month and discussing a topic followed by a related hands-on project that actively engages both Students and Educators.

Reference

- Niskanen, Sampo. OpenRocket vehicle Technical Documentation. 18 July 2011. Web.
- Apke, Ted. "Black Powder Usage." (2009). Print. <<http://www.info-central.org/?article=303>>.
- PerfecFlite. StratoLogger SL100 Users Manual. Andover, NH: Print. <www.perfectflite.com>.
- Roensch, S. (2010). "Finite Element Analysis: Introduction." 2011, from <http://www.finiteelement.com/feawhite1.html>.
- "G-10 Fiberglass Epoxy Laminate Sheet." MATWEB.com. http://www.matweb.com/search/datasheet_print.aspx?matguid=8337b2d050d44da1b8a9a5e61b0d5f85
- "Shape Effects on Drag." NASA Web. 19 Nov. 2011. <<http://www.grc.nasa.gov/WWW/k-12/airplane/shaped.html>>.
- Cavcar, Mustafa. "Compressibility Effects on Airfoil Aerodynamics." (2005). Print.
- "Apogee Paramagnetic Oxygen Gas Experimental Electromagnetic Separator: Preliminary Design Review." Comp. Georgia Tech University Student Launch Initiative. Atlanta: 2009. Print.
- Cheng, David. Field and Wave Electromagnetics. 1st ed. Reading, MA: Addison-Wesley Publishing Company, 1985. Print.
- Millspaugh, Ben, Ph.D. "Civil Air Patrol: Model Rocketry." Leadership Development and Membership Services Directorate, National Headquarter, Civil Air Patrol, Maxwell AFB, AL. Print.

Appendix I: Project A.P.E.S. Gantt Chart

Appendix II: Launch Checklist

1. Prepare payload bay
 - a. Ensure batteries and switches are wired to the altimeters correctly
 - b. Ensure batteries, power supply, switch, data recorder and pressure sensors are wired correctly
 - c. Install fresh batteries into battery holders and secure with tape
 - d. Insert altimeter and payload into the payload bay
 - e. Connect appropriate wires
 - f. Verify payload powers on correctly and is working properly. If it is not, check all wires and connections
 - g. Turn off payload power
 - h. Arm altimeters with output shorted to verify jumper settings. This is to check battery voltage and continuity
 - i. Disarm altimeter, un-short outputs
 - j. Close altimeter bay
2. Assemble charges
 - a. Test e-match resistance and make sure it is within spec
 - b. Remove protective cover from e-matches
 - c. Measure amount of black powder determined in testing
 - d. Put e-matches on tape with sticky side up
 - e. Pour black powder over e-matches
 - f. Seal tape
 - g. Retest e-matches
3. Ensure altimeter is disarmed
4. Connect charges to altimeter bay
5. Turn on altimeter and verify continuity
6. Disarm altimeter
7. Connect drogue shock cord to booster section and altimeter bay
8. Fold excess shock cord so it does not tangle
9. Add Nomex cloth under drogue chute and shock cord
10. Insert altimeter bay into drogue section and secure with shear pins
11. Pack main chute
12. Attach main shock cord to payload bay
13. Fold excess shock cord so it does not tangle
14. Add Nomex cloth under main chute and shock cord
15. Attach altimeter bay to the main section with nylon rivets
16. Connect shock cord to nose cone, install nose cone and secure with shear pins
17. Assemble motor

- a. Follow manufacturer's instructions
- b. Do not get grease on propellant or delay
18. Do not install igniter until at pad
19. Install motor in launch vehicle
20. Secure positive motor retention
21. Inspect launch vehicle. Check CG to make sure it is in safe range; add nose weight if necessary
22. Arm altimeter and ensure both charges read continuity
23. Disarm altimeter
24. Bring launch vehicle to the range safety officer (RSO) table for inspection
25. Bring launch vehicle to pad, making sure to carry it only by the recovery sections.
26. Install on pad, verify that it can move freely (use a standoff if necessary)
27. Install igniter in launch vehicle
28. Touch igniter clips together to make sure they will not fire igniter when connected
29. Make sure clips are not shorted to each other or blast deflector
30. Arm altimeters via switches and wait for continuity check for both
31. Turn on payload via a switch and start stopwatches
32. Return to front line
33. Launch. Stop the stopwatches and record time from arming payload and launch
34. Watch flight so launch vehicle does not get lost
35. Recover launch vehicle
36. Disarm altimeter(s) if there are unfired charges
37. Disassemble launch vehicle, clean motor case, other parts, inspect for damage
38. Record altimeter data
39. Download payload data

Troubleshooting

<i>Test</i>	<i>Problem</i>	<i>Control & Mitigation</i>
Power on payload	Payload does not power on	Check batteries have sufficient charge, check wires are connected correctly
Check E-match resistance	E-match resistance does not match required specifications	Replace e-match before use
Power on altimeters	Altimeters do not power on	Check batteries have sufficient charge, check wires are connected correctly
Check for altimeter continuity after installing e-matches	No continuity	Check wires are connected correctly
Launch Rocket	Engine does not fire	Disconnect power, ensure igniter clips are not touching, ensure power is reaching clips ,ensure motor is assembled correctly

Appendix III: Ground Test Plan

Ground Test Plan

Goals

The A.P.E.S. ground test data will provide the basis for empirical modeling of the force interactions for various configurations of the experiment at various voltages. All actions will be incremented to allow for a detailed model for extrapolation and interpolation of the data for future flight control systems. Goals are detailed in Table 40: Ground Test goals.

Table 40: Ground Test goals

<i>Ground Test Goal</i>	<i>Ground Test Goal Definition</i>
1	DC Steady State Solenoid Testing
2	Map Magnetic Fields
3	Detect force equilibrium
4	Develop model for control of voltage

Test Sequence 1

The static magnetic field of a solenoid will be mapped at various distances and currents utilizing the 3-axis AKM 8975 magnetic sensor. From this, a Response Surface Equation (RSE) will be developed in order to map the total field strength at a given distance and current. The ranges for the distance and current tested are listed in Table 41.

Table 41. Range of test values used during Test Sequence 1.

<i>Parameter</i>	<i>Value</i>
Distance Range	1 cm to 5 cm
Current Range	0 A to 0.86 A

Test Sequence 2

Equilibrium testing with no internal magnetism. A single vertically-oriented solenoid will be utilized to lift the test article to equilibrium points within a cylinder, from 1 cm to 7 cm in steps of 1 cm. Hall-effect sensors will be used to map fields at each equilibrium point identically to



the static field mapping. The optical detection sensors will detect distance from below the cylinder. The optical detection sensors sensor will be lowered to the minimum read distance using MakerBeam. The minimum read distance shall be confirmed by data sheets and calibration.

Test Sequence 3

Equilibrium de-scope testing with internal magnetism. One (1) neodymium magnet shall be placed in the center of the test article and covered with reflective material. A single vertically-oriented solenoid will be utilized to lift the test article to equilibrium points within a cylinder, from 1 cm to 7 cm in steps of 1 cm. Hall-effect sensors will be used to map fields at each equilibrium point identically to the static field mapping. The test setup should allow for both pulling of the test article as well as pushing of the test article.

Test Sequence 4

Similar testing will be completed using a horizontal sheet with the sample placed on top. Solenoids will be used to pull and hold the sample in the middle of the platform at equilibrium. These tests will be completed with the permanent magnet sample. The Camera Cube will allow for object detection. Fields will be mapped at equilibrium.

Test Sequence 5

A permanently magnetic test article will be levitated from rest in 3-dimensions to equilibrium at central points in the test stand. Incrementing of the equilibrium point will allow for greater control of the test article. Object detection will be accomplished with the Camera Cube. Fields will be mapped at equilibrium.

Test Sequence 6

The flight model will be tested and disturbances will be introduced.



Appendix IV: Mathematical and Physical Modeling of Magnetic Fields

In order to accomplish the objective of stabilizing a platform with magnetic fields during the ascent of a launch vehicle, a control system must be developed with inputs of voltages and currents supplied to solenoids and optical sensing feedback for kinematics data. To create the control system, equations and experimentation to model the fields and resultant forces on an object in the field will be derived and conducted, respectively, from the scientific principles governing electromagnetism. Typically, electromagnetic equations are focused on defining axial interactions, while the A.P.E.S. experiment requires a comprehensive understanding of three-dimensional magnetic fields. The following sections will define the governing equations and concepts that are the foundation for the experimental testing and will serve as the basis for a data-centered control system.

Modeling General Magnetic Fields

If two magnets or electromagnets are at a large enough distance from each other, or small enough compared to the distances involved, then they can be modeled as being magnetic dipoles. A magnetic dipole can be thought of as a small current loop; this still creates a non-vanishing magnetic field at distances much larger than the radius of the loop. The magnetic dipole moment of a single current loop is defined as

$$\mathbf{m} = I\mathbf{S} \quad (1)$$

where the \mathbf{S} vector, and hence \mathbf{m} as well, is oriented perpendicular to the planar area of the loop so that curling the fingers of one's right hand in the direction of the current gives the direction of \mathbf{S} as the direction of the thumb. The magnetic potential due to a magnetic dipole of moment \mathbf{m} is

$$\mathbf{A}(\mathbf{r}) = \frac{\mu}{4\pi} \frac{\mathbf{m} \times \mathbf{r}}{r^3} \quad (2)$$

where \mathbf{r} is the vector from the dipole to the field point where the potential is being calculated, r is the magnitude of vector \mathbf{r} , and μ is the permeability of the medium at the field point. The magnetic flux density \mathbf{B} and the magnetic field \mathbf{H} due to the dipole are, respectively,

$$\mathbf{B}(\mathbf{r}) = \nabla \times \mathbf{A} = \frac{\mu}{4\pi r^3} (3(\mathbf{m} \cdot \hat{\mathbf{r}})\hat{\mathbf{r}} - \mathbf{m}) \quad (3)$$

$$\mathbf{H}(\mathbf{r}) = \frac{\mathbf{B}}{\mu} = \frac{1}{4\pi r^3} (3(\mathbf{m} \cdot \hat{\mathbf{r}})\hat{\mathbf{r}} - \mathbf{m}) \quad (4)$$

Where $\hat{\mathbf{r}}$ is the unit vector in the direction of \mathbf{r} , and the distance r is much greater than the radius of the loop.

There are two ways to approximate model the vector potential field, the magnetic field, and the magnetic induction field as produced by a solenoid using these equations. The first method is to model the solenoid as a single dipole of moment $\mathbf{m} = N\mathbf{IS}$ at the center of the solenoid, where N is the number of turns in the solenoid, as a solenoid has N current loops each of moment \mathbf{IS} . However, this does not take into account the fact that each loop of the solenoid is not at the same location. Therefore, a more precise way of modeling the solenoid – albeit still an approximation – would be to place one dipole of moment \mathbf{IS} at the center of each loop that makes up the solenoid, or perhaps one moment per k loops of moment $k\mathbf{IS}$, where we have a choice of k . However, computational difficulty is greatly increased due to the necessity of finite-element solver techniques as the mathematics progresses. The magnetic \mathbf{H} field produced by each model are shown below, where N is taken to be 11 loops (distributed over 2 cm of length for the second model) and $\frac{1}{4\pi}\mathbf{IS}$ is taken to be $\mathbf{k} \text{ A} \cdot \text{cm}^2$. One dipole of moment $11\mathbf{k} \text{ A} \cdot \text{cm}^2$ is placed at the origin in the typical cartesian plane in Figure 70, and 11 dipoles of moment $\mathbf{k} \text{ A} \cdot \text{cm}^2$ are distributed from -1 to 1 along the y-axis in Figure 71, for the sake of simplicity.

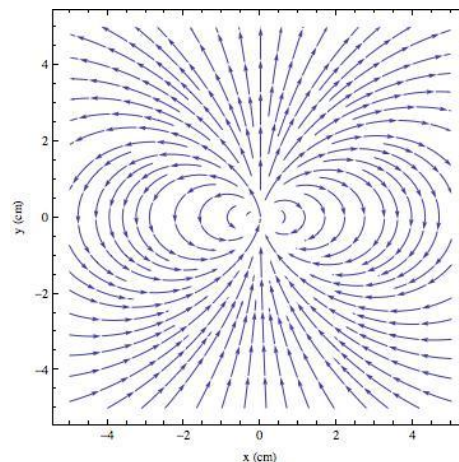


Figure 70: field generated by a single dipole

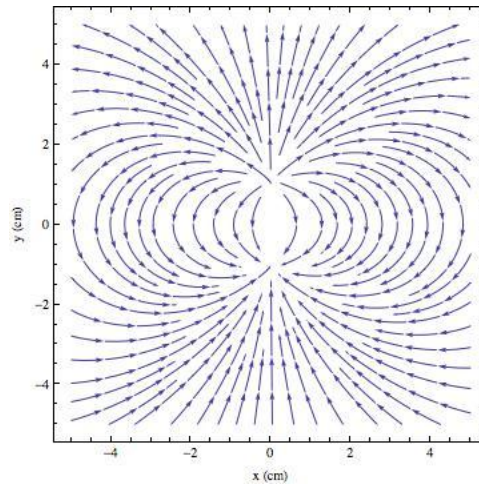


Figure 71: field generated by multiple dipoles

Generation of Magnetic Forces in Materials

All materials are composed of atoms, with a positively charged nucleus and negatively charged electrons. The movement and rotation of these charges form microscopic magnetic dipoles, which have magnetic dipole moments. The magnetization vector, \mathbf{M} , of a material at a point is defined as the volume “density” of magnetic dipole moment, i.e.

$$\mathbf{M} = \lim_{\Delta v \rightarrow 0} \frac{\sum \mathbf{m}_k}{\Delta v} \tag{5}$$

where each \mathbf{m}_k is the magnetic moment of the k th atom in the volume Δv , and the sum is over all the atoms. The force on a magnetic material can be determined by summing the forces on the dipoles in the material due to the field that it is placed in. The magnetization of a material depends on the field it is placed in, and the flux density depends on the field, as follows:

$$\mathbf{M} = \chi_m \mathbf{H} \tag{6}$$

$$\mathbf{B} = \mu_0(\mathbf{H} + \mathbf{M}) = \mu_0\mathbf{H}(1 + \chi_m) = \mu_0\mu_r\mathbf{H} = \mu\mathbf{H} \tag{7}$$

where χ_m is the material’s magnetic susceptibility, μ_r is its relative permeability, and μ is the absolute permeability. The parameters χ_m and μ_r are not always constant, especially in the case

of ferromagnetic materials. However, assuming a linear relationship between \mathbf{M} and \mathbf{H} – approximately true in the case of magnetically soft ferrite – or a constant \mathbf{M} in the case of a permanent neodymium magnet, using the \mathbf{H} field of a dipole or multiple dipoles as the field of the solenoids, the force on the platform due to the fields interacting with the microscopic dipoles in the material can be calculated.

Forces on Materials in Magnetic Fields

The force on an object is the sum of the forces on all of the magnetic dipoles that make up the object. By definition, the magnetic dipole moment of an infinitesimal volume of the object dV is $\mathbf{m} = \mathbf{M} dV$. The force due to the field of a magnetic dipole of moment \mathbf{m}_s on a magnetic dipole of moment \mathbf{m} that is in a material of permeability μ is:

$$\mathbf{F}(\mathbf{r}, \mathbf{m}_s, \mathbf{m}) = \frac{3\mu}{4\pi r^4} [(\mathbf{m}_s \cdot \hat{\mathbf{r}})\mathbf{m} + (\mathbf{m} \cdot \hat{\mathbf{r}})\hat{\mathbf{m}}_s + (\mathbf{m}_s \cdot \mathbf{m})\hat{\mathbf{r}} - 5(\mathbf{m}_s \cdot \hat{\mathbf{r}})(\mathbf{m} \cdot \hat{\mathbf{r}})\hat{\mathbf{r}}] \quad (8)$$

Where \mathbf{r} is the vector from \mathbf{m}_s to \mathbf{m} , and $\hat{\mathbf{r}}$ is again the unit vector in the direction of \mathbf{r} . First the case of a ferrite platform is considered, with approximate constant χ_m and μ . In this case, the force on the platform is calculated to be:

$$\mathbf{F}(\mathbf{r}, \mathbf{m}_s) = \iiint \frac{3\mu\chi_m}{16\pi^2 r^7} [(\mathbf{m}_s \cdot \hat{\mathbf{r}})\mathbf{m}_s - (\mathbf{m}_s \cdot \mathbf{m}_s)\hat{\mathbf{r}} - 4(\mathbf{m}_s \cdot \hat{\mathbf{r}})^2 \hat{\mathbf{r}}] dV \quad (9)$$

Where \mathbf{m}_s is now used as $\mathbf{m}_s = NIS$ for the solenoid and the integral is evaluated over the volume of the platform. If it is assumed that the object is small such that the quantity integrated does not vary significantly over the volume, the force on the platform of volume V , due to the solenoid of moment $\mathbf{m}_s = NIS$, is:

$$\mathbf{F}(\mathbf{r}, \mathbf{m}_s, \mathbf{m}) = \frac{3VN^2I^2S^2\mu\chi_m}{16\pi^2 r^7} [(\hat{\mathbf{n}} \cdot \hat{\mathbf{r}})\hat{\mathbf{n}} - \hat{\mathbf{r}} - 4(\hat{\mathbf{n}} \cdot \hat{\mathbf{r}})^2 \hat{\mathbf{r}}] \quad (10)$$

Where $\hat{\mathbf{n}}$ is the unit vector in the direction of \mathbf{S} – the unit normal to the loop area of the solenoid – and \mathbf{r} is the position vector from the solenoid center to the center of mass of the platform. While approximate, it is clear that the force will vary as the square of current and inversely by

the seventh power of the distance between the solenoid and the platform assuming a magnetically-soft ferrite material. To check the validity of this equation, and assuming that both $\hat{\mathbf{n}}$ and \mathbf{r} are in the positive \mathbf{k} direction in a Cartesian plane, such that the platform is above the dipole, it is found that:

$$\mathbf{F} = \frac{-3VN^2I^2S^2\mu\chi_m}{4\pi^2r^7}\mathbf{k} \quad (11)$$

Or that the platform is pulled towards the dipole, which matches the basic experience of magnetic materials attracted to magnets due to induction.

The equations given above are derived in Appendix 3. However, the validity of these equations is primarily for the case of a single solenoid acting on a platform with constant permeability. Forces originating from more than one solenoid do not add in the conventional sense, as the induction of a ferrite material is highly non-linear. These equations must be re-derived from equation (8), as the fields and magnetization of the platform change in the n-solenoid problem.

Much easier is the case of a permanent neodymium magnet with constant magnetization \mathbf{M} throughout. In this case, the force on the platform is the sum of the force on each $\mathbf{M} dV$ segment,

$$\mathbf{F}(\mathbf{r}, \mathbf{m}_s, \mathbf{M}) = \iiint \frac{3\mu_0}{4\pi r^4} [(\mathbf{m}_s \cdot \hat{\mathbf{r}})\mathbf{M} + (\mathbf{M} \cdot \hat{\mathbf{r}})\hat{\mathbf{m}}_s + (\mathbf{m}_s \cdot \mathbf{M})\hat{\mathbf{r}} - 5(\mathbf{m}_s \cdot \hat{\mathbf{r}})(\mathbf{M} \cdot \hat{\mathbf{r}})\hat{\mathbf{r}}] dV \quad (12)$$

Here, the constant involves μ_0 rather than just μ , since the \mathbf{M} vector is constant and is largely independent of \mathbf{H} . Again, the exact value of the expression is highly dependent on the shape of the volume integrated upon. However, if the volume V is small, the force can be taken due to the solenoid field NIS as:

$$\mathbf{F}(\mathbf{r}, \mathbf{m}_s, \mathbf{m}) = \frac{3VNIS\mu_0}{4\pi r^4} [(\hat{\mathbf{n}} \cdot \hat{\mathbf{r}})\mathbf{M} + (\mathbf{M} \cdot \hat{\mathbf{r}})\hat{\mathbf{n}} + (\hat{\mathbf{n}} \cdot \mathbf{M})\hat{\mathbf{r}} - 5(\hat{\mathbf{n}} \cdot \hat{\mathbf{r}})(\mathbf{M} \cdot \hat{\mathbf{r}})\hat{\mathbf{r}}] \quad (13)$$

Where $\hat{\mathbf{n}}$ is defined as before. Equation (11) is also an approximate solution, but here it is evident that the force on a permanent magnet varies only directly on the current in the solenoid and inversely by the fourth power of the distance, rather than by the square of current and inversely by the seventh power of distance in the case of forces from induction in a ferrite platform. The force will also depend on the orientation of \mathbf{M} . Unlike for the case of a material with constant permeability, the forces on a permanent magnet due to multiple solenoids *do* add in the conventional sense, greatly simplifying computational analysis.

Appendix V: Recovery MATLAB code

```

%% Author: Akshaya Srivastava
% Date: 12/19/2011
% Purpose: USLI Recovery System Design and Analysis

clc
clear
close all

%% Main Parachute Sizing and Ejection Optimization Code
% Code will find optimal height and main parachute size for deployment
% given a certain speed. The Drogue Chute Area is assumed constant based
% on a worst case scenario. Ejection charges will also be calculated based
% on user choosing what height the main chute should deploy at based on
% 3D plots created by code. Equations have been derived in notebook (an
% image of the design process is available upon request). Limitations and
% constraints have been extracted from the USLI Handbook. All units are in
% SI for calculations. Conversion code is implemented as required, for ease
% of checking whether requirements in the USLI Handbook are met. All
% Parachutes are assumed to be one inch thick. Drift is considered and
% program won't end until the drift conditions have been satisfied. Drift
% Conditions include 1) a maximum total drift of 2500 ft [USLI HANDBOOK]
% and 2) a maximum drift between drogue and main chute deployments
% of 1800 ft.

%% Assumptions made
% 1) Cd of Drogue = 1.2 (can be updated with testing)
% 2) Cd of Main = 1.4 (can be updated with testing)
% 3) STP Conditions at Landing
% 4) Need to Pressurize all the Volume (needs to be updated with
% actual model)
% 5) Thickness of all parachutes is assumed to be 1-inch to account for
% harness, shroud lines, and other hardware.
% 6) Drogue Descent Speed was assumed to be 50 fps
% 7) Once a chute is deployed, the time the rocket takes to reach
% terminal velocity/descent rate is negligible
% 8) Drogue Drift shouldn't exceed 1800 ft.
% 9) The main chute will reach the ground after deployment in 30 seconds

% Constants with direct effect on flight profiles
mass_si = 18.1653; %kg
ke_max_possible_si = 376.8; %J - Found in PDR and USLI HANDBOOK
v_max_possible_si = sqrt((2*ke_max_possible_si)/mass_si); %m/s
drift_total = 2501; %ft-limit used for loop
wind_eng = 0:5:20; %mph - provided by USLI Handbook
wind_si = wind_eng *.44704; %m/s - Converting to SI
delta_t = 2500/22; %s - 2500 ft at 15 mph (=22 ft/s) [USLI HANDBOOK]

% Constants with indirect effect on flight profiles
C_d_main = 1.4; %dimensionless assumed quantity for now...

```

```

C_d_drogue = 1.2; %dimensionless assumed quantity for now...
rho_si = 1.225; %for now take air density at landing(2000ft=95% of sea lvl)
g_si = 9.81;%m/s^2
R_air_si = 287.04; %J/(kg*K) - molecular gas constant of air
R_air = 53.3533; %(ft*lb)/(lb*R) - molecular gas constant of air
V_drogue = ((1/3)*pi()* (4.7)^2)*(25.5); %in^3-volume of drogue chamber
V_main = 12*(pi()* (5)^2); %in^3-volume of main chamber accounting for stuff
R_combust = 22.16*12; %in*lb)/(lb*R) - gas combustion constant (FFFF BP)
T_combust = 3307; %R - gas combustion temperature (FFFF BP)

%% Defining Drogue Data
% All Drogue Data is computed here
v_drogue_si = 15.24;%15.24m/s=50ft/s
temp_drogue = -.0036*5280+59.007 + 459.67;%R-at a mile high
temp_drogue_si = (temp_drogue-32-459.57)*(5/9) + 273.15; %K-for press. calc
rho_drogue = rho_si * .8549;%SI units at a mile high
drogue_area = g_si*(mass_si^2* sqrt((wind_si(length(wind_si))^2+...
    v_drogue_si^2)))/(C_d_drogue*(.5*mass_si*v_drogue_si^2)*15.24...
    *(rho_drogue));%m^2-Worst case scenario (ke is calculated)

% Converting Drogue Chute Area and Diameter
drogue_area = drogue_area * 10.7639104 %ft^2 (Shown)
drogue_dia = sqrt((4*drogue_area)/pi()) %ft (Shown)

pressure_drogue_si = R_air_si*rho_drogue*temp_drogue_si; %Pascals
pressure_drogue = pressure_drogue_si * .000145037738; % lbf/in^2

eject_drogue = (((V_drogue-drogue_area)*(23.7-pressure_drogue))/...
    (R_combust*T_combust))*454 %grams (Shown)

%% Calculating Main Chute Data
% Defining loops to iterate and make graphs. One graph of velocity vs
% optimal height per wind speed. The area of the parachute will also be
% displayed per wind speed and velocity.

v_val = 1:.2:v_max_possible_si; %m/s-Values of velocity to iterate through

chute_area = zeros(length(wind_si),length(v_val)); %m^2- used to store the
    %values of chute sizing

optimal_h = zeros(length(wind_si),length(v_val)); %m-used to store
    %minimum height

drift = zeros(length(wind_si),length(v_val)); %m-used to store drift values

for u = 1:length(wind_si)
    for v = 1:length(v_val)
        chute_area(u,v) = g_si*(mass_si^2* sqrt((wind_si(u))^2+...
            (v_val(v))^2)))/(C_d_main*ke_max_possible_si*rho_si*v_val(v));
    %m^2-done
    %with assumed
    %values
    
```

```

    optimal_h(u,v) = (v_val(v))*delta_t; %m-Minimum deployment height
    drift(u,v) = sqrt((wind_si(u))^2+(v_val(v))^2)*delta_t; %m-drift

    %placing an upper bound on drift for plots [USLI HANDBOOK]
    if (drift(u,v)*3.2808399 > 2500)
        drift(u,v) = NaN;
    end
end
end

%% Creating 3D plots to show results
chute_area = chute_area - drogue_area; %m^2 - finding main chute area
chute_dia = real(sqrt(4*chute_area/pi)); %m - getting main chute diameter

v_mat = [v_val;v_val;v_val;v_val;v_val]; %terminal velocity mesh for plots
u_mat = []; %wind velocity mesh for plots
for i = 1:length(v_val)
    u_mat = [u_mat transpose(wind_si)]; %filling in wind velocity mesh
end

% 3D plot and labels - English Units
figure
surf(v_mat.*3.2808399,chute_dia.*3.2808399,optimal_h.*3.2808399)
xlabel('Descent Rate (ft/s)')
ylabel('Diameter of Main Parachute (ft)')
zlabel('Minimum Deployment Height (ft)')
title('Descent Rate - Size - Height (English)')

% 3D Plot to show drift with respect to wind velocity and terminal velocity
% English units
figure
surf(v_mat.*3.2808399,u_mat.*3.2808399,drift.*3.2808399)
xlabel('Descent Rate (ft/s)')
ylabel('Wind Velocity (ft/s)')
zlabel('Drift (ft)')
title('Wind - Descent Rate - Drift (English)')

%Loop to keep drift in bounds.
while (drift_total>2500)
    drogue_drift = 2001;
    while (drogue_drift > 1800)
        prompt = ['Based on figures displayed, Choose a height to' ...
            ' deploy the main chute (ft): '];%prompt for user input
        h_chosen = input(prompt); %ft-Asks user to choose a height.
        h_chosen_si = h_chosen*3.2808399; %m-Used only in calculations
        drogue_drift = wind_si(4)*((1609-h_chosen)/50)*3.2808399;
        %ft-keeping drift
        %within bounds
    end
end

```



```

%% Calculation of Ejection Charge for Main Chute

temp_main = 59.007-.0036*h_chosen + 459.67;%R-at altitude chosen;
temp_main_si = (temp_main-32-459.57)*(5/9) + 273.15; %K-for pressure
rho_main = rho_si *((h_chosen^2)*.00000002914 - h_chosen * ...
    .0029+99.995)/100;%SI-done by percent change density at altitude

pressure_main_si = R_air_si*rho_main*temp_main_si; %Pascals
pressure_main = pressure_main_si * .000145037738; % lbf/in^2

%% Displaying Specific Data for Chosen Height
delta_t_chosen = 30; %sec-chosen and can be modified (Shown)

chute_area_chosen = ((2*mass_si*g_si*delta_t_chosen^2)/(rho_main*...
    C_d_main*(h_chosen/3.2808399)^2))*10.7639104 %ft^2 (Shown)

v_chosen = h_chosen/delta_t_chosen %ft/sec (Shown)
drift_chosen = sqrt(15^2+v_chosen^2)*delta_t_chosen %ft-Shown
chute_chosen_diameter = sqrt(4*chute_area_chosen/pi()) %ft-Shown
drift_total = drogue_drift+drift_chosen;%ft-shows drift at 15ft/s winds
%condition to go back into loop
if (drift_total > 2500)
    drogue_drift = 2001;
else
    drift_total
end

eject_main = ((V_main-chute_area_chosen)*(24.7-pressure_main))/...
    (R_combust*T_combust))*454 %grams (Shown)
end

% Extra plot to show drift at various windspeeds
figure

plot(wind_eng,sqrt(wind_si.^2+(v_chosen/3.2808399)^2)*delta_t_chosen*3.280839
9)
xlabel('Wind Velocity (ft/s)')
ylabel('Drift (ft)')
title('Wind - Drift (English)')

end

```

Appendix VI: FIRST LEGO League Lesson Plan

Electricity and Magnetism

January 28th, 2012

Main Concepts

- ✓ How electricity works.
- ✓ The difference between conductors and insulators.
- ✓ How electricity is related to magnetism.

Activities

ACTIVITY ONE: Electric Bug

To make a bug:

- 1 D battery
- 1 light bulb
- poster putty
- colored paper
- wire
- pipe cleaners

Materials:

- compass

Hook: Do you think you can get the bug to light up?

- ❖ Make the bug light up. Right now the light bulb is lit. *How do you think the light is on?* It's not connected to the wall. *Is it magic?*
- ❖ Inside the bug is a battery and when the bulb is on the circuit is complete and electricity is flowing. *Do any of you know what electricity? Can you explain it?*
- ❖ Everything is composed of atoms and in atoms there are these things called electrons. Sometimes electrons jump from one atom to another. When there are a lot of atoms doing this we call it an electric current. In some materials the electrons can jump a lot and in other materials they can't jump at all. When the electrons can jump around the material is called a conductor and when the electrons can't jump the material is called an insulator.
- ❖ I have a bunch of different materials here. *Which ones do you think are conductors? Which ones do you think are insulators?*
- ❖ Try to make the bulb light with the different materials. Once you have tried all the materials put the conductors on one side and the insulators on the other.

- ❖ Okay, so these are conductors and these are insulators. *What is different about them?*
- ❖ The conductors are all metal and the insulators are not metal. So in metals the electrons can jump around a lot.

End: This is how electricity works. This is how the lights in your house turn on when you flip the switch.

Appendix VII: Civil Air Patrol (CAP) Model Rocketry Program Lesson Plan

Model Rocketry Program

March 2012

Main Concepts

The CAP Model Rocketry Program is broken up into three (3) stages.

Stage One – REDSTONE

- ✓ Identify historical facts about the development of rockets
- ✓ Describe the major contributions of the four great rocket pioneers.
- ✓ Recall facts about the rocket pioneers' lives and accomplishments.
- ✓ Design, build and launch two non-solid fuel hands-on rocket options

Stage Two – TITAN

- ✓ Explain Newton's three Laws of Motion. -Describe the aerodynamics of a rocket.
- ✓ Design, build and launch two of the hands-on rocket options.
- ✓ Demonstrate knowledge of the NAR safety code.

Stage Two – SATURN

- ✓ Describe altitude tracking.
- ✓ Explain baseline distance.
- ✓ Describe the ingredients of a model rocket engine.
- ✓ Define Newton seconds. -Define total impulse.
- ✓ Demonstrate knowledge of the NAR safety code.
- ✓ Design, build and launch one rocket in the Saturn stage.

Activities

ACTIVITY ONE: Electric Bug

Materials:

- Civil Air Patrol Model Rocketry Handbook
- Appropriate supplies for all rocket builds